ABSTRACT

Title of Document: RIBOSOME INTEGRITY AND TRANSLATIONAL FIDELITY REQUIRE ACCURATE MODIFICATION AND PROCESSING OF rRNA IN THE YEAST *SACCHAROMYCES CEREVISIAE*

Jennifer Lynn Baxter Roshek, Ph.D., 2006

Directed By: Associate Professor Dr. Jonathan D. Dinman, Department of Cell Biology and Molecular Genetics

Translating mRNA sequences into functional proteins is a fundamental process necessary for the viability of organisms throughout all kingdoms of life. The ribosome carries out this process with a delicate balance between speed and accuracy. Although kinetic and biochemical studies along with high resolution crystal structures have provided much information about the ribosome, many of the underlying mechanisms of ribosome function are still poorly understood. This work seeks to understand how ribosome structure and function are affected by changes in rRNA as caused by two very different mechanisms. *mof6-1*, originally isolated as a recessive mutation which promoted increased efficiencies of programmed -1 ribosomal frameshifting, was found to be an allele of *RPD3* which encodes a histone deacetylase that is involved in transcriptional activation and silencing. This mutant demonstrated a delay in ribosomal RNA (rRNA) processing leading to changes in reading frame

maintenance and ribosomal A-site specific defects. To understand the role of *cis*-acting changes to rRNA, yeast strains deficient in rRNA modifications in the peptidyl transferase center of the ribosome were monitored for changes in ribosome structure and translational fidelity. Analyses revealed mutant phenotypes including sensitivity to translational inhibitors; changes in reading frame maintenance, nonsense suppression and aa-tRNA selection; and increased rates of A-site tRNA binding to the mutant ribosome. One mutant in particular, *spb1DA*/*snr52*Δ, promoted increased rates of programmed -1 ribosomal frameshifting, increased rates of near cognate tRNA selection and A-site tRNA binding. Structural analysis of *spb1DA*/*snr52*Δ revealed changes consistent with a more accessible ribosomal A-site. These results suggest that rRNA nucleotide modifications produce small but distinct changes in ribosome structure and function contributing to overall translational fidelity.

Taken together, these data suggest that rRNA, a main component of the ribosome, contributes directly to translational fidelity. Defects in rRNA caused by changes in both its processing and modification can cause changes in reading frame maintenance, nonsense suppression, aa-tRNA selection and binding as well as ribosome structure.

RIBOSOME INTEGRITY AND TRANSLATIONAL FIDELITY REQUIRE ACCURATE MODIFICATION AND PROCESSING OF rRNA IN THE YEAST *SACCHAROMYCES CEREVISIAE*

By

Jennifer Lynn Baxter Roshek

Dissertation submitted to the Faculty of the Graduate School of the
University of Maryland, College Park, in partial fulfillment
of the requirements for the degree of
Doctor of Philosophy
2006

Advisory Committee:
Associate Professor Jonathan D. Dinman, Ph.D., Chair
Associate Professor Steve Mount, Ph.D.
Professor Donald Nuss, Ph.D.
Professor Philip Farabaugh, Ph.D.
Professor Dorothy Beckett, Ph.D., Dean's Representative

© Copyright by
Jennifer Lynn Baxter Roshek
2006

Dedication

I would like to extend my love and thanks to my mother. Her years of sacrifice, support and encouragement have made this journey possible. She is a part of all that I have become.

Acknowledgements

I would like to thank my advisor Dr. Jonathan D. Dinman for years of support. This work would not have been possible without him. I would also like to thank every member of the Dinman Laboratory for their assistance, helpful advice, and countless discussions.

This work was supported in part by a National Institutes of Health Virology Training Grant at the University of Maryland and by National Institutes of Health grant NIH R01 GM58859

Table of Contents

Dedication ii
Acknowledgements iii
Table of Contents iv
List of Tables vi
List of Figures vii
List of Abbreviations ix
Chapter 1: An Ingress 1
Introduction 1
rRNA Modification 3
Translation 8
Overview 8
Initiation 10
Cap-Independent Initiation 12
Elongation 13
Termination 20
Translational Recoding 22
Programmed Ribosomal Frameshifting 22
Programmed -1 Ribosomal Frameshifting 23
Programmed +1 Ribosomal Frameshifting 28
Nonsense Suppression 31
Summary 33
Chapter 2: Delayed rRNA processing results in significant ribosome biogenesis and functional defects 34
Introduction 34
Materials and Methods 36
Strains, media, and genetic methods 36
Plasmid and strain constructs, programmed ribosomal frameshift, and transcriptional derepression 38
in vivo [^{35}S]Methionine Incorporation 40
Pulse-Chase Labeling of rRNA 41
Polysome and 2-dimensional NEPHGE analyses 41
Preparation of tRNAs and of donor and acceptor fragments 42
Purification of ribosomes and tRNA binding assays 43
Puromycin reaction with tRNA fragments 44
Results 45
mof6-1 is an allele of RPD3 45
Correlation of growth and frameshifting defects in the rpd3 mutants 52
Deletion of other genes linked to heterochromatin-associated functions also result in the Mof$^-$ phenotype 56
Mutation of genes involved in the histone deacetylation apparatus result in 60S ribosomal subunit biogenesis defects 58

Ribosome biogenesis defects are not due to global defects in ribosomal protein expression 60
The mutants result in aminoacyl-tRNA binding in defects 60
Ribosomes from mof6-1 cells have decreased peptidyl transfer activities 65
Discussion 65
Chapter 3: Effects of rRNA modifications in the PTC of yeast ribosomes on translational fidelity and ribosome structure 70
Introduction 70
Materials and Methods 75
Strains, media, and genetic methods 75
Killer virus assay and viral dsRNA analyses 76
Dual Luciferase Assays 77
Drug Sensitivity 77
Ribosome isolation 78
Purification of aminoacyl-tRNA synthetases 79
Synthesis of aminoacyl-tRNA and acetylated aminoacyl-tRNA 80
Characterization of peptidyl transferase activity 81
tRNA binding activity 82
Structure Probing on Ribosomes in vitro 84
Results 84
rRNA modification mutants show sensitivity to translation inhibitors 85
Virus propagation in rRNA modification mutants 88
rRNA modification mutants cause defects in translational fidelity 92
Changes in aminoacyl-tRNA binding and peptidyl transfer rates 96
Structure changes observed in the PTC of a modification deficient ribosome 98
Discussion 104
Chapter 4: Conclusions and Future Directions 118
Appendix A: Yeast Strains 122
Appendix B: Plasmid List 124
Appendix C: Oligonucleotide List 126

List of Tables

Table 1: Summary of phenotypes for rRNA modification mutants 103

Table.2: Yeast strains 122

Table.3: Plasmid List 124

Table.4: Oligonucleotide List 126

List of Figures

Figure 1.1: rRNA processing in *S. cerevisiae* 2

Figure 1.2: H/ACA and C/D box snoRNAs 7

Figure 1.3: Eukaryotic cap-dependent translation initiation 9

Figure 1.4: Translation elongation cycle 11

Figure 1.5: Schematic representation of the hybrid-states translocation cycle 14

Figure 1.6: Kinetic scheme of aa-tRNA selection and the two stages of proofreading 16

Figure 1.7: Computer simulated amino-acyl tRNA accommodation into the A-site .. 18

Figure 1.8: Schematic of general translation termination 21

Figure 1.9: Programmed -1 ribosomal frameshifting 25

Figure 1.10: The "killer" virus sytem in yeast 27

Figure 1.11: Programmed +1 ribosomal frameshifting 30

Figure 2.1: *mof6-1* is an allele of *RPD3* 47

Figure 2.2: *RPD3* allele-specific effects on -1 PRF and viral maintenance 50

Figure 2.3: Transcriptional repression 51

Figure 2.4: Correlation of growth and frameshifting defects in *rpb3* mutants 53

Figure 2.5: Decreased rates of protein synthesis in cells expressing the mof6-1p form of Rpd3p 55

Figure 2.6: Frameshifting defects in heterochromatin-associated mutants. 57

Figure 2.7: Delayed 35S rRNA processing in histone deacetylation associated mutants 59

Figure 2.8: 60S ribosomal subunit biogenesis and polysome defects 61

Figure 2.9: Sensitivity to translational inhibitors 63

Figure 2.10: Decreased aa-tRNA binding in *mof6-1 ribosomes* 64

Figure 2.11: Decreased peptidyl transfer activities in *mof6-1* mutant ribosomes 66

Figure 3.1: Secondary structure map of rRNA modification sites 71

Figure 3.2: Ribosomal large subunit with the PTC highlighted 86

Figure 3.3: Modified 25S rRNA residues in the PTC of yeast 87

Figure 3.4: Sensitivity to translational inhibitors 89

Figure 3.5: M_1 virus propagation in rRNA modification mutants. 91

Figure 3.6: Bicistroni dual luciferase reporter system. 93

Figure 3.7: Programmed ribosomal frameshifting in rRNA modification mutants 95

Figure 3.8: aa-tRNA selection in rRNA modification mutants 97

Figure 3.9: Nonsense suppression phenotypes in rRNA modification mutants 99

Figure 3.10: Phe-tRNA binding to A-site 100

Figure 3.11: Ac-Phe-tRNA binding to P-site 101

Figure 3.12: Peptidyl transfer rates as measured by the puromycin reaction 102

Figure 3.13: *in vitro* structure probing analyses 105

Figure 3.14: Three dimensional depiction of structural changes revealed by structural probing 108

Figure 3.15: Interactions between RF-2 and the *E. coli* LSU 112

Figure 3.16: Interaction of RF1 with the PTC ribosomal large subunit 113

List of Abbreviations

aa-tRNA	Aminoacyl-tRNA
ASL	Anticodon stem loop
CMCT	1-cyclohexyl-3-(2-morpholinoethyl) carbodiimide metho-p-toluene
CrPV	Cricket Paralysis Virus
CFU	Colony forming unit
DLR	Dual luciferase reporter
DMS	Dimethyl sulfate
dsRNA	Double stranded RNA
DTE	1,4-dithioerythritol
EDTA	Ethylenediaminetetraacetic acid
EF	Elongation Factor
eIF	Eukaryotic initiation factor
EMCV	Encephalomycarditis virus
eRF	Eukaryotic release factor
GAC	GTPase associated center
GTP	Guanosine triphosphate
HCV	Hepatitis C Virus
HPLC	High Performance Liquid Chromatography
IRES	Internal ribosome entry site
LSU	Large subunit of the ribosome
mRNA	Messenger RNA
Nm	2'-*O*-ribose methylation
NTR	Non-translated region
OD	Optical density at specified wavelength
ODC	Ornithine decarboxylase
ORF	Open Reading Frame
PMSF	Phenylmethylsulfonyl fluoride
Ψ	Pseudouridine
PT	Peptidyl transfer
PTC	Peptidyl transferase center

PRF	Programmed Ribosomal Frameshifting
rDNA	Ribosomal DNA
RDRP	RNA dependent RNA polymerase
RF	Release factor
rRNA	Ribosomal RNA
snoRNA	Small nucleolar RNA
snoRNP	Small nucloelar RNA-protein complexes
snRNA	Small nuclear RNA
SSU	Small subunit of the ribosome
tRNA	Transfer RNA

Chapter 1: An Ingress

Introduction

Translation, the decoding of information contained within messenger RNA (mRNA) into its corresponding protein, is a fundamental process carried out in all kingdoms of life and is crucial for cell growth and proliferation. This process is mediated primarily by the ribosome in conjunction with associated protein factors. In all growing cells, a vast amount of energy and resources is dedicated to the biosynthesis of ribosomes. It has been estimated that a growing cell manufactures as many as 2000 ribosomes per minute (Warner, 1999). In the face of such intense energetic demands, it is essential that the many steps involved in ribosome biogenesis be efficient and well coordinated. The ribosome is made up of two subunits, each of which consists of ribosomal RNA (rRNA) and as many as 70 to 100 ribosomal proteins. In eukaryotes, ribosome biogenesis begins in the nucleolus where a large precursor rRNA is synthesized by RNA polymerase I (Pol I). This precursor rRNA undergoes a series of cleavage events, nucleotide modifications and folding steps resulting in mature rRNA species. In the yeast *Saccharomyces cerevisiae*, a 35S rRNA precursor is processed into three mature rRNA species: 18S, 5.8S and 25S (Figure 1.1) (Decatur and Fournier, 2003). An additional rRNA component required for ribosome formation is 5S rRNA, which is independently transcribed by RNA polymerase III (Pol III), processed and exported into the nucleolus for assembly. In

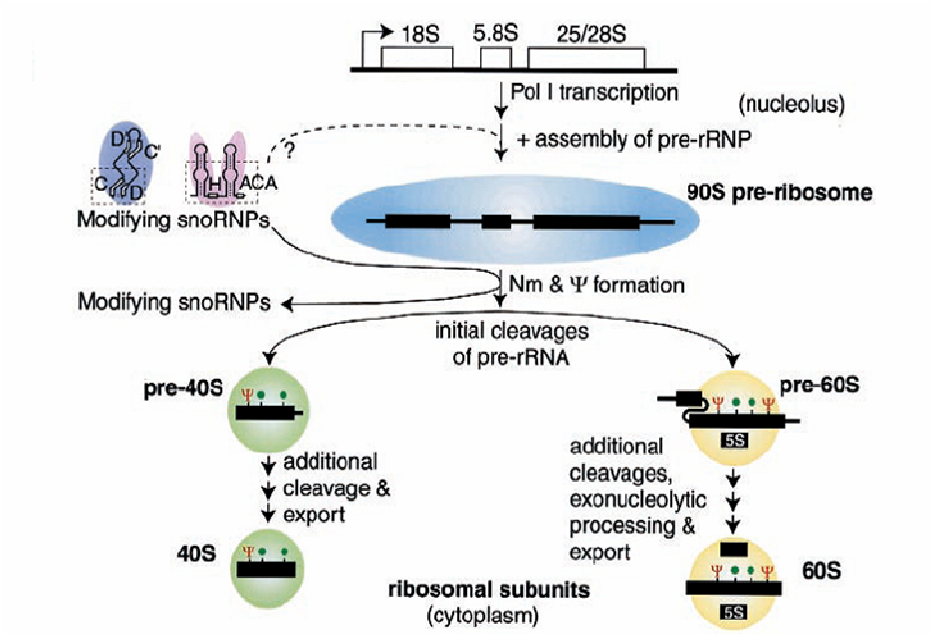

Figure 1.1

rRNA processing in yeast

A general overview of ribosome biogenesis. Figure adapted from Decatur and Fournier, 2003.

addition to mature rRNAs, production and assembly of the mature 60S (large) and 40S (small) subunits that comprise a complete 80S yeast ribosome requires approximately 80 ribosomal proteins and greater that 150 accessory proteins and small RNAs. In yeast, this process is completed in the cytoplasm with the final processing of the small subunit 20S pre-rRNA to mature 18S rRNA (Vanrobays et al., 2001).

rRNA Modification

One vital component of ribosome biogenesis involves pre-rRNA nucleotide modification. Such rRNA modifications are found in all known ribosomes, although their location and abundance vary among phylogenetic kingdoms (Rozenski et al., 1999). There are over 200 modified nucleotides in human rRNA, over 100 in the yeast *S. cerevisiae*, and close to 40 modified nucleotides found in the eubacteria *E. coli* rRNA. Three general nucleotide modifications occur in rRNA: 1) pseudouridylation – the conversion of uridine to pseudouridine (Ψ), 2) methylation- addition of a methyl group to the ribose 2'hydroxyls (Nm), and 3) other modifications- primarily base methylation at various positions. The most abundant modifications are pseudouridylation and 2'-*O*-methylation. In eukaryotes, two classes of small nucleolar RNA-protein complexes (snoRNPs) labeled H/ACA and C/D type snoRNPs mediate each of these modification reactions[1]. They are classified as such because they each contain a small nucloelar RNA (snoRNA) harboring

[1] In eubacteria, only specific protein enzymes are required to carry out nucleotide modification without RNA guides. In archaea, small guide RNAs, called sRNAs, form snRNPs and are involved in site-specific RNA modification in an evolutionarily related process to eukaryotes. Eukaryotic modifications and its machinery will be the focus of this work.

conserved H and ACA or C and D sequence motifs (often called 'boxes') (Balakin et al., 1996a). The snoRNPs of both classes consist of a snoRNA, which serves as a guide sequence, and at least four specific proteins. During the modification reaction, the snoRNA provides site specificity through base pairing with the target RNA allowing the enzymatic protein to catalyze the modification of a specific nucleotide. The residue ultimately modified resides within the target RNA sequence that is base paired to the guide snoRNA and at a specific location relative to the H/ACA or C/D boxes. Pseudouridylation and 2'-O-methylation reactions are performed by H/ACA and C/D box snoRNPs respectively.

SnoRNA molecules are short, usually ranging between 80-400 nucleotides (nt)[2]. They exist in a wide range of eukaryotes[3] with the vast majority of research performed in yeast and mammalian systems. Most H/ACA and C/D box snoRNAs are transcribed by RNA polymerase II (Pol II). Their genomic locations vary among eukaryotes. Most mammalian snoRNAs are located in the introns of protein-coding genes, while most yeast snoRNAs are processed from polycisronic transcripts or are transcribed from independent genes. Both intronic and polycistronic transcriptional units yield pre-snoRNAs which require processing to mature. Intronic snoRNAs are processed in two ways. The primary pathway involves debranching the spliced lariat followed by exonucleolytic digestion of extraneous sequence. The second pathway operates independent of splicing, where the snoRNAs are excised from the introns through endonucleotytic cleavage followed by trimming. SnoRNAs encoded by

[2] Some exceptions are snR30 consisting of 608 nt and snR59 with 78nt.
[3] SnoRNAs have been found in eukaryotes including but not limited to humans, mice, *Xenopus*, *D. melanogaster, C. elegans*, *A. thaliana*, *S. cerevisiae*, *S. pombe*, *E. gracilis*, and trypanosomes.

polycistronic transcription units undergo endonucleolytic cleavage followed exonucleolytic processing to remove excess nucleotides.

All guide H/ACA snoRNAs share a hairpin-hinge-hairpin-tail secondary structure with the conserved sequence ANANNA (H box) in the hinge region and the ACA motif exactly three nucleotides from the 3'end in the tail structure (Figure 1.2b). Guide H/ACA snoRNAs facilitate pseudouridylation through complementary base pair interactions with a 6-20 nucleotide stretch of the target rRNA encompassing the targeted U residue. This interaction occurs in such a way as to leave the targeted U residue unpaired in a hairpin bulge creating a 'pseudouridylation pocket' thereby making it available to the pseudouridine synthase (Ni et al., 1997; Ganot et al., 1997a). Formation of Ψ is known to require the breakage of the N_1-glycosyl bond, rotation of the uracil ring by 180° followed by formation of the C_5-glycosyl bond (Chu et al., 1976). Guide H/ACA RNAs associate with at least four proteins to form a functional snoRNP complex. The snoRNA-directed pseudouridylation is carried out by yeast Cbf5fp (mammalian/human Nap57p/dyskerin) (Lafontaine et al., 1998; Zebarjadian et al., 1999). The other guide H/ACA snoRNA associated proteins in yeast include Gar1p, Nhp2p, and Nop10p (Balakin et al., 1996b; Ganot et al., 1997b; Henras et al., 1998; Watkins et al., 1998).

The methylation C/D snoRNAs contain the conserved C (consensus sequence RUGAUGA, where R stands for any purine) and D (consensus CUGA) boxes near their 5' and 3' ends, respectively (Figure 1.2a) (Kiss, 2001). These boxes are often

brought together by a short base pair interaction between the termini. C/D snoRNAs also contain second set of motifs that resemble the boxes C/D called C' and D' boxes, which are located more internal to the RNA (Kiss-Laszlo et al., 1998). These snoRNAs direct methylation through base-pairing the target RNA with a 10-21 nt region of complementarity located immediately upstream of the box D (or D') region of the snoRNA (Cavaille and Bachellerie, 1998). The nucleotide targeted for methylation is located within the base-paired region 5 bp upstream of the D (or D' box) of the snoRNA. Nm formation involves a methytransfer reaction between S-adenosyl methionine and the target RNA. Box C/D snoRNAs are complexed with at least three proteins to form a mature C/D snoRNP. C/D snoRNA guided 2'-*0*-methylation of rRNA is performed by yeast Nop1p (human fibrillarin) methytransferase (Schimmang et al., 1989). Other associated proteins in yeast (and humans) include Nop56p (hNop56p), Nop58p (hNop58p) and Snu13p (15.5 kDa) (Gautier et al., 1997; Lafontaine and Tollervey, 1999; Lafontaine and Tollervey, 2000).

It is important to note that nucleotide modification is not limited to rRNA. Other small stable RNAs such as splicing snRNAs (small nuclear RNAs) and tRNAs are also modified. U2 snRNA contains a Ψ residue highly conserved among eukaryotes (Zhao and Yu, 2004), that greatly facilitates splicing (Valadkhan and Manley, 2003) by establishing a favorable branch site conformation. Most knowledge obtained about modified nucleotides, however, has originated from the extensive studies on tRNA modification. Posttranscriptional modification of tRNA residues occurs

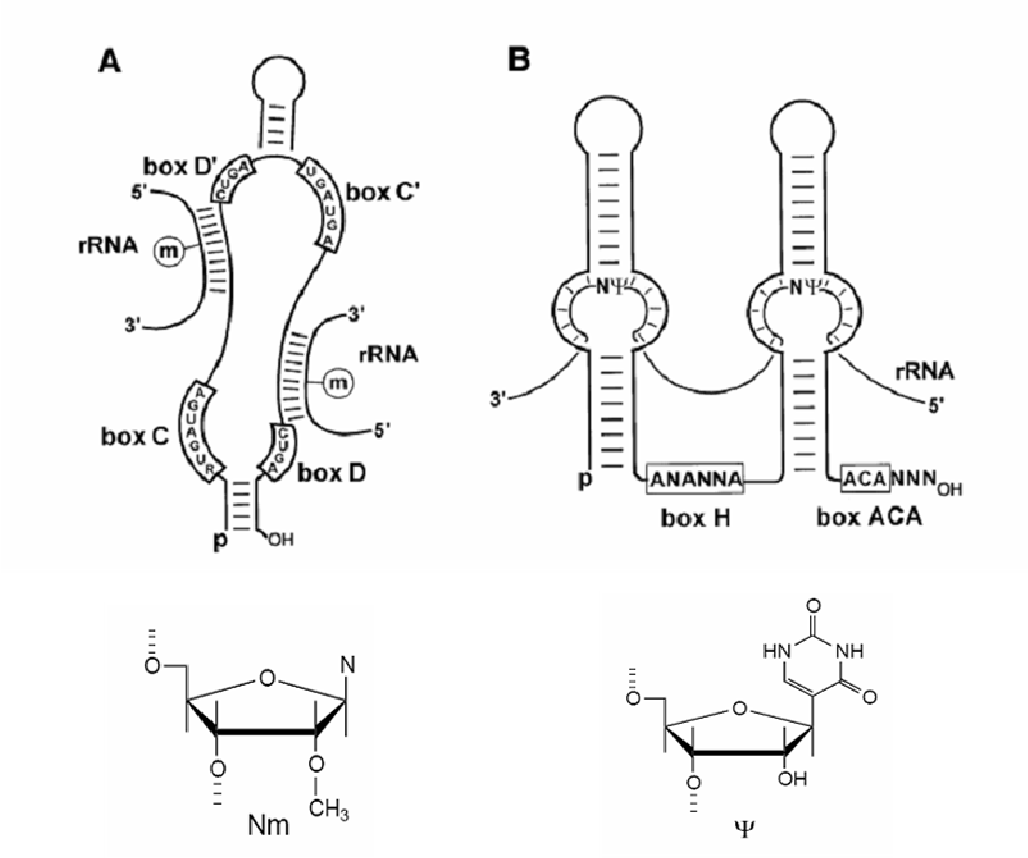

Figure 1.2

H/ACA and C/D box snoRNAs

Models of snoRNA structures their interactions with the pre-rRNA they modify. Each modified nucleotide is depicted below its respective model. **(A)** Box C/D snoRNA guiding 2'-O-ribose methylation. **(B)** Box H/ACA snoRNA guiding pseudouridylation. Figure adapted from Kiss, 2001.

throughout the molecule on the sugar or the base. These modifications in the core of the molecule function to facilitate proper folding and increase stability either through direct interaction or as a mediator for magnesium ion binding (Kowalak et al., 1994; Agris, 1996; Durant et al., 2005). Modifications in the anti-codon loop of the tRNA can contribute to the specificity and stability of the codon:anti-codon interactions between the tRNA and mRNA within the ribosome (Sundaram et al., 2000). tRNA modification has also been shown to contribute to its own nuclear export (Kutay et al., 1998).

Translation

Overview

Ribosomes, along with the rest of the translation machinery, have evolved to promote efficient and accurate translation, a delicate balance between speed and fidelity. Translation can be divided into three stages: initiation, elongation and termination. During initiation, ribosomes are loaded onto the mRNA, elongation factors are added and exchanged while the start codon is located and outfitted with a Met-$tRNA_i^{Met}$ (methionyl initiator transfer RNA) in the ribosomal peptidyl (P) site. Elongation involves docking of aminoacyl-tRNAs (aa-tRNA) into the acceptor (A) site of the ribosome. This is followed by decoding, whereby the cognate aa-tRNA is recognized and accommodated into the A-site. The third step is peptidyl transfer, the ribosome catalyzed formation of a peptide bond between the amino acids located at the 3' ends of the A- and P- site tRNAs. Translocation then occurs, allowing the

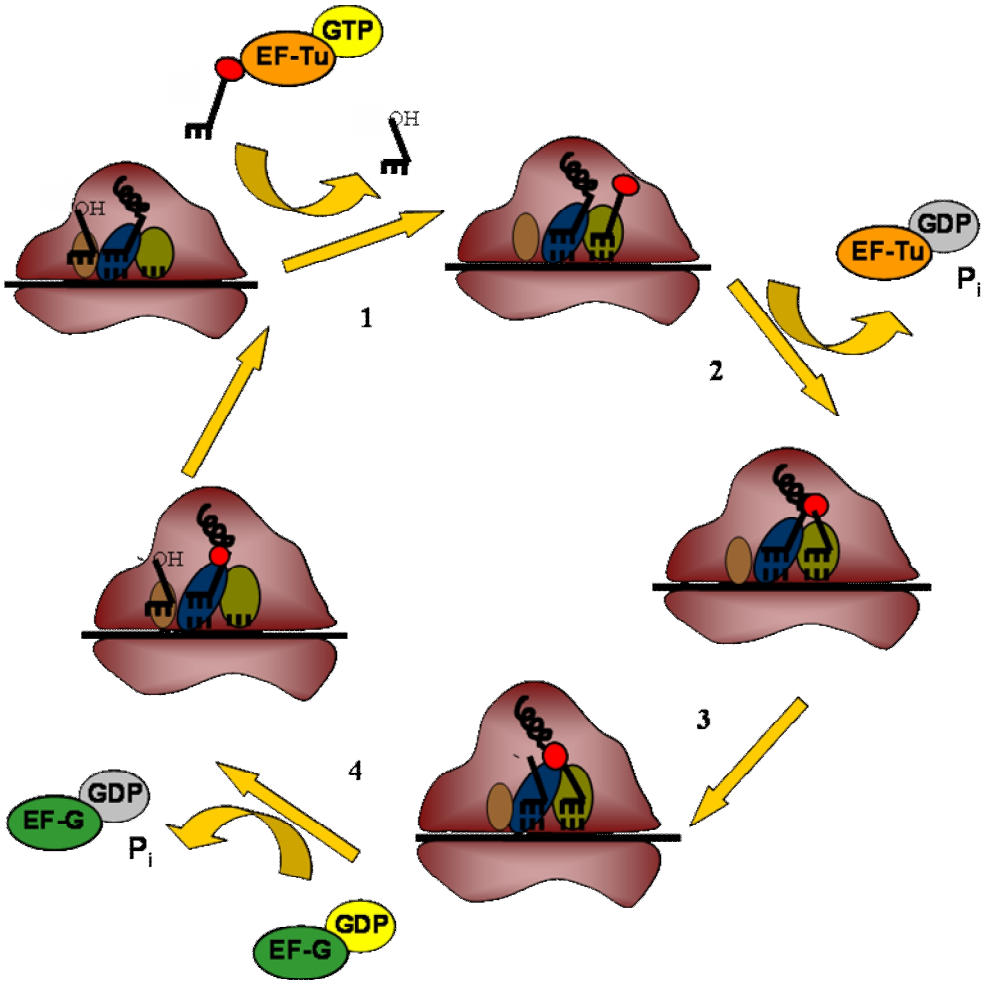

Figure 1.3

Translation elongation cycle

(1) aa-tRNA delivered to the ribosome in a ternary complex with EF-Tu:GTP. (2) GTP hydrolysis, aa-tRNA accommodation and EF-Tu:GDP dissociation. (3) Petidyl transfer (4) Translocation. Large subunit A-site (blue), P-site (green) and E-site (brown). Amino acid on the incoming aa-tRNA (red)

ribosome to encounter the next codon in its A- site so the elongation cycle can begin again (Figure 1.3). This iterative process continues until the ribosome encounters a stop codon in its A-site, which stimulates peptide release resulting in translation termination.

Initiation

In eukaryotes[4], translation initiation begins with formation of the eIF2/GTP/Met-$tRNA_i$ ternary complex (Figure 1.4). This complex binds ribosomal 40S SSU (small subunit) along with eIF1, eIF1A, eIF5 and eIF3 to create the 43S pre-initiation complex. The eIF4F complex recruits the 43S pre-initiation complex to the mRNA. The components of the eIF4F complex interact with the 7-methylguanosine (m^7G) cap located at the 5'end of the mRNA molecule and with poly A binding protein (PABP) bound to the 3' end poly A tail thereby circularizing the message. The initiation complex scans the message in a 5' to 3' direction in search of the correct initiation (AUG) codon, which is located in a favorable sequence context. Initiation codon recognition is thought to involve base-pair formation with the initiator tRNA resulting in GTP hydrolysis by eIF2. This triggers release of eIF2-GDP and the other initiation factors which facilitates ribosomal 60S LSU binding to the 40S/Met-$tRNA_i$/mRNA complex. The end result of translation initiation yields 80S ribosomes bound to the mRNA with the Met-$tRNA_i$ base-paired to the AUG codon positioned in the P-site of the ribosome.

[4] Translation initiation differs between prokaryotes and eukaryotes in execution but not outcome. Differences in prokaryotes include absence of mRNA 5'cap and start codon recognition involving a Shine-delgarno sequence rather than ribosome scanning. For review see (Kozak, 1999). Eukaryotic initiation will be discussed here.

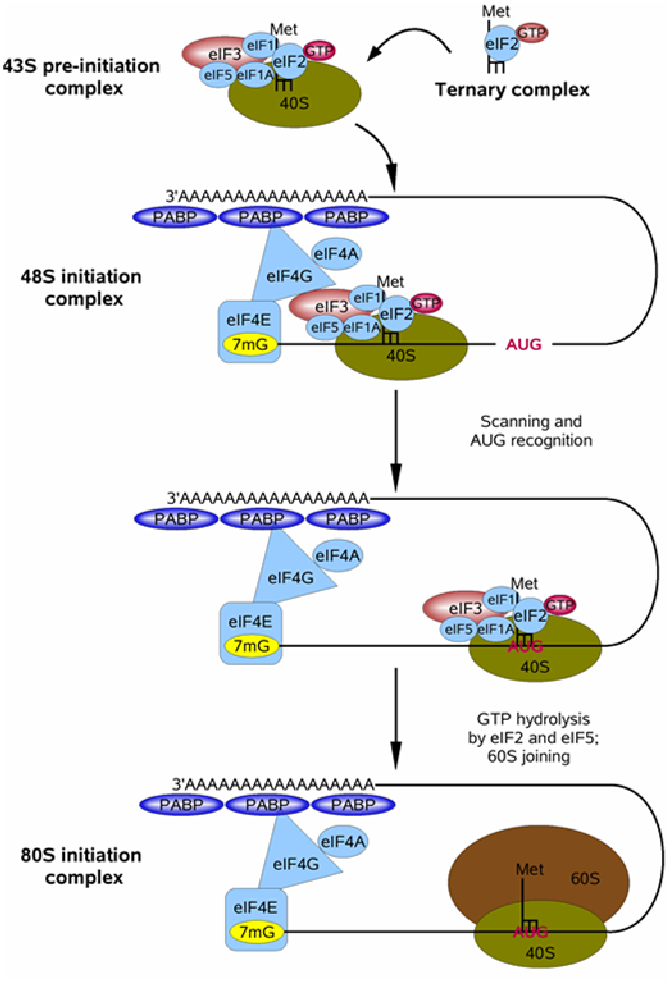

Figure 1.4

Eukaryotic cap-dependent translation initiation

Cap-Independent Initiation

Translation can also be initiated through 5' cap-independent mechanisms. Such initiation is mediated by ribosomes binding to highly structured regions in the 5' NTR (non-translated regions) of RNAs called IRESs (internal ribosome entry site). IRES elements are present in viral mRNAs and vary in size, structure and in the trans-acting factors required for efficient translation (Pisarev et al., 2005). Some picornavirus IRESs, like encephalomycarditis virus (EMCV), requires initiation factors eIFs 2, 3 and 4 for 40S subunit recruitment. In contrast, the hepatitis C virus (HCV) IRES can recruit 40S ribosomal subunits near the initiation codon without any initiation factors, but requires the initiation ternary complex for correct positioning (Pestova et al., 1998). Remarkably, the cricket paralysis virus (CrPV) IRES mediates initiation in a factor independent manner. The IRES can correctly assemble and position 80S ribosomes and to begin translation in the absence of any eIFs or the ternary complex (Wilson et al., 2000).

Mammalian cellular mRNAs have been identified which also contain naturally occurring IRES elements (Hellen and Sarnow, 2001). The structures, trans-acting elements, and functional mechanisms for cellular mRNA IRESs are largely unknown. While viral IRES elements often contain one highly ordered structural element which is essential for IRES activity, some cellular mRNA IRES elements identified so far contain several noncontiguous elements that each have individual IRES activity. IRES containing mRNAs encode growth factors, transcription and translation factors, and oncogenes, among other proteins. Interestingly, cellular mRNAs containing

IRES elements have been identified that are cell cycle and apoptosis regulated (Pyronnet et al., 2000; Stoneley et al., 2000; Hellen and Sarnow, 2001).

Elongation

Unlike initiation, translation elongation is highly conserved between prokaryotes and eukaryotes[5]. Translation elongation consists of three steps: aa-tRNA accommodation, peptidyl transfer, and translocation. These steps can be represented as tRNA passage through the ribosome (hybrid-states model; Figure 1.5) (Moazed and Noller, 1989; Noller et al., 2002) and subdivided into 7 distinct kinetic stages (Figure 1.6). Elongation begins with delivery of an aa-tRNA to a waiting ribosome, which contains a peptidyl-tRNA in the P-site and an empty A-site. The aa-tRNA is delivered in a ternary complex consisting of elongation factor Tu (EF-Tu) bound to GTP[6]. This initial binding is rapid and the aa-tRNA is positioned in the A/T hybrid state on the ribosome such that the aa-tRNA anti-codon end is located in the decoding center of the ribosome while its 3' acceptor end has not yet been accommodated into the ribosome and does not interact with it (Figures 1.5 and 1.7). Subsequently, codon:anti-codon base-pairing occurs stabilizing interactions between the mRNA and aa-tRNA (Pape et al., 1999). Correct codon:anti-codon interaction is monitored through a complex series of interactions and conformational changes involving the 16S RNA, aa-tRNA and the LSU (Gabashvili et al., 1999; Ogle et al., 2001). Correct

[5] Since most kinetic, biochemical and structural experiments were performed in *E. coli*, its nomenclature is used unless otherwise noted.
[6] eEF-1:GTP in eukaryotes

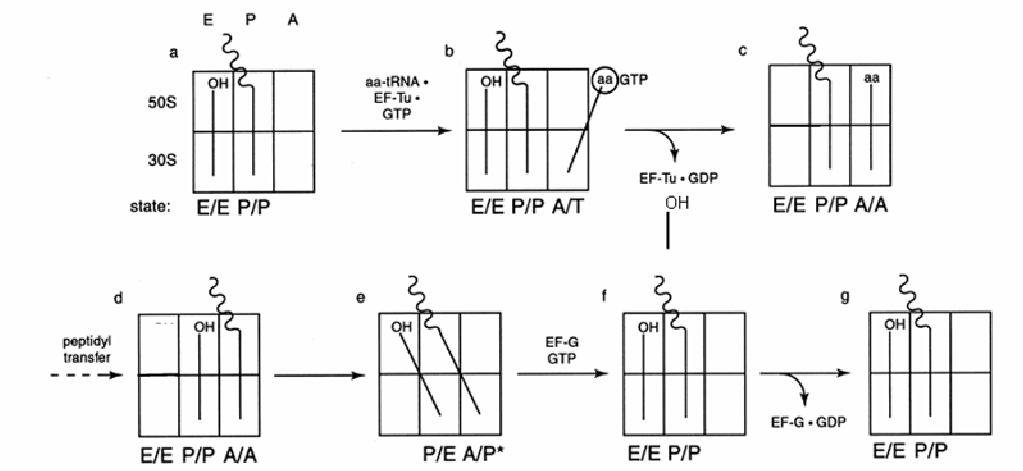

Figure 1.5

Schematic representation of the hybrid-states translocation cycle

The ribosome is represented as the rectangle, with the top section as the large subunit and the bottom section the small subunit. Ribosomal E, P and A sites are represented by the vertically delineated segments. Figure adapted from Noller et al., 2002.

interactions and conformational changes are transduced to EF-Tu promoting rapid GTP hydrolysis (Rodnina et al., 1995; Gromadski and Rodnina, 2004). EF-Tu:GDP adopts a different conformation which is unfavorable to ribosome binding and quickly dissociates (Nissen et al., 1995; Pape et al., 1998). EF-Tu release allows the 3'-CCA end of the aa-tRNA to enter the LSU in the A/A site thereby finalizing accommodation (Figures 1.5 and 1.7).

aa-tRNA discrimination takes place at two distinct stages of the translation elongation cycle described above (Figure 1.6) (Ogle and Ramakrishnan, 2005). Initial selection takes place prior to GTP hydrolysis. During this step, cognate and near cognate codon:anti-codon interactions are stabilized by the codon recognition step and proceed to GTP hydrolysis, whereas non-cognate tRNAs, having no significant codon:anti-codon interactions, promote a severely decreased rate of GTPase activation (providing a ~650 fold selection for cognate vs. non-cognate aa-tRNA (Gromadski and Rodnina, 2004)) and dissociate from the ribosome (Yarus et al., 2003). Thus, correct codon:anti-codon interactions serve to slow dissociation of the cognate tRNA from the ribosome and increase the rate of GTP activation (Rodnina et al., 2005). The majority of non-cognate tRNAs are rejected during the initial selection step. The proofreading step takes place after GTPase hydrolysis but prior to accommodation. Most of the discrimination between cognate and near cognate tRNAs occurs at this step. Any near-cognate tRNAs that have made it through initial aa-tRNA selection can be rejected and dissociate at this step

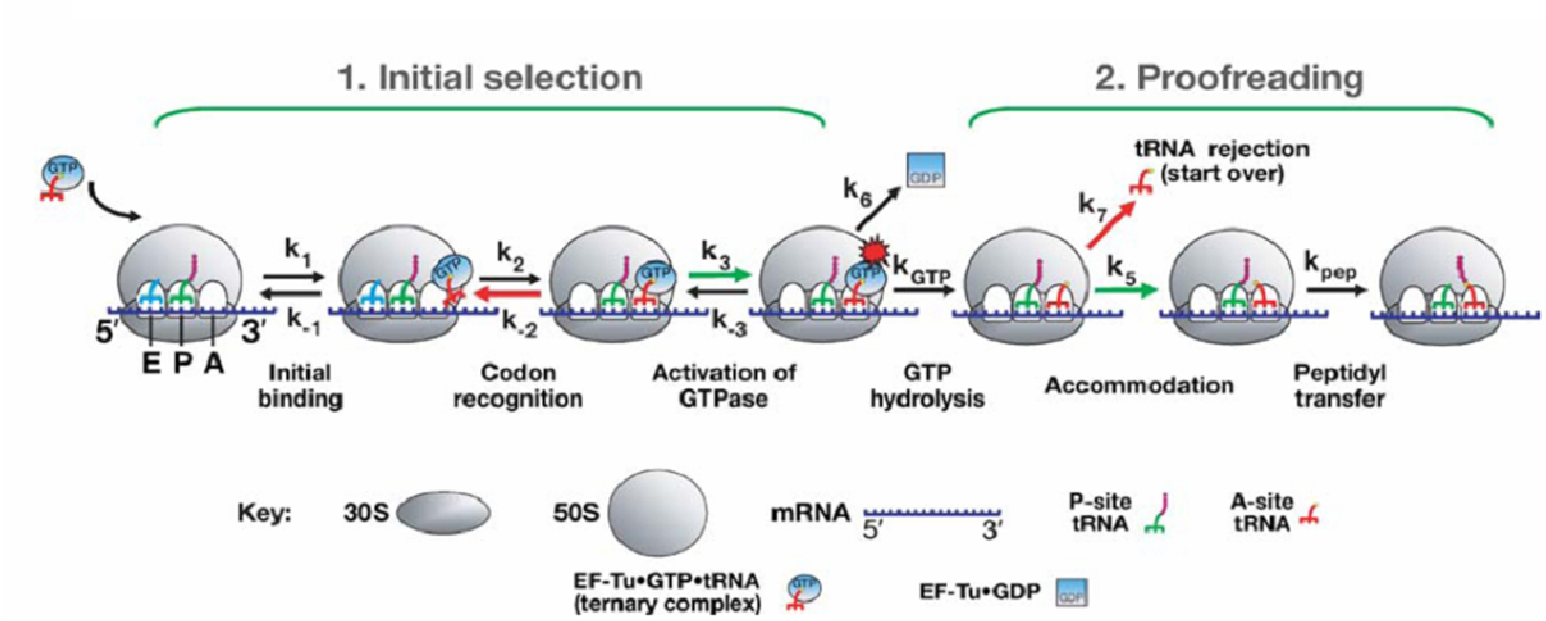

Figure 1.6

Kinetic scheme of aa-tRNA selection and the two stages of proofreading.

Figure adapted from Ogle and Ramakrishnan, 2005.

(Pape et al., 1999; Rodnina et al., 2005). Cognate tRNAs bind more stably and have increased rates of accommodation while near cognate tRNAs dissociate more readily and have much reduced rates of accommodation.

A computer simulation has been performed which shows the path of the aa-tRNA as it accommodates into the ribosomal LSU (Figure 1.7a) (Sanbonmatsu et al., 2005). The simulation shows the aa-tRNA 3' end slips along helix 89 (h89) and h90 and then encounters two "gates" which cause the aa-tRNA to pause as it accommodates into the ribosome (Figure 1.7b). The first gate consists of two nucleotides: U2860 of h89 (*E.coli* U2492) and h92 A-loop residue C2924 (*E. coli* C2556). The second gate, which immediately follows the first, is formed by h90 nucleotide U2941 (*E. coli* C2573). Therefore, altering the local conformation of the ribosome or the incoming aa-tRNA could result in changes in accommodation and suggest a means for detecting near- and non- cognate aa-tRNAs in the accommodation proofreading step. It should be noted that helices of the LSU rRNA involved in the accommodation of the aa-tRNA 3'-CCA end through the ribosome (helices 89, 90 and 92) contain several modified nucleotides.

Peptidyl transfer occurs after accommodation and involves the transfer of the growing peptide chain situated on the 3' end of the peptidyl-tRNA onto the amino acid located on the 3'end of the aa-tRNA. This reaction is extremely fast and is mediated only by the 23S rRNA[7] as no cofactors, ribosomal proteins or metal ions come into contact with the site of peptidyl transfer

[7] 25S in *S. cerevisiae*.

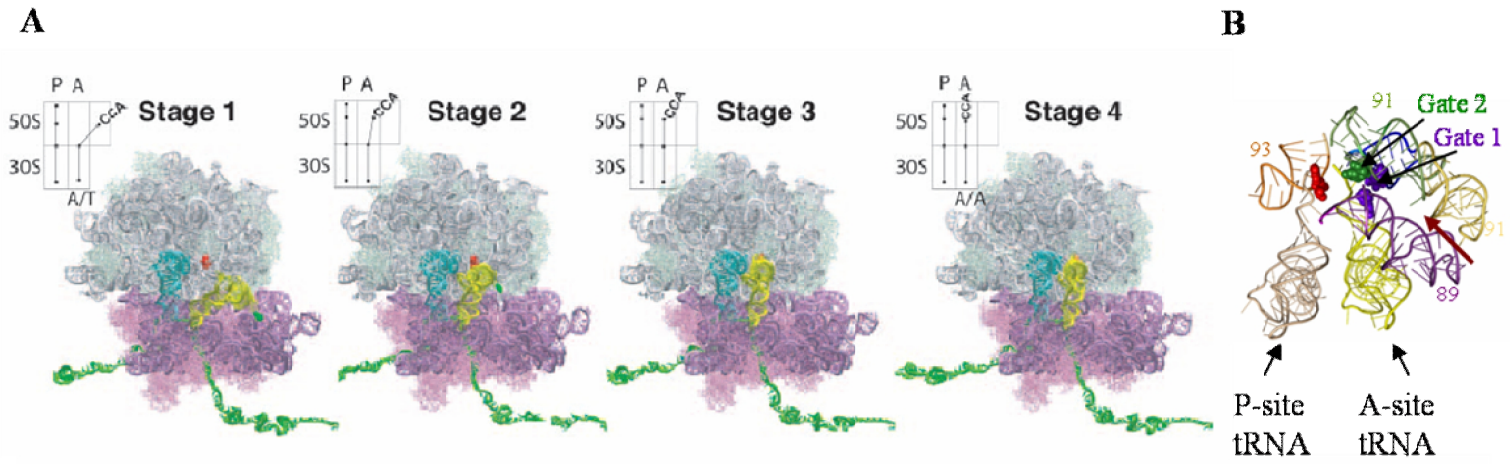

Figure 1.7

Amino-acyl tRNA Accommodation into the A-site

(A) Computer simulation of aa-tRNA accommodation. Large subunit (light blue), small subunit (purple), mRNA (green), aa-tRNA (yellow), peptidyl-tRNA (dark blue), 23S A loop residue G2553 (yeast Gm2921) (red). Figure adapted from Sanbonmatsu et al., 2005. **(B)** Depiction of the three "gate" residues which monitor the path of aa-tRNA into the A-site. Residues of the first gate, U2860 and C2924, are shown in indigo. The second gate residue, C2573, is colored green. Helix 89 (violet); h90 (olive); h91 (gold); h92 (blue); h93 (orange); A2819 (red) The A-site tRNA is colored yellow in both panels. *S. cerevisiae* numbering used. Red arrow indicates the path of the 3'end of the aa-tRNA as it accommodates into the A-site.

(Nissen et al., 2000; Steitz and Moore, 2003). Despite many rapid advances in the biochemical and crystallographic studies of peptidyl transfer, the exact nature of the reaction is unknown. A few models have been suggested including acid-base catalysis (Muth et al., 2000), substrate assisted (Weinger et al., 2004), and an induced fit mechanism (Schmeing et al., 2005b). The induced fit mechanism postulates that, upon accommodation, conformational changes in the peptidyl transferase center (PTC) in the ribosomal LSU serve to position the peptidyl-tRNA and its peptide chain in such a way as to facilitate spontaneous nucleophilic attack of the carbonyl bond between the peptidyl-tRNA and its peptide chain by the amino group of the aa-tRNA amino acid. After peptidyl transfer takes place, it is proposed that the P- and A-site tRNAs adopt the P/E and A/P hybrid states in the ribosome respectively (Figure 1.5). The now empty 3'-end of the P-site tRNA moves into the E site of the ribosome while its anti-codon end is still in the P-site. Simultaneously, the 3'-end of the A-site tRNA, which now carries the growing peptide chain, is located in the P-site while its anti-codon end still resides in the A-site. It should be noted that while some evidence for these intermediates has been found, the true state of the tRNA within the ribosome is understandably elusive and thus remains uncertain (Blanchard et al., 2004; Sharma et al., 2004).

Translocation involves the movement of the tRNA:mRNA complex relative to the ribosome by three nucleotides causing the deacylated P/E site tRNA to move entirely into the E-site, the A/P tRNA carrying the peptide chain to move entirely into the P-site (P/P), which leaves the A-site devoid of tRNA but harboring the codon

previously 3' adjacent on the mRNA (Figure 1.5). EF-G:GTP[8] binds the ribosome and mediates GTP hydrolysis which is required for efficient translocation. The precise mechanism of translocation is unknown. Experiments show that both the large and small ribosomal subunits undergo conformational changes during translocation (Wilson and Noller, 1998; Gabashvili et al., 1999; Agrawal et al., 1999). Cryo-EM studies have revealed ratchet-like motion of the SSU relative to the LSU during translocation (Frank and Agrawal, 2000; Spahn et al., 2004).

Termination

Translation elongation continues codon after codon until a termination codon is encountered in the ribosomal A-site. The three natural nonsense or stop codons are UAA, UAG, and UGA. In eukaryotes[9], all stop codons are decoded by the class 1 eukaryotic release factor eRF1 with help from the class 2 release factor eRF3 and GTP. This triggers the release of the polypeptide chain through the hydrolysis of the ester bond that connects it to the peptidyl-tRNA. It is then thought that eRF3 mediated GTP hydrolysis occurs releasing the termination factors from the ribosome (Figure 1.8).

The mechanism of elongation termination is not known. X-ray crystallographic studies revealed similarities in shape between class 1 release factors and the ternary complex suggests termination may begin in a similar way to accommodation, however, the mechanism of stop codon recognition is not yet completely understood

[8] eEF-2:GTP in eukaryotes
[9] Translation termination differs between prokaryotes and eukaryotes. Eukaryotic termination will be discussed here.

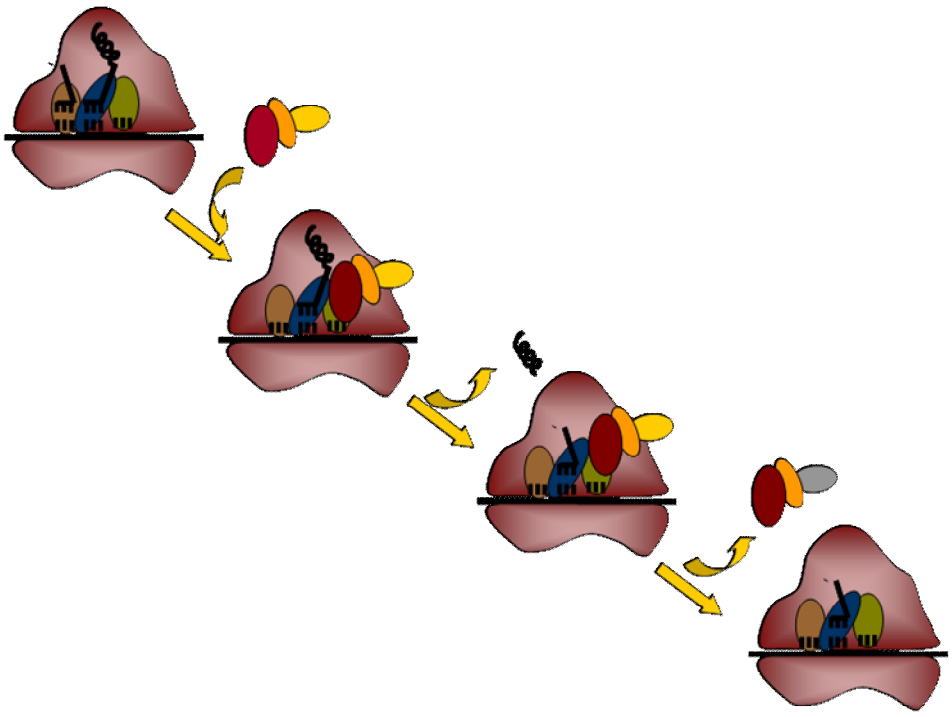

Figure 1.8

Schematic of general translation termination

Complex of eRF1 (red), aRF3 (orange) and GTP (yellow) binds to the A-site of the ribosome (green) when it is occupied by a stop codon. The complex stimulates hydrolysis of the peptide chain from peptidyl-tRNA in the P-site (blue). GTP hydrolysis is known to be required converting GTP to GDP (grey) although the exact mechanism is unknown.

(Ito et al., 1996; Song et al., 2000; Chavatte et al., 2002). In sharp contrast to translation elongation, ester bond hydrolysis requires entry of a water molecule into the PTC of the ribosome. It has been proposed that eRF1 serves to coordinate the water molecule for ester bond hydrolysis (Song et al., 2000) or that conformational changes upon eRF1 binding would both allow water entry into the PTC and make the ester bond susceptible to nucleophilic attack (Frolova et al., 1999; Schmeing et al., 2005a).

Translational Recoding

Translating ribosomes normally remain in a single reading frame for the duration of polypeptide chain elongation. Occasionally, however, ribosomes are directed by *cis*-acting mRNA signals to abandon the standard decoding rules of translation. This "recoding" can result from phenomena such as bypassing (hopping over long stretches of mRNA), programmed stop codon read-through/redefinition, and programmed ribosomal frameshifting (Baranov et al., 2002; Namy et al., 2004). These recoding events, or "programmed mistakes", can be exploited as powerful tools for elucidating mechanisms influencing translational fidelity.

Programmed Ribosomal Frameshifting

Programmed ribosomal frameshift signals on an mRNA cause translating ribosomes to shift reading frame, usually by a single nucleotide in the 5' (-1) or 3' (+1) direction, and continue elongation in the new frame (Brierley, 1995; Dinman, 1995; Gesteland and Atkins, 1996; Farabaugh, 2000; Baranov et al., 2002; Harger et

al., 2002). This is termed Programmed Ribosomal Frameshifting (PRF) because the frameshift is non-random; it is directed by specific signals contained in the mRNA message. This type of recoding occurs during elongation. PRF is utilized in a wide variety of organisms and can be used to regulate gene expression as well as a range of cellular processes.

Programmed -1 Ribosomal Frameshifting

Programmed –1 ribosomal frameshifting is utilized by animal, plant, and fungal viruses, bacteriophages and some cellular genes. This list includes mammalian retroviruses, coronaviruses, astroviruses, arteriviruses, and toroviruses; fungal totiviruses; plant viruses such as tetraviruses and tombusviruses; T7 (Condron et al., 1991) and λ (Hayes and Bull, 1999) (Levin et al., 1993) bacteriophages; bacterial insertion sequences (Chandler and Fayet, 1993); and *dnaX* in *E.coli* (Blinkowa and Walker, 1990). Programmed –1 ribosomal frameshifting (-1 PRF), as it applies to eukaryotic systems, will be the form of recoding focused on here. –1 PRF was first discovered in Rous sarcoma virus, where the frameshift allows for the production of the *gag-pol* fusion protein (Jacks and Varmus, 1985). The majority of confirmed –1 frameshift signals are found in RNA viruses. A consensus has been defined for the basic components of all known eukaryotic viral –1 frameshift signals ranging from the relatively simple yeast L-A virus to a more complex virus such as HIV-1.

Although the molecular mechanism of –1 PRF is not completely understood, the cis-acting signal components for eukaryotic viral systems have been well

characterized. The frameshift signal is always found to contain a slippery-site, a spacer region and a downstream stimulator such as mRNA secondary structure, most commonly a pseudoknot. The 'simultaneous slippage model' (Jacks and Varmus, 1985; Jacks et al., 1988) was proposed to explain how this signal directed frameshifting occurs. The mRNA pseudoknot directs the translating ribosome to pause (Tu et al., 1992; Somogyi et al., 1993), and the spacer region ensures that the pause occurs with the ribosome bound amino-acyl and peptidyl tRNAs paired at the slippery site (Figure 1.9). The slippery site is a heptameric sequence described as X XXY YYZ where X's are any three identical nucleotides, Y's are all A or all U, and Z is not G. In the zero frame, the XXY and YYZ codons are base paired with their cognate tRNAs in the P- and A-sites respectively. The sequence of the slippery site is such that as the ribosome pauses, the ribosome-bound tRNAs can slip back one nucleotide in the –1 direction and all non-wobble bases can correctly re-pair with the mRNA. Peptidyl transfer occurs locking the new frame into place and the pseudoknot melts out enabling the ribosome to continue elongation in the –1 frame (Harger et al., 2002; Plant et al., 2003).

The yeast L-A virus is a well-studied model system for understanding –1 PRF (Figure 1.10). The L-A viral genome consists of a double stranded RNA (dsRNA) containing two overlapping open reading frames (ORFs) joined by a –1 PRF signal. The first ORF encodes *Gag*, the capsid protein, and the downstream ORF encodes *Pol*, the viral RNA dependant RNA polymerase (RDRP) (Dinman et al., 1991). If no frameshift event takes place, *Gag* protein is produced. If the translating ribosome

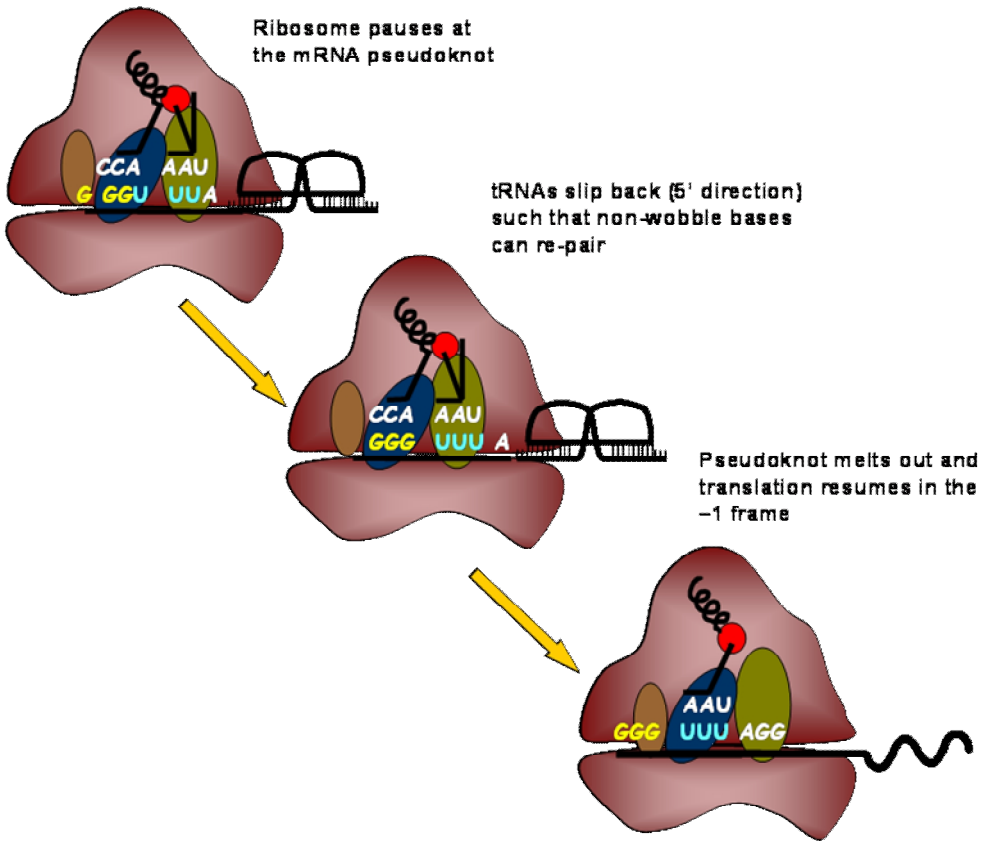

Figure 1.9

Programmed -1 Ribosomal Frameshifting

Schematic describing the mechanism of -1PRF. Slippery site from the yeast L-A virus frameshift signal depicted here. Ribosome depicted as in Figure 1.3.

encounters the frameshift signal and slips back one nucleotide in the 5' direction to continue translating in the –1 frame, a *Gag – Pol* fusion protein is produced. The ratio of *Gag* to *Gag-Pol* proteins is dictated by –1 PRF efficiency. The L-A virus supports a satellite virus named M_1. It encodes no enzymatic or structural proteins of its own and relies completely on L-A for capsid and RDRP proteins. M_1 has a small dsRNA genome that encodes a secreted protein toxin and immunity to that toxin. Cells harboring the L-A and M_1 viruses excrete the toxin killing surrounding M_1 minus yeast cells, thereby conferring a growth advantage and an easily assayable phenotype (Figure 1.10). Increases or decreases in –1 PRF have been shown to disrupt viral particle formation interfering with L-A and M_1 virus propagation (Dinman and Wickner, 1992).

Programmed –1 ribosomal frameshift signals have also been found in cellular genes of higher eukaryotes. The mouse embryonal carcinoma differentiation regulated (*Edr*) gene, a developmentally regulated mammalian gene, utilizes –1 PRF for production of its C-terminal end (Shigemoto et al., 2001; Manktelow et al., 2005). The human paraneoplastic antigen Ma3 gene contains a functional –1 PRF signal first identified through a bioinformatic approach (Wills et al., 2006). The exact function of this gene as well as the role of its –1 PRF frameshift signal is so far unknown, however, Ma3 is expressed in the brain and testis and immunity to Ma3 is associated with serious brain related defects.

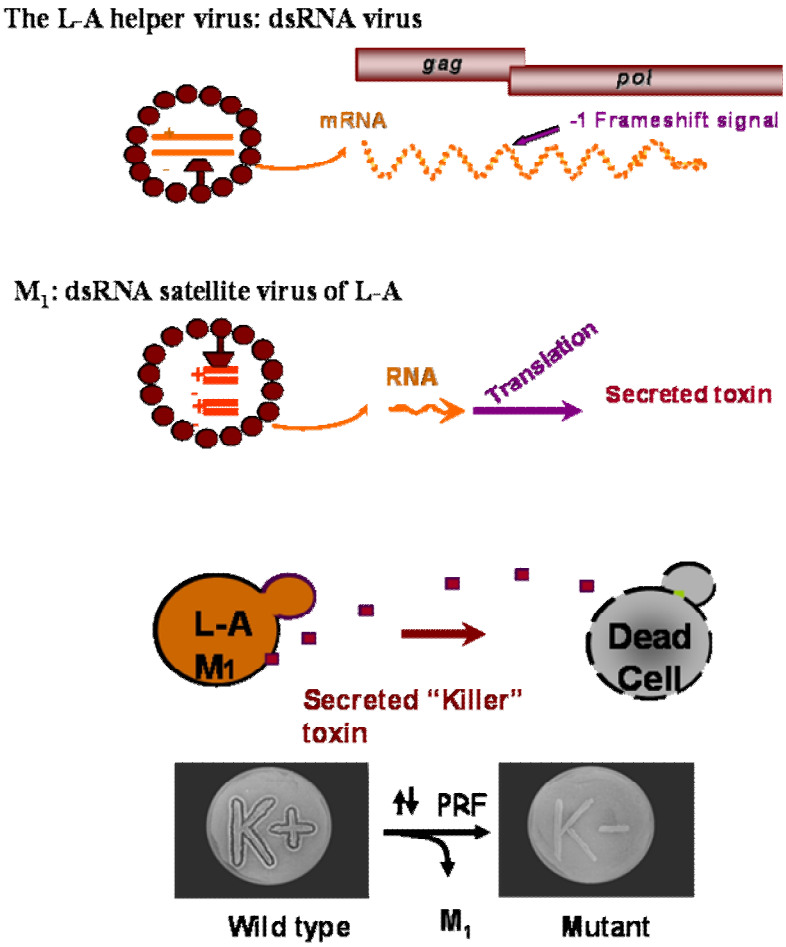

Figure 1.10
The "killer" virus system in yeast

Programmed +1 Ribosomal Frameshifting

Programmed +1 Ribosomal Frameshifting (+1 PRF) results in a translational reading frame shift of one nucleotide in the 3' direction. Although the precise mechanisms differ, +1 PRF signals are composed of a slippery sequence in the mRNA and a stimulator that enhances frameshifting. +1 PRF signals can be found in retrotransposons and in both prokaryotic and eukaryotic genes (Farabaugh, 1996). There is also a high frequency of +1 PRF signals found in ciliates (Aigner et al., 2000; Klobutcher and Farabaugh, 2002).

One of the first examples of programmed +1 frameshifting was identified in *E. coli* and occurs in the *prfB* gene, which encodes the peptide release factor 2 (RF2). *prfB* gene expression is negatively regulated by its +1 PRF signal. The frameshift signal consists of a slippery site sequence of CUU UGA C[10]. The CUU occupies the ribosomal P-site paired to a peptidyl-tRNA and the UGA codon occupies the vacant A-site. If there is sufficient RF2 present in the cell, the stop codon is immediately recognized and termination takes place. If the RF2 abundance is low, the ribosome pauses allowing the peptidyl-tRNA:ribosome complex to shift one nucleotide in the 3' direction thus avoiding the stop codon. Translation continues in the +1 frame and more RF2 is produced. Experiments *in vitro*, show that over expression of RF2 decreases the +1 PRF for the *prfB* gene, and that expression of defective RF2 increased +1 frameshifting to almost 100% *in vivo* (Craigen and Caskey, 1986; Donly et al., 1990).

[10] Incoming frame codon organization indicated by the spaces

The yeast Ty*1* retrotransposon +1 PRF signal has a slippery sequence comprised of CUU AGG C[11] (Figure 1.11). The CUU occupies the ribosomal P-site paired to a peptidyl-tRNA and the AGG codon occupies the vacant A-site. The AGG codon is decoded by the low abundance $tRNA^{Arg}$. The elongating ribosome pauses, waiting for the rare $tRNA^{Arg}$. This pause increases the chance for the petidyl-tRNA occupied ribosome to slip forward one nucleotide such that the GGC codon now occupies the vacant A-site. This GGC codon corresponds to an abundant $tRNA^{Gly}$. Accommodation of the $tRNA^{Gly}$ occurs and translation elongation continues in the new +1 reading frame. Five fold over expression of hungry codon $tRNA^{Arg}$ caused a 43-fold decrease in +1 PRF (Belcourt and Farabaugh, 1990). Likewise, deletion of the hungry codon $tRNA^{Arg}$ caused +1 PRF to approach 100% (Kawakami et al., 1993).

All known antizymes require +1 PRF for their gene expression (Ivanov et al., 2000). An example in higher eukaryotes is rat ornithine decarboxylase (ODC) antizyme (Matsufuji et al., 1995). Ornithine decarboxylase converts ornithine to putrescine, and is the rate-limiting step in polyamine biosynthesis (Pegg, 1986). ODC antizyme regulates ODC expression by binding to ODC dimers causing them to dissociate and targeting them for degradation (Hayashi and Murakami, 1995). ODC antizyme gene expression is regulated by a +1 PRF signal whose efficiency is regulated by polyamines (Rom and Kahana, 1994). Full length active ODC antizyme is only produced in the event of a +1 frameshift which is regulated by polyamine concentrations.

[11] Incoming frame codon organization indicated by the spaces

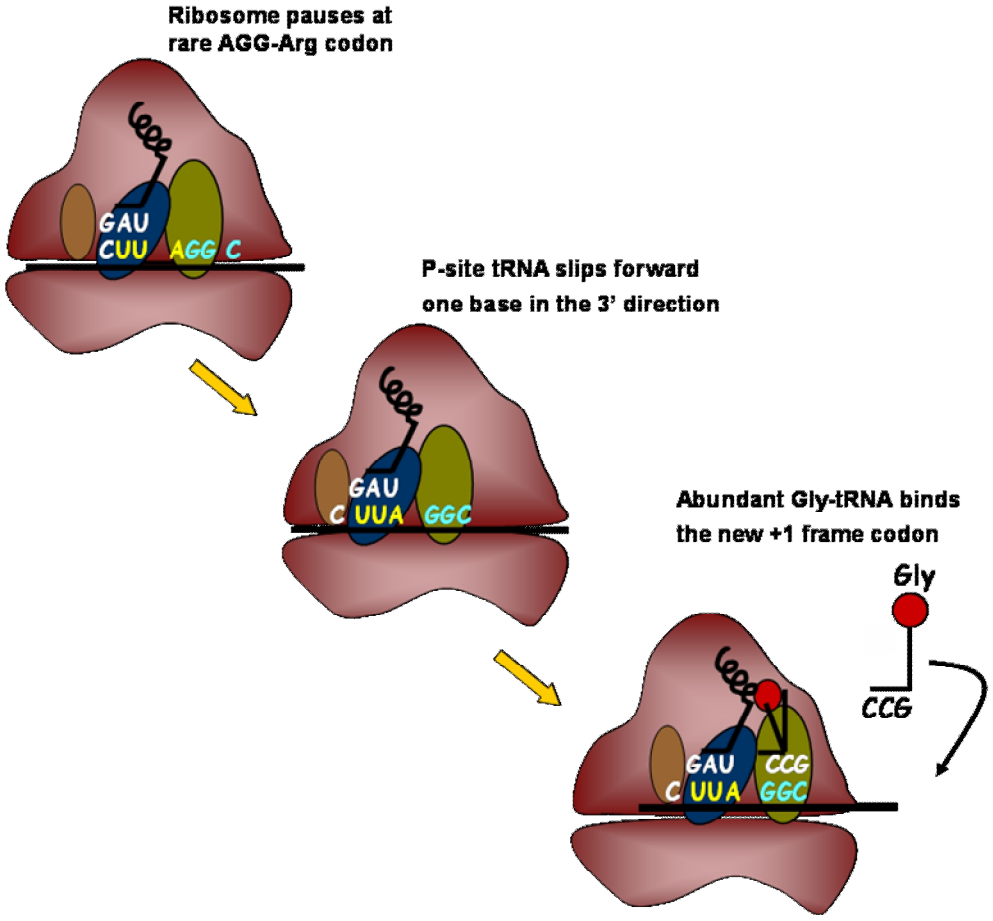

Figure 1.11

Programmed +1 Ribosomal Frameshifting

Schematic describing the mechanism of +1PRF. Slippery site from the yeast Ty*1* retrotransposon frameshift signal depicted here. Ribosome depicted as in Figure 1.3.

Nonsense Suppression

Nonsense suppression, also called stop codon read-through, occurs when a termination codon is decoded either by a natural suppressor tRNA (non-programmed) or by stop codon redefinition (programmed), and subsequent translation continues in the 3' direction. The stop codon can be redefined as a natural amino acid or as an unusual amino acid such as selenocystein or pyrrolysine[12] (Hatfield and Gladyshev, 2002). Different organisms utilize programmed nonsense suppression for the production of certain genes including viruses (Skuzeski et al., 1991) and *Drosophila* (certain developmental genes *oaf*, *kelch* and *hdc*) (Robinson and Cooley, 1997; Steneberg and Samakovlis, 2001).

Non-programmed nonsense suppression (the term 'nonsense suppression' will be used throughout this text for simplicity) allows the formation of multiple polypeptides from one message and is utilized extensively by RNA viruses. Naturally occurring nonsense suppressor tRNAs are found in prokaryotes and eukaryotes including yeast and mammals and serve to decode the stop codons. All known nonspecific nonsense suppressor tRNAs are cellular tRNAs that also decode cognate codons. Consequently, unconventional codon:anti-codon interactions are required for nonsense suppression. Suppressor tRNAs vary. For example, the UAG stop codon can be decoded by $tRNA^{Gln}$ with a CUG anticodon in *S. cerevisiae*, and by $tRNA^{Tyr}$ with an anti-codon of GΨA in *Drosophila*. Viruses that utilize stop codon read-through infect a wide

[12] Selenocysteine incorporation: mechanism conserved for all kingdoms except higher plants and fungi; Pyrrolysine: mechanism seen in bacteria.

range of hosts including plants (tomato bushy stunt virus, TBSV) and animals (murine leukemia virus, MuLV). MuLV utilizes stop codon read-through for its reverse transcriptase production. As the sole means of reverse transcriptase enzyme, nonsense suppression is required for viral propagation. The precise mechanism of nonsense suppression is not fully known. However, the surrounding sequence and structural environment of both the mRNA stop codon and nonsense suppressor tRNAs are crucial for nonsense suppression (Kuchino and Muramatsu, 1996; Beier and Grimm, 2001). It has been suggested that interactions between the mRNA surrounding the stop codon with the ribosomal small subunit rRNA may be involved (Namy et al., 2001).

Defects in stop codon read-through can occur through two distinct mechanisms. The first is a decrease in fidelity resulting in misincorporation events such that a near or non-cognate tRNA can more easily decode a stop codon. The second involves a reduction in the efficiency and accuracy of the termination machinery itself. Mutations that lead to increase rates of stop codon read-through have been identified on both the large and small subunits of the ribosome. On the small subunit rRNA, mutation C1054A in *E. coli* (Pagel et al., 1997), and its yeast counterpart (Chernoff et al., 1996) were shown to cause increased rates of nonsense suppression. In *E. coli*, these effects were shown to be caused by decreased rates of association of the release factor to the ribosome (Arkov et al., 2000) and of subsequent peptidyl-tRNA hydrolysis (Arkov et al., 1998). In the large subunit of the *E. coli* ribosome, the

mutation G1093A in the GTPase center of the ribosome also results in increased nonsense suppression (Arkov et al., 2002).

Summary

The ribosome is a complex machine made of rRNA and proteins that performs the translation process efficiently and accurately. Biochemical and kinetic studies along with new advances in ribosome x-ray crystal structures have allowed researchers to begin the tremendous task of understanding the process of translation and the underlying mechanics of the ribosome. Despite the myriad of recent advances, there are still may questions left unanswered. This dissertation seeks to elucidate the effects of changes in ribosomal RNA on the translational fidelity and structure of ribosomes in *S. cerevisiae*. Chapter 2 explores the effects a histone deacetylase which causes defects in rRNA processing, has on cell growth and translational fidelity. Chapter 3 investigates the affect modified rRNA residues in the peptidyl transferase center of the yeast ribosome have on ribosome structure and the resulting translational fidelity in yeast. Chapter 4 discusses how changes in ribosome structure can lead to changes in fidelity for different stages of the translation cycle, as well as exploring future directions of rRNA modification research.

Chapter 2: Delayed rRNA processing results in significant ribosome biogenesis and functional defects

Introduction

A growing yeast cell devotes a large amount of energy and resources to the production of ribosomes, each of which must be able to translate mRNAs with extremely high accuracy (Warner, 1999). Although a premium has been placed on fidelity of the translational apparatus, programmed recoding events, such as -1 PRF, provide a convenient means to probe the molecular mechanisms underlying ribosome structure/function relationships as well as providing a unique window into the translation elongation cycle. There are a number of parameters that can influence the ability of ribosomes to maintain translational reading frame (Harger et al., 2002). These include: changes in the residence time of ribosomes at a particular PRF signal, and the precise step of the elongation cycle that such a kinetic change might occur; changes in the stabilities of ribosome-bound tRNAs due to alterations in intrinsic ribosomal components such as ribosomal proteins and rRNAs; and defects in the abilities of ribosomes to recognize and correct errors. In combination with the current high-resolution structural understanding of ribosomes, this approach is leading to new insights into ribosome structure/function relationships.

In the course of these studies, alleles of several yeast chromosomal genes have been characterized that specifically increase -1 PRF efficiency. Nine chromosomal *mof* mutants (Maintenance Of Frame) were originally described (Dinman and Wickner, 1992; Dinman and Wickner, 1994; Dinman and Wickner, 1995), and alleles

of other translation-associated genes with Mof$^-$ phenotypes have also been identified (Jones et al., 1995; Balasundaram et al., 1994; Dinman and Kinzy, 1997; Ruiz-Echevarria et al., 1998; Meskauskas and Dinman, 2001). Concomitant loss of the killer virus occurs in strains harboring the *mof1-1, mof2-1, mof4-1, mof5-1, mof6-1* alleles (Dinman and Wickner, 1994). *MOF2* and *MOF4* are allelic to *SUI1* (Cui et al., 1998) and *UPF1* (Cui et al., 1996) respectively. This work focuses on the cloning and characterization of *MOF6*. We show that *mof6-1* is an allele of *RPD3*, the well-characterized histone deacetylase, that is involved in transcriptional activation and silencing (Struhl, 1998; Suka et al., 1998). The defect is dependent on the histone deacetylase activity of the gene product, and can be rescued by the human homolog, HDAC1. Expression of the mutant *rpd3* alleles results in delayed exit from lag-phase growth and premature auxotrophic shift, suggestive of a defect in carbon source mobilization and utilization. The frameshifting defect is most pronounced in early log phase, when demand for newly synthesized ribosomes is greatest. The demonstration that deletion of either the *SIN3* or the *SAP30* genes (Sun and Hampsey, 1999) also promoted frameshifting and virus maintenance defects suggests a heterochromatin-associated defect. Processing of the 35S precursor-rRNA was delayed in isogenic strains harboring mutant *rpd3* alleles and in cells containing gene knockout alleles of *SIN3* and *SAP30*. In actively growing cells, this delay in rRNA processing appears to be the primary event that results in a 60S ribosomal subunit biogenesis defect. The resulting unstable ribosomes have specific aminoacyl-tRNA binding defects that result in decreased peptidyl transferase activities. This in turn results in decreased rates of peptidyl transfer, allowing ribosomes stalled at the -1 PRF signal more time

to slip. We suggest that the heterochromatic-associated Rpd3p/Sin3p/Sap30p complex (Sun and Hampsey, 1999) could be physically involved in helping to coordinate a very early and critical step in the ribosome biogenesis process. Alternatively, abrogation of the function of this complex may result in repression of synthesis of the snoRNAs responsible for modification of bases in the large subunit rRNA that are associated with A-site. Lastly, the observed phenotypic defects may result from an uncharacterized function of Rpd3p involving direct modification of ribosomal or other proteins associated with the ribosome biogenesis machinery.

Materials and Methods

Strains, media, and genetic methods

The *S. cerevisiae* strains used in this study are presented in Table 2. Oligonucleotides were synthesized and purchased from Integrated DNA Technologies (IDT) and are listed in Table 4. DNA sequence analysis was performed by the RWJMS DNA Synthesis and Sequencing Laboratory. *E. coli* strains DH5∀ and MV1190 were used to amplify plasmids, and *E. coli* transformations were performed using the standard calcium chloride method as described previously (Sambrook et al., 1989). Yeast were transformed using the alkali cation method (Ito et al., 1983). YPAD, YPG, SD, synthetic complete medium (H-) and 4.7 MB plates for testing the killer phenotype were used (Wickner and Leibowitz, 1976). Cytoduction of L-A and M_1 from strain JD758 into rho-o strains were as previously described (Dinman and Wickner, 1994). Restriction enzymes were obtained from Promega, MBI Fermentas,

and Roche. T4 DNA ligase and T4 DNA polymerase were obtained from Roche, and precision Taq polymerase was obtained from Qiagen. Radioactive nucleotides were obtained from NEN. Dr. Michael Hampsey generously provided the *rpd3)*, *sin3Δ*, and *sap30Δ* yeast strains, and the transcription derepression defective *ume6* strains were gifts from Dr. Andrew Vershon.

To monitor temperature sensitivity, cells were grown to saturation and equal numbers, spotted on selective media and grown at either the permissive temperature (30°C) or the restrictive temperature (37°C) for 3 days. Lack of, or severely reduced growth was indicative of temperature sensitivity. Similarly, 10-fold serial dilutions of cells were spotted onto medium containing sparsomycin (5μg/ml), anisomycin (5μg/ml), or paromomycin (800μg/ml) to monitor sensitivities to these drugs. To monitor sensitivity to cycloheximide, cells were grown to saturation and 0.1 OD_{595} were spread on selective media. A sterile filter disk containing 100ng of cycloheximide was placed in the center of each plate. Cells were grown for three days and zones of growth inhibition measured.

The killer virus assay was done by replica plating *S. cerevisiae* colonies onto 4.7MB plates (Wickner and Leibowitz, 1976) with a freshly seeded lawn of strain 5x47 (0.5 ml of a suspension at 1 unit of $O.D._{550}$ per ml per plate). After 2-3 days at 20EC, killer activity was observed as a zone of growth inhibition around the killer colonies. dsRNA of L-A and M_1 viruses were prepared as described (Fried and Fink, 1978; Liermann et al., 2000) and separated by electrophoresis through 1.0% non-

denaturing agarose gels and visualized by ethidium bromide staining. RNA blotting was used as previously described (Dinman and Wickner, 1994) to monitor the abundance of L-A and M_1 dsRNAs.

Plasmid and strain constructs, programmed ribosomal frameshift, and transcriptional derepression

A YCp50 based *S. cerevisiae* genomic library was purchased from ATCC (Rose et al., 1987). The genomic clone that complemented the *mof6-1* ts- phenotype was given the name pJD155. Subclones of pJD155 were generated by partial digestion with *EcoR* I, and self ligated using the Roche rapid ligation kit. The pRS series of plasmids have been previously described (Sikorski and Hieter, 1989; Christianson et al., 1992). Full length *RPD3*, *PEX6*, and *AAD14* genes were amplified from genomic DNA from JD932D by polymerase chain reaction using the oligonucleotide primers 1+2 (*rpd3* alleles), 3+4 (*PEX6*), and 5+6 (*AAD14*) (See Table 2B), cloned into pRS314 and pRS316, and were designated pRPD3, pPEX6 and pAAD14. The *mof6-1* allele was amplified from genomic DNA obtained from strain JD469-2C using primers 1+2. PCR reactions using the oligonucleotide primers 1+2 were carried out under the following conditions: Denaturation of dsDNA for 30 seconds at 95^{O}C, annealing at 48^{O}C for 45 seconds, 4 min elongation. PCR products were purified using a Qiagen kit, digested with *Xho* I and *Pst* I, and were ligated into pRS314, or pRS316 (Sikorski and Hieter, 1989). PCR reactions using oligonucleotide primers 3+4 (*PEX6*) or 5+6 (*AAD14*) were carried out under the following conditions: 30 seconds at 95^{O}C denaturation of dsDNA, 45 sec. annealing at 48^{O}C, 6 minutes

elongation time. PCR products were purified using a Qiagen kit, digested with *Kpn* I and *Sal* I (*PEX6*), or *Xho* I and *Pst* I (*AAD14*), and ligated into pRS314. To make pHDAC1, the 1.5 kb *Bam* HI fragment containing the HDAC1 cDNA (a generous gift from Dr. S. L. Schreiber) was excised from pBJ5/HDAC1-F (Taunton et al., 1996) and inserted into *Bam* HI digested pG-1 (Schena and Yamamoto, 1988), thus placing the human gene under control of the constitutive yeast *PGK1* promoter. The synthetic oligonucleotide H151A (Table 2B) was used to create pH151A using standard methods (Kunkel, 1985). Subcloning PEX6 into pRS306 (Sikorski and Hieter, 1989) generated plasmid pPEX6, which was used to integrate the *URA3* into the *PEX6* locus of yeast strain LNY95. pRPD3, pSIN3 and pSAP30 were generous gifts from Dr. M. Hampsey.

Plasmids p-1 and p0, which were used to monitor programmed ribosomal frameshifting, have been described previously (Tumer et al., 1998). Briefly, in these plasmids, transcription is driven from the yeast *PGK1* promoter into an AUG translational start site. The *E. coli lacZ* gene serves as the enzymatic reporter, and transcription termination utilizes the yeast *PGK1* transcriptional terminator. In the p0 plasmids, *lacZ* is in the 0-frame with respect to the translational start site, and measurement of ∃-galactosidase activity generated from cells transformed with these plasmids serve as the 0-frame controls. In the p-1 series, *lacZ* is in the -1 frame with respect to the translational start site, and is 3' of the L-A programmed -1 ribosomal frameshift signal such that ∃-galactosidase can only be produced as a consequence of a programmed -1 ribosomal frameshift. The efficiency of programmed ribosomal

frameshifting is calculated by determining the ratio of ∃-galactosidase activity produced by cells harboring either p-1 divided by the ∃-galactosidase activity produced by cells harboring p0, and multiplying by 100%. All assays were performed in triplicate.

Plasmids pAV73 and pAV138 were used to monitor transcriptional derepression in cells harboring alleles of *RPD3* (Vershon et al., 1992). pAV73 is a *URA3*, *2μ*, *CYC-LacZ* fusion reporter plasmid that is used as a control to establish a baseline. PAV138 contains a URS1 site from the *HOP1* promoter cloned into the *Xho* I site of pAV73. It represses *lacZ* expression in a Ume6p/Sin3p/Rpd3p dependent manner. The pAV73/pAV138 ratios of β-galactosidase activities were used to calculate the ability of the *RPD3* variants to derepress *lacZ* reporter gene transcription as previously described (Vershon et al., 1992). All assays were performed in triplicate.

in vivo [^{35}S]Methionine Incorporation

Labeled methionine incorporation assays were performed as previously described (Carr-Schmid et al., 1999). Briefly, isogenic *rpd3Δ* strains containing wild type pRPD3 or p*mof6-1* were grown in 30 ml of -met -trp medium at 30°C to an O.D.$_{595}$ of 1.0. Unlabeled methionine was added to a concentration of 50 μM and [^{35}S]methionine and [^{35}S]cystine (Expre^{35}S^{35}S Label, NEN Life Science Products) were added to each culture to final specific activities of 1.1 μCi/mL. Samples were harvested at 0 min and at 15 min intervals for 60 min. Incorporation of the [^{35}S]-

labels was monitored by cold trichloroacetic acid precipitation. For each time point, 1.2 mL aliquots were harvested from which 0.2 mL was used to determine the $O.D._{595}$ of the cultures. One ml of ice-cold 20% trichloroacetic acid (TCA) was added to the remaining 1 ml of each aliquot, incubated on ice for 10 min, heated to 70°C for 20 min, and filtered through pre-wet Whatman GF/C filters. Filters were sequentially washed with 10 ml of ice cold 5% TCA and 10 ml of 95% ethanol, dried, and radioactivity of samples was determined by scintillation counter. All time points were taken in triplicate. Experiment performed in duplicate.

Pulse-Chase Labeling of rRNA

Pulse-chase labeling with L-[methyl-^{3}H]methionine was carried out on the isogenic wild-type, *mof6-1*, *rpd3Δ*, *rpd3-H151A*, *sin3Δ*, and *sap30Δ* strains as previously described (Dunbar et al., 1997; Lee and Baserga, 1999). Twenty thousand cpm per sample was resolved on a 1.2% formaldehyde-agarose gel. Labeled RNAs were transferred to a zeta-probe membrane (Bio-Rad), sprayed with EN^{3}HANCE (Dupont), and exposed to x-ray film.

Polysome and 2-dimensional NEPHGE analyses

For polysome analyses, cytoplasmic extracts, prepared as described by (Baim et al., 1985), were fractionated on 7% - 47% sucrose gradients buffered with 50 mM Tris-acetate, pH 7.4, 50 mM NH_4Cl, 12 mM $MgCl_2$, 1 mM DTT. Gradients were centrifuged in an SW41 rotor at 40,000 rpm for 135 min at 4°C, fractionated and analyzed by continuous monitoring of A_{254} (Ohtake and Wickner, 1995b). For

NEPHGE analyses, 40S and 60S ribosomal subunits were separated by ultracentrifugation through a 7% - 27% sucrose gradient in the presence of 500mM EDTA. Purified ribosomal subunits (≈195 μg /sample) were separated by non-equilibrium pH gradient gel electrophoresis (pH gradient of 3.5% -- 11.5% in the first dimension, 12.5% polyacrylamide separating gel in the second dimension) and were visualized by silver staining by the Kendrick Laboratories (Madison WI).

Preparation of tRNAs and of donor and acceptor fragments

Yeast tRNAs were charged with [^{14}C]phenylalanine as previously described (Harris and Pestka, 1973; Meskauskas and Dinman, 2001). Briefly, a 400 μl reaction mix composed of 200 Φg of yeast tRNA (Sigma), 25 mM Tris-HCl pH 7.5, 20 mM $MgCl_2$, 10 mM ATP, 50 nmol phenylalanine (313 mCi/mmol, NEN), 50 μl aminoacyl-tRNA synthetase (Sigma, 9U/ml) was incubated for 25 min at 37EC. After addition of 40 ml of 3M sodium acetate (pH 5.0) the mixture was extracted twice with an equal volume of water-saturated phenol and once with chloroform. It was then precipitated with 2.5 vol of ethanol at –20EC for 1 hour. After centrifugation for 10 min, the pellet was resuspended in 50 ml of 2 mM potassium acetate (pH 5.0). [^{14}C]Phe-tRNA^{Phe} was separated from uncharged tRNAs by anion exchange chromatography (DEAE). Acetylation of charged tRNAs was performed as previously described (Haenni and Chapeville, 1966). Briefly, [^{14}C]Phe-tRNA^{Phe} was resuspended in 200 μl of 0.2 M sodium acetate (pH 5.0) followed by addition of 2.5 μl of acetic anhydride. After 1-hour incubation on ice, another 2.5 μl of acetic

anhydride was added and incubation at 0EC continued for an additional hour. The tRNA was precipitated by addition of 2.5 vol of ethanol. The [^{14}C]Phe-tRNA^{Phe} and acetyl-[^{14}C]Phe-tRNA^{Phe} were subsequently digested with 500U of RNase T1 in 200 µl of 0.3 M sodium acetate (pH 5.0) for 1 hour at 37EC, and the reaction mixtures were purified using DEAE Sephadex as previously described (Pestka et al., 1970). The resulting A-site specific [^{14}C]Phe-CACCA (acceptor) and P-site specific acetyl-[^{14}C]Phe-CACCA (donor) fragments were used as substrates for the tRNA fragment binding assays.

Purification of ribosomes and tRNA binding assays

Salt washed ribosomes were purified as previously described (Merrick, 1979; Meskauskas and Dinman, 2001). Briefly, yeast cells were grown in 0.5 L of YPAD overnight, collected by centrifugation, and washed twice with buffer A (20 mM Tris-HCl pH 7.5, 10 mM $MgCl_2$, 1 mM DTT, 0.1 mM EDTA, 0.25 M sucrose). The cell pellet was suspended in 20 ml of buffer A, 30g of glass beads (0.45mm diameter) were added, and cells were disrupted by vortexing. The yeast lysate was centrifuged twice for 15 min at 15,000 rpm in a Sorvall S34 rotor, and the supernate was pelleted at 100,000 x g for 3 hrs. The pellet was suspended in 6 ml of buffer B (20 mM Tris-HCl pH 7.5, 10 mM $MgCl_2$, 1 mM DTT, 0.1 mM EDTA, 0.25 M sucrose, 0.5 M KCl), and placed on a cushion of 3 ml of buffer C (20 mM Tris-HCl pH 7.5, 10 mM $MgCl_2$, 1 mM DTT, 0.1 mM EDTA, 1 M sucrose, 0.5 M KCl). After centrifugation at 50,000 rpm for 4 hours (SW55 Ti) the pellet was dissolved in 1 ml of buffer A. After a clarifying spin for 1 min in a microfuge, OD_{260} readings were taken (1 A_{260} unit =

19 pmol ribosomes, see (Abraham and Pihl, 1983). Protein content of ribosomes was also estimated using Protein Assay Reagent (Biorad). Ribosomes were suspended in buffer A at concentration 4 pmol/μl, and stored at –70^{o}C.

The whole-tRNA and tRNA fragment binding assays followed a modification of the previously published protocol (Harris and Pestka, 1973; Meskauskas and Dinman, 2001). Briefly, ribosomes (400 pmol) were incubated with 800 pmol of whole tRNAs, donor, or acceptor fragments in 500 μl of a buffer containing 70 mM Tris-acetate pH 7.2, 40 mM magnesium acetate, 0.4 M potassium acetate, and 50 mM NH_4Cl. Ethanol was added to a final concentration of 30%, and 20Φl aliquots were taken during the time course at 24EC. Samples were diluted to 1ml with cold buffer (50 mM Tris-HCl, pH 7.2, 0.4 M KCl, 40mM $MgCl_2$, 30% Ethanol), immediately precipitated onto a Millipore filter, washed with 1 ml of the dilution buffer, and counted in a scintillation counter. The reaction mix without ribosomes was used as control. All assays were performed in triplicate.

Puromycin reaction with tRNA fragments

Puromycin reactions were performed as previously described (Diedrich et al., 2000) with slight modifications. Ribosomes (20 pmol) were incubated with 5 pmol of CACCA[^{14}C]AcPhe (682 d.p.m./pmol) in 300 μl of PR Buffer [25 mM HEPES-KOH pH 7.4, 135 mM NH_4Cl, 250 mM KCl, 20 mM $MgCl_2$, 33% EtOH] at 0^{o} C for 10 min. Puromycin was added to final concentrations of 1 mM, and reaction mixtures were incubated on ice. At indicated time points 50 μl aliquots were taken and

reactions stopped by the addition of equal volumes of a 0.3 M NaOAc solution saturated with $MgSO_4$. Puromycin was extracted with 1 ml of EtOAc and the radioactivity was determined by liquid scintillation counting. In all the studies controls were performed in the absence of puromycin to determine the nonspecific extraction of CACCA[^{14}C]AcPhe. Control values (generally less than 2%) were subtracted from the values obtained in the presence of puromycin.

Results

mof6-1 is an allele of RPD3

The ts$^-$ phenotype of *mof6-1* cells (Dinman and Wickner, 1994) provided a simple selective trait for the cloning of the wild type gene. *mof6-1* cells (JD469-2D) transformed with a YCp50 based genomic library(Rose et al., 1987) were replica plated to selective media and subsequently shifted to non-permissive temperature (37°C). Approximately 1.2 x 10^4 colonies were screened (4.8 genome equivalents) and three that grew at the restrictive temperature were isolated. Positive plasmids were rescued from yeast into *E. coli*, and reintroduction into *mof6-1* cells confirmed their abilities to confer growth at the non-permissive temperature. The inserts in all of the genomic clones were approximately thirteen Kb in length, and sequence analysis mapped them all to the same region of chromosome XIV. One of the genomic clones, pJD155, was used for the subsequent characterization of *MOF6*. Meiotic linkage analysis was used to ascertain whether pJD155 harbored *MOF6* as opposed to a second site suppressor. The *URA3* gene was inserted into the *PEX6*

locus of a *MOF6 ura3* strain (JD 972A) (Figure 2.1a), providing a scorable phenotype for genetic linkage analyses. Diploid cells (JD972A x JD469-2D) were sporulated, and the genotypes of 26 tetrads were determined. All of the tetrads scored as parental ditypes, i.e., 2:2 segregation of Ura^+ ts^+: Ura^- ts^-. The absence of crossover events demonstrates tight genetic linkage between the *MOF6* and the site of *URA3* integration (*PEX6*), confirming that *MOF6* was present in the yeast genomic DNA insert of pJD155.

Partial restriction analysis of pJD155 revealed four *Eco* RI restriction fragments, which were designated A, B, C, D based on their relative mobilities (Figure 2.1a). All subclones generated from partial *Eco* RI digestion which did not contain the B fragment were unable to complement the temperature sensitive phenotype (e.g. pJD155.CAD). Sequence analysis revealed that the B fragment contained *RPD3*. To determine whether *MOF6* is *RPD3*, or whether the B fragment contained other genetic information required for transcription initiation or 3' end formation of flanking genes, clones of the individual open reading frames that were present on the genomic clone were generated by PCR as described in Materials and Methods. *mof6-1* cells harboring either pJD155 or p*RPD3* but not p*PEX6* or p*AAD14* were able to grow at restrictive temperatures (Figure 2.1). Further, an *RPD3* clone generated from *mof6-1* genomic DNA, p*mof6-1*, was not able to compliment the ts^-

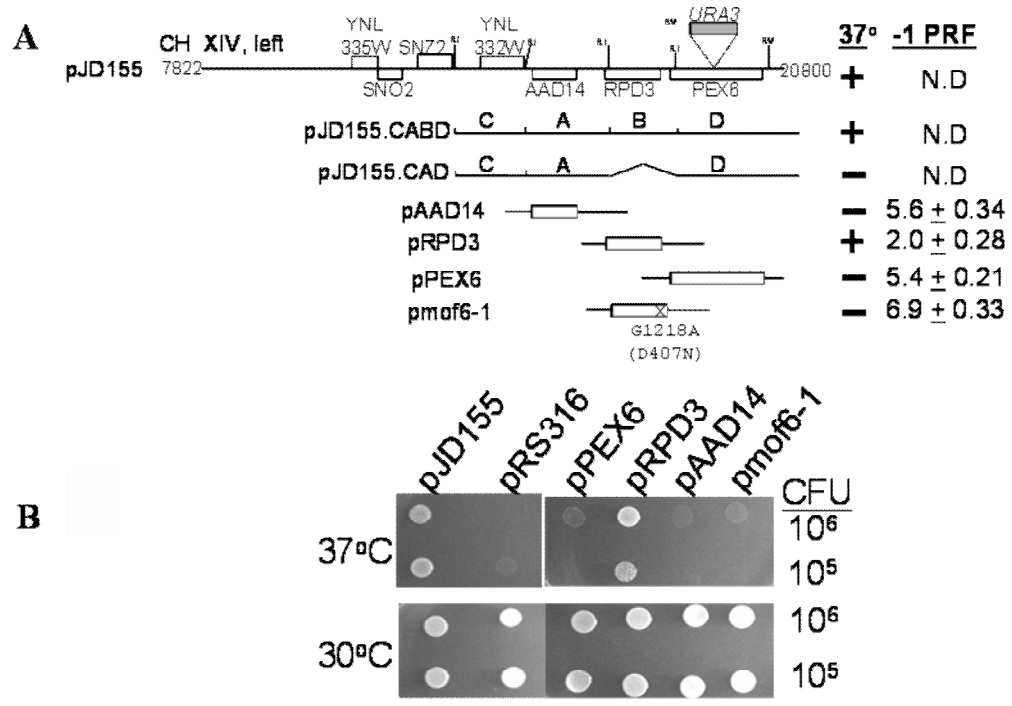

Figure 2.1

***mof6-1* is an allele of *RPD3*.**

(A) Cloning of *MOF6*. At the top is the schematic representation of the ≈ 13 kb insert isolated from the YCp50 plasmid library (pJD155). The subclones of the plasmid pJD155, and of PCR generated clones are indicated (left), and their effects on growth and -1 PRF are shown on the right. The position of the G to A transition position 1218 of the coding sequence in the *mof6-1* allele is shown. (B) Complementation of the temperature sensitive phenotype by *RPD3*. *mof6-1* strains harboring the indicated clones were spotted onto selective media and incubated at the either the permissive (30°C) or the non-permissive temperature (37°C) for four days. Experiments performed by J. Yashenchak.

(Meskauskas et al., 2003)

phenotype, confirming that *RPD3* is both necessary and sufficient to complement the *mof6-1* ts^- phenotype (Figure 2.1). .

Programmed ribosomal frameshifting assays were used to examine whether p*RPD3* could complement the *mof6-1* frameshifting defect. The frameshift test plasmids p-1 and the 0-frame control p0 were introduced into *mof6-1* cells harboring p*RPD3,* p*PEX6,* p*AAD14*, or p*mof6-1* and the affects on -1 PRF were assayed. Whereas introduction of the wild-type gene p*RPD3* restored –1 PRF efficiencies to wild type levels (approximately 2.0%), frameshifting efficiencies remained elevated in cells harboring the other clones (Figure 2.1a). Sequence analysis of *mof6-1* clones isolated from three independent PCR reactions revealed the presence of a single base transition, G1218A, corresponding to change at the amino acid level of aspartatic acid to asparagine (GAT → AAT) at position 407, approximately 30 residues from the C-terminus of the protein (data not shown). A ClustalW analysis (Thompson et al., 1994) reveals that yeast has an acidic residue at this position while the *RPD3* homologs from humans, mice and *Arabdopsis* contain the basic arginine, suggesting that there may be a requirement for a charged residue in this environment. Unfortunately, the lack of structural information pertaining to this region of the protein precludes additional speculation on the functional role of this amino acid residue.

Two additional plasmid-borne *rpd3* alleles were constructed for further studies. Since the *mof6-1* mutation did not occur in the putative deacetylation motif (Kasten et al., 1997), we constructed an allele in this domain changing the histidine at

position 151 to an alanine residue (pH151A), which was previously shown to nearly abrogate Rpd3p deacetylase activity (Kadosh and Struhl, 1998). In addition, since HDAC1 is the most homologous of the at least seven different human histone deacetylases to *RPD3* (see (Taunton et al., 1996; Wang et al., 1999), we used a clone in which transcription of the human HDAC1 cDNA was driven from the yeast *PGK1* promoter (pHDAC1). In order to further characterize *mof6-1* independent of strain-specific background effects, all subsequent experiments were performed with plasmid-borne alleles in a the *rpd3::LEU2* gene disruption strain YMH270. The resulting isogenic strains were subsequently transformed with the p-1 and p0 frameshift test vectors, and -1 PRF efficiencies were determined. Frameshifting efficiencies were significantly elevated in cells harboring pmof6-1, pH151A, and vector alone, while addition of the wild-type gene or the human homolog reduced –1 PRF efficiencies to wild-type levels (Figure 2.2a).

To examine the affects of the different *rpd3* alleles on killer virus maintenance, L-A and M_1 were first introduced by cytoplasmic mixing into the *rpd3)* strain harboring the wild-type *RPD3* gene on a *URA3* based *CEN* plasmid, and stable $Killer^+$ colonies were identified. The resulting strain was then transformed with low copy *TRP1* vectors harboring the different *RPD3* alleles, or with a vector control. In parallel to the frameshifting results, increased – 1 frameshifting efficiencies correlated with loss of the killer phenotype (Figure 2.2b) and with loss of the M_1 satellite virus (Figure 2.2c). Assays for transcriptional repression (Figure 2.3) and cycloheximide hypersensitivity (data not shown) also demonstrated correlations

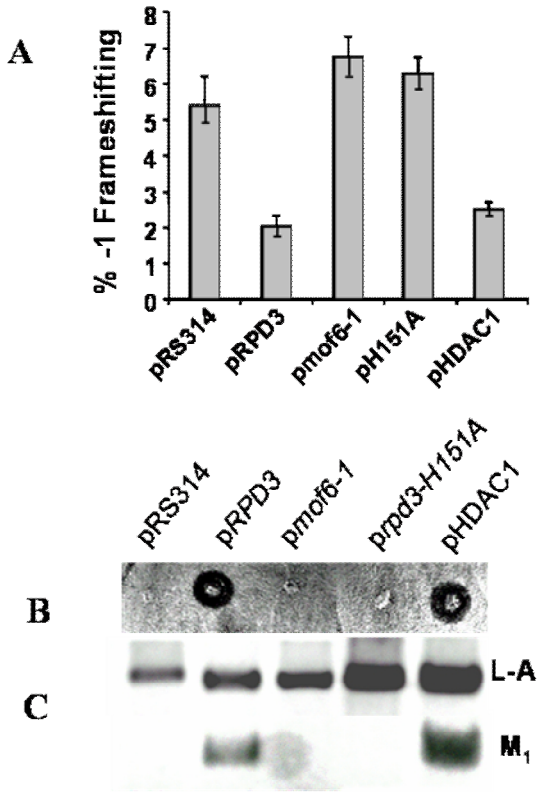

Figure 2.2

***RPD3* allele-specific effects on -1 PRF and killer virus maintenance.**

(A) Frameshift test plasmids p0 or p-1 were introduced into cells and -1PRF efficiencies were determined as described in the materials and methods. All assays were performed in triplicate. Percent error is indicated. **(B and C)** The L-A and M1 viruses were introduced into the isogenic strains harboring the various *RPD3* variants. The killer phenotypes are shown in **(B)**. **(C)** Total nucleic acids were extracted from these cells, separated through a 1.0% non-denaturing agarose gel, denatured in the gel, transferred to a nylon membrane and hybridized with L-A and M1 specific (+) strand probes. Hybridizing bands were visualized by autoradiography. Positions of L-A and M1 are shown. Experiments implemented by J. Yasenchak and E. Carr.

(Meskauskas et al., 2003)

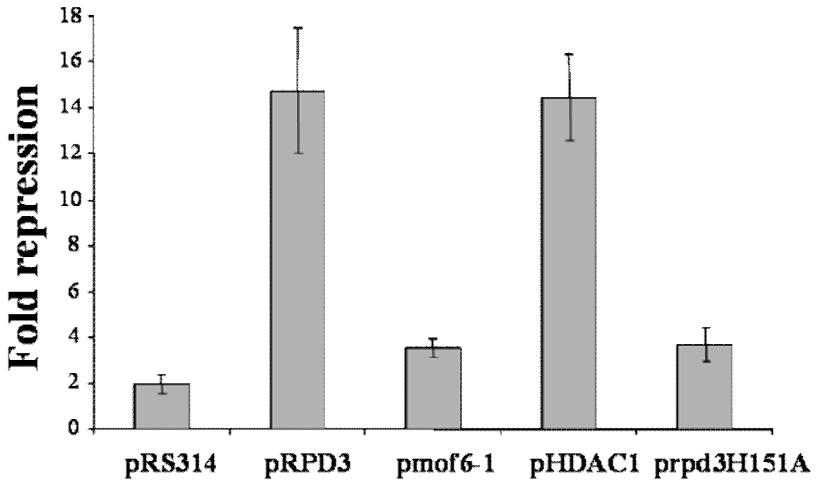

Figure 2.3

Transcriptional repression

The transcriptional derepression phenotype of the *mof6-1* allele is similar to those of the other loss of *RPD3* function alleles. De-repression phenotypes of the *RPD3* variants were determined as described in materials and methods. Experiments performed by J. Yasenchak and E. Carr.

(Meskauskas et al., 2003)

between these classic *rpd3*-associated phenotypes and defects in programmed –1 ribosomal frameshifting. In addition, introduction of pmof6-1into wild-type cells had no effect on –1 frameshifting efficiencies, demonstrating that this does not represent a gain of function allele (data not shown). Taken as a whole, these data define the *mof6-1*, *rpd3-H151A* and *rpd3)* as *mof*-specific alleles of *RPD3*.

Correlation of growth and frameshifting defects in the rpd3 mutants

It was observed that the initial appearance and subsequent growth of colonies of *rpd3Δ* cells transformed with the various plasmid-borne mutant alleles of *rpd3* was delayed relative to those containing the wild-type gene. Measurement of growth rates revealed significant quantitative differences. In logarithmic growth, doubling times of cells harboring either vector alone or the pH151A allele were approximately 1.4-fold longer than wild-type controls. The growth defect was even greater in *mof6-1* cells where doubling times were increased approximately 1.6-fold compared to isogenic wild-type cells. Shifting cells from stationary phase growth to fresh medium, and subsequent monitoring of cell growth rates revealed that the mutants also exhibited significantly different effects on the quality of growth as compared to isogenic wild-type controls. Particularly striking was that the mutants remained in lag-phase growth for approximately 2 hr longer than wild-type controls (Figure 2.4a), suggestive of a defect in the ability of the biosynthetic apparatus to respond to the presence of a rich nutrient source. Similarly, the onset of diauxic shift occurred approximately 2 hours earlier for cells harboring pmof6-1, and 1 hour early for

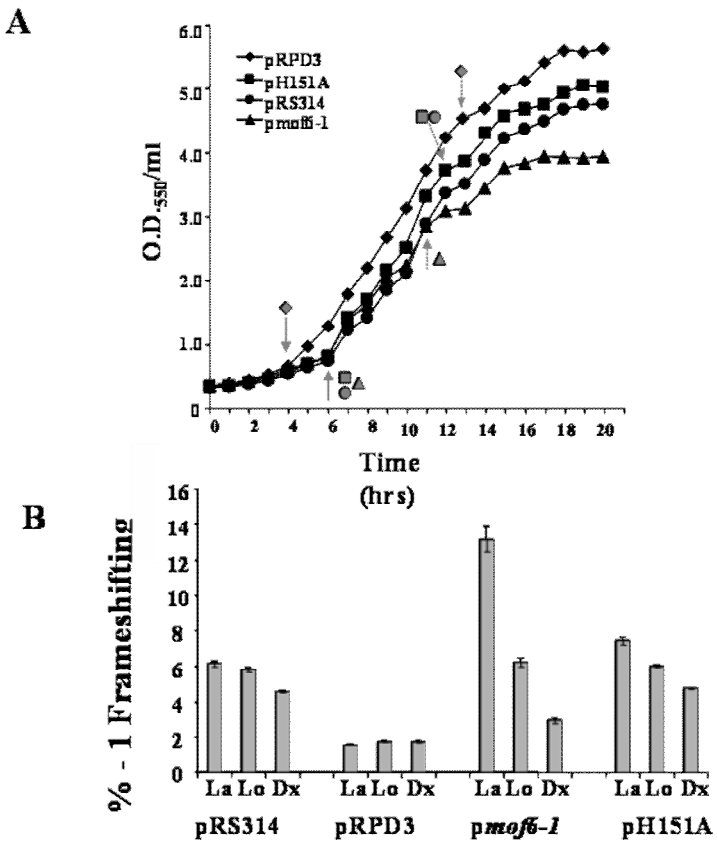

Figure 2.4

Correlation of growth and frameshifting defects in the *rpd3* mutants.

(A) Growth curves for *rpd3* mutants and isogenic wild-type yeast strains. Data shown represents the mean averages of each timepoint through three repetitions of the experiment. Standard deviations were <5%. Solid arrows indicate the approximate point of exit from lag-phase. Dotted arrows indicate diauxic shift. Experiment performed by J. Baxter Roshek **(B)** Programmed –1 ribosomal frameshifting efficiencies were determined in isogenic *rpd3*Δ strains harboring vector alone (pRS314), or the indicated plasmid borne alleles of *RPD3* during the three different phases of cell growth. La: lag-phase growth; Lo: log-phase growth; Dx: after diauxic shift. Error bars denote percent error. Experiment carried out by E. Carr.

(Meskauskas et al., 2003)

pH151A and vector alone as compared to those expression the wild-type gene. This result suggests inefficient utilization of carbon source by the mutants.

Given the original translation-associated defect of *mof6-1*, we examined whether these cells exhibited any gross defect in protein synthesis. Rates of incorporation of [^{35}S] labeled methionine and cysteine into newly synthesized protein were determined in mid-logarithmically growing cells as described in the materials and methods. The results (Figure 2.5) demonstrate that that rates of protein synthesis in *mof6-1* cells were approximately 75% that of wild-type cells.

Previous experiments had demonstrated that programmed –1 ribosomal frameshifting efficiencies remain stable throughout the growth cycle in wild-type cells (Dinman et al., 1991). In light of the effects of the mutants on cell growth, –1 PRF efficiencies were monitored during lag-phase, log-phase, and after diauxic shift in isogenic *rpd3Δ* cells harboring vector alone, pRPD3, pmof6-1, and pH151A. The results of these experiments show that –1 PRF defects were maximized in the mutants in lag-phase, becoming less severe as cells progressed through the growth curve (Figure 2.4b). The effect was most notable in *mof6-1* cells. The results suggest that the frameshifting defects were maximized in the mutants when demand for ribosomes was the greatest, and that –1 frameshifting efficiencies decreased in parallel with the demand for newly synthesized ribosomes. That no such effect was observed in wild-type cells is in line with the bioeconomic model of regulation of ribosome

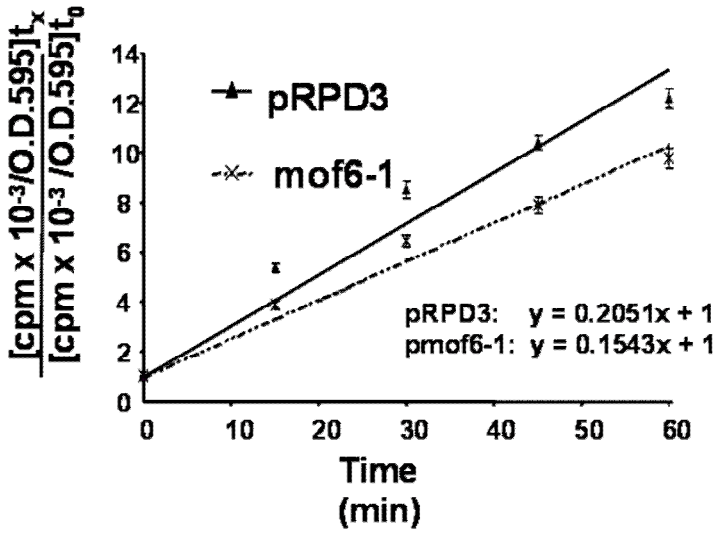

Figure 2.5

Decreased rates of protein synthesis in cells expressing the Mof6-1p form of Rpd3p. [^{35}S]methionine and [^{35}S]cystine were added to mid-logarithmically growing isogenic *rpd3Δ* strains containing wild type pRPD3 or p*mof6-1* and samples were harvested at 0 min and at 15 min intervals for 60 min. Incorporation of the [^{35}S]-labels was monitored by cold trichloroacetic acid precipitation as described in materials and methods. The data were plotted using the formula y = mx +B where m is the slope, x is the sample and B is the y intercept. Rates of protein synthesis correspond to m. All time points were taken in triplicate and the experiment was repeated twice. Experiment performed by J. Baxter Roshek.

(Meskauskas et al., 2003)

biosynthesis (Warner, 1999), and suggests a defect in the regulation of ribosome biosynthesis (see below).

Deletion of other genes linked to heterochromatin-associated functions also result in the Mof⁻ phenotype

Deacetylation of histones by Rpd3p promotes local chromatin condensation, resulting in transcriptional repression of nearby RNA pol II transcribed genes (reviewed in (Courey and Jia, 2001). Although Rpd3p is able to deacetylate histones *in vitro*, *in vivo* deacetylation of histones by Rpd3p requires the co-factors. Mutations in any of the components of the Rpd3p/Sin3p/Ume6p repression complex lead to gene-specific derepression of RNA pol II regulated genes and concomitant transcriptional activation (Hassig et al., 1997; Kadosh and Struhl, 1998). Conversely, mutations in any of the components of the Rpd3p/Sin3p/Sap30p repression complex lead to the opposite effect, i.e. enhanced transcriptional silencing of RNA pol II transcribed genes artificially inserted into heterochromatin contexts (Sun and Hampsey, 1999).

Given the model describing the histone deacetylase complex, if *mof6-1* is acting through either of these complexes, then *sin3* mutants would also exhibit Mof⁻ phenotypes. Further, if the effect is on a heterochromatin-associated function, e.g. transcription or maturation of rRNAs, *sap30* mutants should also promote increased –1 PRF efficiencies. Conversely, *ume6* mutants should promote increased –1 PRF efficiencies if the effect is on genes found in euchromatin, e.g. ribosomal protein

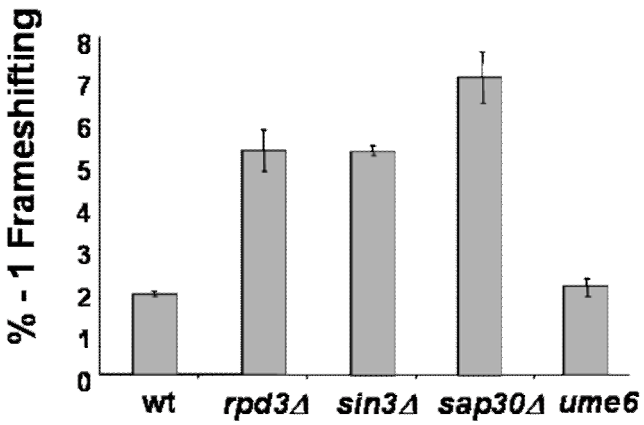

Figure 2.6

Frameshifting defects in heterochromatin-associated mutants

The frameshift test vectors p0 and p-1 were introduced into isogenic wild-type, *rpd3Δ*, *sin3Δ*, and *sap30Δ* strains, along with four strains harboring different alleles of UME6, and programmed –1 ribosomal frameshift efficiencies were determined. All assays were performed in triplicate. Error bars denote percent error. Experiments carried out by J. Yasenchak and E. Carr.

(Meskauskas et al., 2003)

genes. Figure 2.6 shows that deletion of either *SIN3* or *SAP30* resulted in increased -1 PRF efficiencies, while three separate *ume6* alleles did not. The *sin3Δ* and *sap30Δ* strains also had significant killer virus maintenance defects, whereas *ume6* strains were able to stably maintain the killer virus (data not shown). These results demonstrate that 1) the histone deacetylation apparatus is involved in a process that results in a specific translational fidelity defect, and 2) the effect is likely to involve a process in the heterochromatin environment.

Mutation of genes involved in the histone deacetylation apparatus result in 60S ribosomal subunit biogenesis defects

That a defect involving heterochromatin should result in a translational fidelity defect suggested a ribosome biogenesis defect involving rRNA transcription or processing. Given the involvement of the histone deacetylase complex in transcription-associated processes, the effects of these alleles on rRNA transcription and processing were examined by pulsing cells with [^{3}H]-methylmethionine, which specifically labels the methylated RNAs, the most abundant of which are those transcribed from the 35S operon. Though no differences were observed with regard to either the rates of 35S pre-rRNA synthesis, nor in its eventual maturation to 18S and 25S rRNAs, the amount of time required for the initial processing step of the 35S pre-rRNA in the mutant cells was delayed by approximately 3 min as compared to wild-type controls (Figure 2.7). A steady state analysis revealed that there was no accumulation of any precursors in the mutant cells (data not shown). Polysome analyses of ribosomes

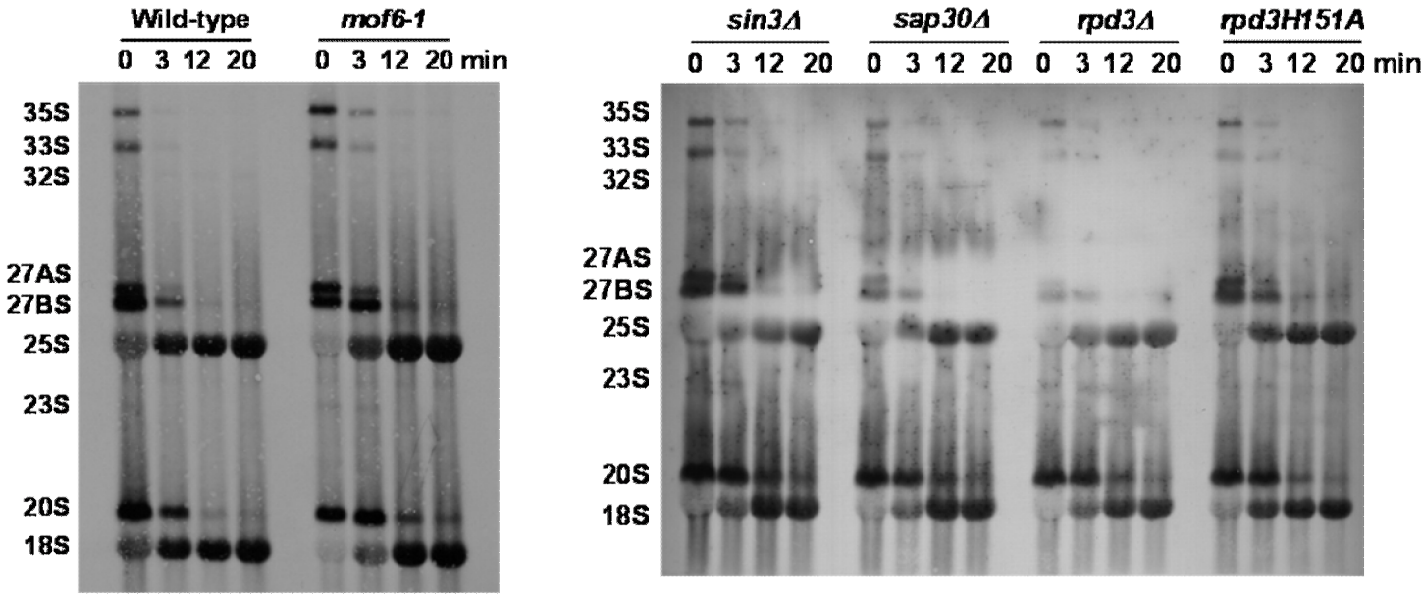

Figure 2.7

Delayed 35S rRNA processing in histone deacetylation associated mutants

Pulse-chase labeling with L-[methyl-^{3}H]methionine was carried out on the isogenic wild-type, *mof6-1*, *rpd3*Δ, *rpd3-H151A*, *sin3*Δ, and *sap30*Δ strains. Twenty thousand cpm per sample was resolved on a 1.2% formaldehyde-agarose gel. Labeled RNAs were transferred to a zeta-probe membrane (Bio-Rad), sprayed with EN3HANCE (Dupont), and exposed to x-ray film. Experiments performed by S. Baserga and J. Gallagher.

(Meskauskas et al., 2003)

isolated from isogenic wild-type, *rpd3Δ, mof6-1*, *rpd3-H151A*, *sin3Δ*, and *sap30Δ* strains were suggestive of biogenesis defects in the 60S ribosome subunits as evidenced by decreased levels of 60S ribosomal subunits, increased areas under the 80S peaks, and decreased polysome peaks (Figure 2.8).

Ribosome biogenesis defects are not due to global defects in ribosomal protein expression.

We have previously found that defects in specific ribosomal proteins result in increased programmed ribosomal frameshifting efficiencies (Peltz et al., 1999; Meskauskas and Dinman, 2001). Thus, one possible explanation for the observed effects could be that these alleles promote altered expression of ribosomal proteins (RPs). To address this, approximately 200μg samples of 60S and 40S ribosomal subunits isolated from isogenic wild-type and mutant cells were separated in two dimensions by nonequlibrium pH gradient electorphoresis (NEPHGE), and RPs were visualized by silver staining. No gross differences in the staining patterns were observed between wild-type and mutant samples (data not shown). These results demonstrate that the effects of the *rpd3* mutants on programmed ribosomal frameshifting and ribosome biogenesis are not due to defects on the synthesis of ribosomal proteins.

The mutants result in aminoacyl-tRNA binding in defects

One previously unexplained phenotype of *rpd3* mutants has been their sensitivity to cycloheximide, a translational inhibitor (Vidal and Gaber, 1991). In light of our

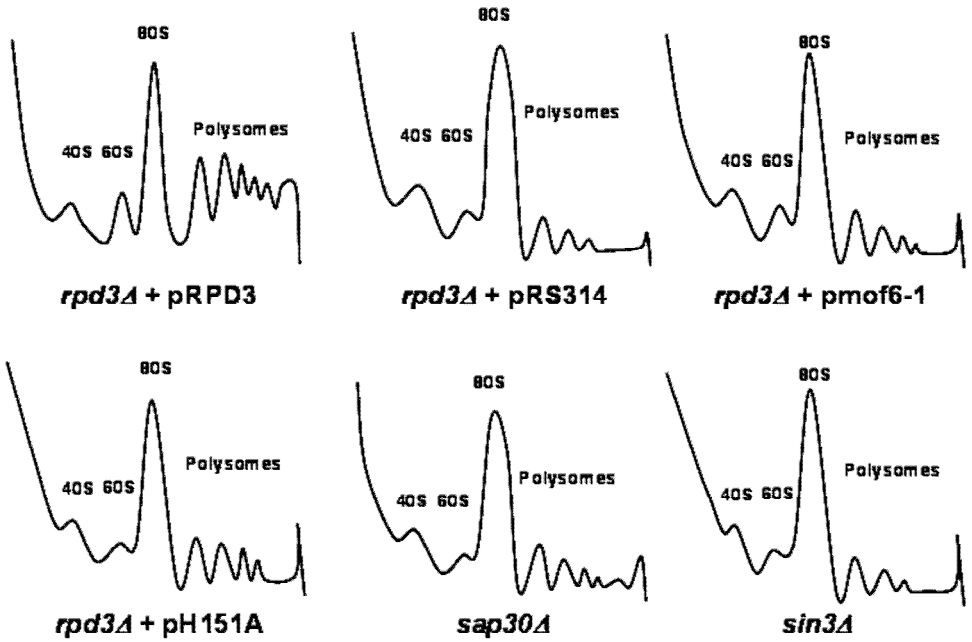

Figure 2.8

Polysome profiles

Cytoplasmic extracts from *mof6-1* and other heterochromatin associated mutant strains as well as their isogenic wild-type were fractionated though sucrose gradients as described in the materials and methods. Gradients were centrifuged in an SW41 rotor at 40,000 rpm for 135 min at 4°C, fractionated and analyzed by continuous monitoring of A_{254}. Experiments implemented by A. Meskauskas.

(Meskauskas et al., 2003)

data showing that these classes of mutants promote a ribosome biogenesis defect specific to 60S subunits, we employed a pharmacogenetic approach using well characterized antibiotics to investigate the specificity of the defects. Sparsomycin, which increases the affinity of ribosomes for the 3' (donor) end of peptidyl-tRNAs (Jayaraman and Goldberg, 1968; Herner et al., 1969; Moazed and Noller, 1991) was used as a P-site specific probe. Anisomycin, which decreases ribosomal affinities for the 3' (acceptor) ends of aminoacyl-tRNAs (Grollman, 1967; Carrasco et al., 1973; Schindler, 1974) and, paromomycin, which stabilizes binding of near-cognate tRNAs in the decoding center of the small subunit rRNA (Carter et al., 2000; Ogle et al., 2001; Vicens and Westhof, 2001) served as probes for A-site specific defects. Figure 2.9 shows that although sparsomycin had no effect relative to wild type on cells harboring the various *rpd3* alleles (*rpd3Δ*, *mof6-1*, and *rpd3-H151A*), or the *sin3Δ* and *sap30Δ* mutants, all of the mutants were hypersensitive to anisomycin, and all but *sap30Δ* were hypersensitive to paromomycin. These data indicate that the translational defect caused by mutations in these genes is specific to the ribosomal A-site. To further investigate the biochemical basis for these observations, tRNA binding experiments were performed comparing isogenic wild-type and *mof6-1* ribosomes. Although no differences were observed in the binding of the 3' ends of either donor or acceptor fragments (data not shown), the binding profiles for intact aa-tRNAs were dramatically different (Figure 2.10). Specifically, *mof6-1* ribosomes had decreased initial rates of aa-tRNA binding, and had lower overall affinities for aa-tRNAs. In addition, precipitous dropoff in aa-tRNA binding at the 60 min time point suggests that *mof6-1* ribosomes are less stable than their wild-type counterparts.

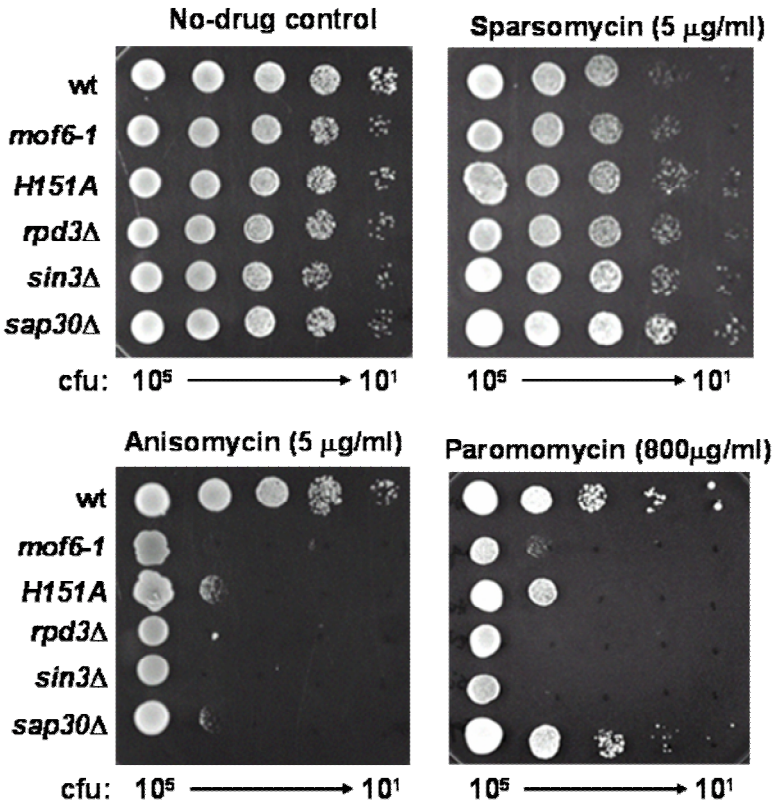

Figure 2.9

Sensitivity to translational inhibitors

Ten-fold dilutions from 10^5 to 10^1 colony forming units (CFU) of isogenic wild-type, *rpd3*Δ, *mof6-1*, *rpd3-H151A*, *sin3*Δ, and *sap30*Δ strains were spotted onto selective (H-trp) medium containing the indicated concentrations of drugs, or no-drug controls and incubated at 30°C for three days. Experiment executed by J. Baxter Roshek.

(Meskauskas et al., 2003)

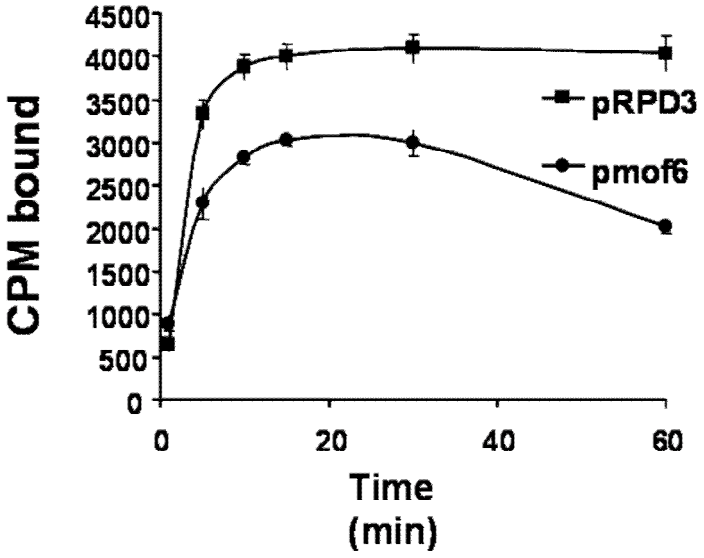

Figure 2.10

Ribosomes from *mof6-1* cells have decreased binding for aa-tRNA.

Ribosomes purified from isogenic wild-type and *mof6-1* strains were incubated with molar excess amounts of [^{14}C]Phe-tRNA and salt washed ribosomes were diluted at the indicated time points and quickly filtered through nitrocellulose filters. After drying, the filters were counted by liquid scintillation. Assays were performed in triplicate. Data points and error bars indicate mean and standard deviation. Experiment performed by A. Meskauskas with assistance from J. Baxter Roshek.

(Meskauskas et al., 2003)

Ribosomes from mof6-1 cells have decreased peptidyl transfer activities

We previously demonstrated that peptidyl transfer defects can specifically promote increased–1 PRF efficiencies (Dinman et al., 1997). It is possible that a defect in binding of aa-tRNA could result in diminished peptidyl transferase activities. This in turn might enable elongating ribosomes to pause longer at the programmed –1 ribosomal frameshift signal, providing them with more time to shift. To test this hypothesis, we compared the peptidyl transferase activities of ribosomes isolated from isogenic wild-type and *mof6-1* strains using the puromycin reaction. Figure 2.11 shows that ribosomes purified from *mof6-1* cells have significantly reduced peptidyl transferase activities as compared to wild-type controls. These findings illuminate the biochemical basis for the Mof⁻ phenotypes of these cells.

Discussion

mof6-1 was originally isolated as a recessive mutation in *S. cerevisiae* that promoted increased efficiencies of programmed -1 ribosomal frameshifting and rendered cells unable to maintain the killer virus (Dinman and Wickner, 1994). In the present study, we have shown that *MOF6* is a unique allele of *RPD3*, that it does not represent a gain-of-function allele, and that the deacetylase function of Rpd3p is required for maintaining wild-type levels of frameshifting, maintenance of the yeast killer virus, and proper timing and extent of downstream rRNA processing events and ribosome maturation.

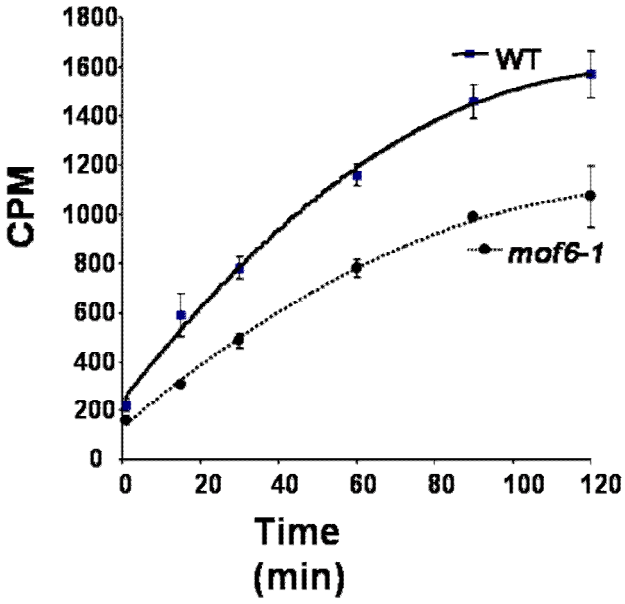

Figure 2.11

Ribosomes from *mof6-1* cells have decreased peptidyltransferase activities.

Time course of the formation of [^{14}C]Phenylalanine-puromycin product in assays using ribosomes isolated from isogenic *rpd3D* cells expressing wild-type or the *mof6-1* forms of Rpd3p. Ethyl acetate soluble radioactivity was determined by liquid scintillation counting. Control studies were performed in the absence of puromycin to determine the nonspecific extraction of CACCA[^{14}C]AcPhe. Control values (generally less than 2%) were subtracted from the values obtained in the presence of puromycin. All experiments were performed in triplicate. Data points and error bars indicate mean and standard deviation. Experiment performed by A. Meskauskas with assistance from J. Baxter Roshek.

(Meskauskas et al., 2003)

We previously demonstrated that peptidyl transfer defects can specifically promote sensitivity to translational inhibitors anisomycin and paromomycin, these data suggest an A-site specific defect which results in increases in -1PRF. This frameshifting defect is most severe during lag phase of growth, when the demand for ribosomes is highest. Mutant cells also display delayed exit from lag-phase growth in which may indicate defects in ribosome production and integrity. As the demand for new ribosomes outpaces the ability of the cell to supply them, the cell would tend to produce a greater fraction of defective ribosomes in an attempt to keep up with demand. Additionally, the mutants strains enter into diauxic shift before the wild-type. These data could suggest that these cells are inefficiently utilizing the carbon source in the growth medium due to their functionally compromised ribosomes producing a large amount of inaccurately translated, inactive protein products. Such an unproductive use of cellular and environmental resources could account for the increased lag time and early entry into diauxic shift.

Specific interactions of the Rpd3p-Sin3p complex with other factors, e.g. Ume6p or Sap30p, have been genetically shown to have differential effects on RNA Pol II transcribed genes in either euchromatin or heterochromatin environments (Sun and Hampsey, 1999). Our observation that mutants of *RPD3*, *SIN3* and *SAP30*, but not of *UME6*, affect programmed –1 ribosomal frameshifting and virus maintenance suggest that these translation-associated defects are due to effects in the heterochromatin environment. The data also demonstrated no quantitative effect on rates of 35S rRNA

synthesis suggesting that defects in ribosome biogenesis and function was not due to an rRNA transcriptional defect. Rather, we have shown that the defect is a delay at the earliest stage in the 35S pre-rRNA processing program. Since processing of the 35S pre-rRNA is co-transcriptional (Fath et al., 2000), and since the histone deacetylase complex is known to influence chromatin structure, one possible explanation for our observations could be that deviations from the wild-type heterochromatin environment cause defects in the early stages of ribosome biogenesis possibly by altered production of the involved machinery.

In light of the well defined steps involved in rRNA maturation (Kressler et al., 1999; Venema and Tollervey, 1999; Leary and Huang, 2001)our data suggest the possibility that the defect may be at the level of rRNA base modification, e.g. 2'-*O*-ribose methylation (Nm) and/or pseudouridylation. These types of base modification have been specifically shown to localize to "functional" regions of the ribosome (Decatur and Fournier, 2002). Of particular interest with regard to the ribosomal A-site specific defect observed here are the large numbers of modified bases clustered in regions of the large subunit rRNA that are associated with the A-site/aa-tRNA interactions, and the peptidyl transferase center (Decatur and Fournier, 2002; Ofengand, 2002). These include 1) the peptidyl transferase center core region, 2) the region of helix 38 that forms an "A-minor motif" with 5S rRNA (Nissen et al., 2001), 3) helix 69, which appears to form an important bridge between the aa- and peptidyl-tRNAs (Stark et al., 2002), and 4) the A-loop at the end of helix 92 (though the lack of effect of *mof6-1* ribosomes on acceptor fragment binding argue against the defect

affecting this particular structure). Thus, an alternative to the altered heterochromatin topology hypothesis could be that a deficiency in the histone deacetylation machinery could result in repression of the RNA polymerase II transcribed box C+D and/or box H+ACA snoRNAs, which act as essential guides for base-specific rRNA modification (Decatur and Fournier, 2002; Ofengand, 2002), resulting in the observed delay in 35S rRNA processing.

Whatever its origin, the early delay in rRNA maturation is affecting a series of downstream processes involved in the biogenesis and functionality of ribosomes. These effects are specific to the formation and/or the function of the A-site. The resulting ribosomes are less accurate than their wild-type counterparts and have decreased peptidyl transferase activities.

Chapter 3: Effects of rRNA modifications in the PTC of yeast ribosomes on translational fidelity and ribosome structure

Introduction

Extensive research into rRNA modification has enabled mapping of the majority of Ψ and Nm residues in eukaryotic and archaeal ribosomes, as well as identifying the snoRNA molecules that guide their modification. However, little is understood about the functional roles of nucleotide modification. It is known that nucleotide modifications within the ribosome are not located randomly. This is most clearly seen in the ribosomal large subunit (Figure3.1), where modifications cluster in highly conserved areas of the ribosome devoted to peptidyl transfer, A- and P site tRNA binding sites, the peptide exit tunnel and intersubunit bridges (Samarsky and Fournier, 1999; Ban et al., 2000; Yusupov et al., 2001; Decatur and Fournier, 2002). This clustering is seen in organisms ranging from *E. coli* to humans with the number of modifications increasing with evolutionary complexity (Ofengand et al., 1995).

Despite this high degree of conservation, most snoRNAs responsible for guiding these modifications can be individually deleted with minimal detriment to the organism indicated as small or no change in growth (Lowe and Eddy, 1999; Samarsky and Fournier, 1999). Disrupting/deleting pseudouridine synthase proteins responsible for modification of only two or three residues in *E. coli* did not produce discernable differences in exponential growth rates between wild-type and mutant

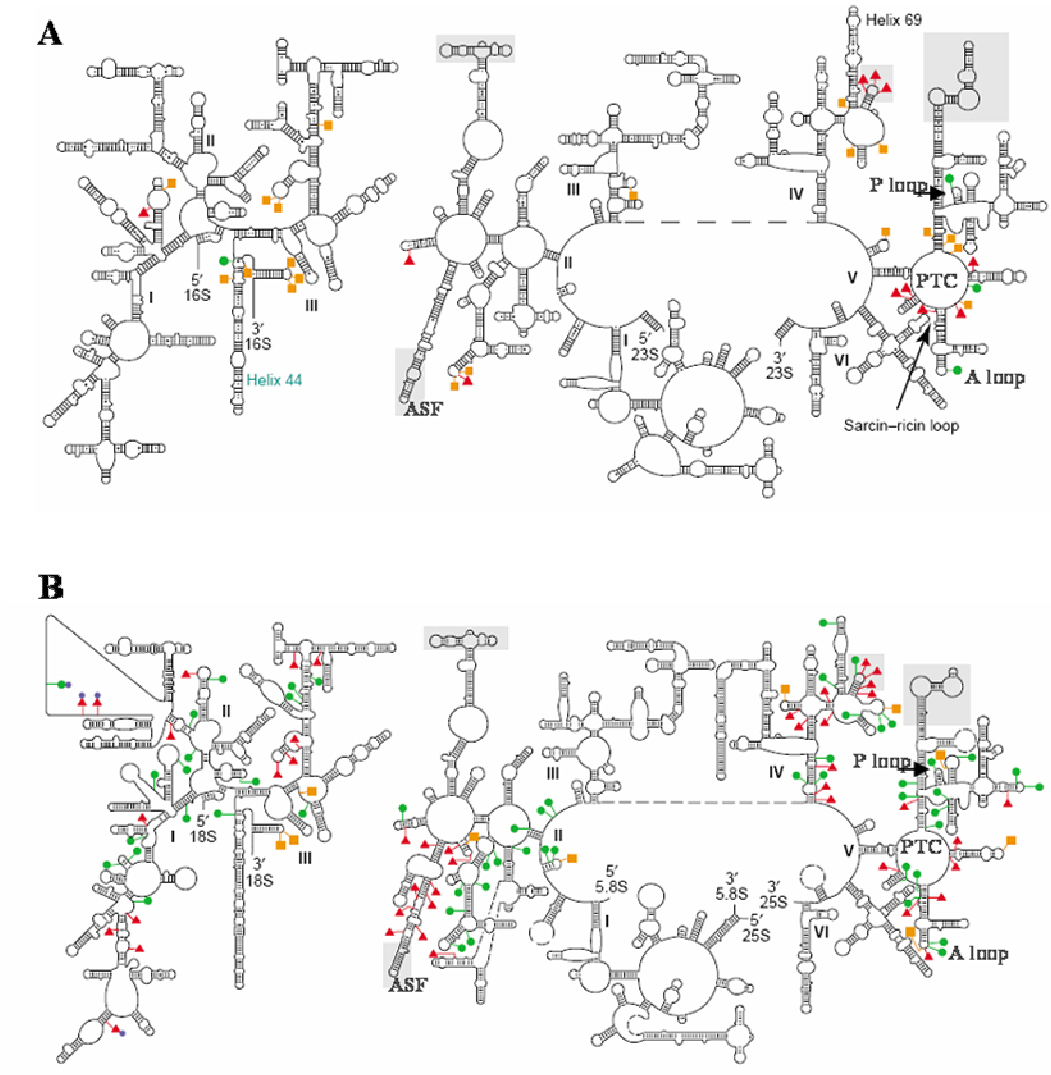

Figure 3.1

Secondary structure map of rRNA modification sites

Distribution of (A) *E. coli* and (B) *S. cerevisiae* rRNA modifications demonstrating their evolutionary conservation and high density in areas of functional importance. Ψ(red), mN (orange), Nm (green). Figure adapted from Decatur and Fournier, 2002.

stains *in vivo*. However, when grown together the mutants strains were strongly out competed by the wild-type suggesting a growth advantage conferred by the modifications (Raychaudhuri et al., 1998; Raychaudhuri et al., 1999). *E. coli* ribosomes reconstituted *in vitro* without posttranscriptional rRNA modifications are severely defective in catalytic activity (Green and Noller, 1996). Interestingly, global disruption of Ψ or Nm formation *in vivo* results in strong growth defects in yeast, as seen resulting from point mutations of yeast modification enzymes Cbf5p and Nop1p; proteins encoded by essential genes in yeast (Tollervey et al., 1993; Zebarjadian et al., 1999). Modifications found to be essential are often performed by a snoRNP that harbors a component also essential for rRNA processing. These results in aggregate suggest that rRNA modifications may be individually dispensable for survival, but together serve to optimize rRNA structure for production of accurate and efficient ribosomes.

While it is has become clear that modified residues in ribosomal RNA can contribute to ribosome function, how these modified residues accomplish this feat is still largely unknown. Based on the chemical properties of Ψ and Nm residues, possible functional roles can be inferred but not established. It has been suggested that Ψ residues contribute to stability by producing increased potential for base stacking, as well as by offering an extra hydrogen bond donor as compared to uridine (Charette and Gray, 2000; Helm, 2006). Nm residues offer protection against hydrolysis by bases and nucleases and can create structural changes by changing the hydration sphere around the oxygen, blocking sugar edge interactions and favoring

the 3'endo ribose configuration (Williams et al., 2001; Helm, 2006). Thermodynamic and NMR based studies of Ψ containing hairpin RNAs revealed that a Ψ residue is stabilizing when located at a stem loop junction and slightly destabilizing when located in single-stranded loop regions when compared to unmodified RNAs (Meroueh et al., 2000). Recent NMR studies of the highly conserved and highly modified LSU H69 of the human ribosome observed discernable but subtle secondary structure differences between rRNA with and without the modifications (Sumita et al., 2005).

Functional and structural studies beyond growth characterization and stability measurements have been performed implicating rRNA modification defects as causing changes in translation rates and ribosome integrity. In *E. coli*, mutants lacking methylation of the m^1G745 residue located in the LSU exhibit a decreased growth rate, decreased rate of polypeptide chain elongation rate, defects in ribosome profiles and showed resistance to the antibiotic viomycin (Gustafsson and Persson, 1998). In yeast, knockout strains were created which lack each of six snoRNA genes that guide pseudouridylation of residues in the PTC of the ribosome, as well as one strain that lacked all six genes (King et al., 2003). The resulting mutants were characterized and only one individual mutant, the snR10 deletion strain, had phenotypic defects. However, deletion strains of all six snoRNA genes promoted moderate defects in growth and translation rates, sensitivity to the drug paromomycin, and changes in ribosome profiles. These defects were more pronounced in the six snoRNA deletion strain than with the snR10 deletion alone. This suggests that at least

one or some combination of the additional hypo-modified residues present in the six gene deletion strain was necessary to produce the increased severity of phenotypic defects seen in the multiple snoRNA deletion strain. Structure probing experiments also revealed altered LSU rRNA structure for the multiple snoRNA deletion strain.

Other functional studies have centered around two methylated nucleotides, mU_{2920} and mG_{2921}, in the A loop of the yeast ribosome. There are two components thought to be involved in the methylation of these rRNA residues: the guide snoRNA snR52, and the site-specific methyltransferase Spb1p, an essential yeast nucleolar protein. Primer extension analysis revealed a functionally redundant pathway whereby snR52 or Spb1p could methylate residue Um_{2920} (Bonnerot et al., 2003). Later TLC (thin layer chromatography) experiments revealed a different mechanism whereby Spb1p and snR52 were responsible for methylation of Gm_{2921} and Um_{2920} respectively, and showing that Spb1p could methylate residue Um_{2920} in the absence of snR52 (Lapeyre and Purushothaman, 2004). Despite this discrepancy, it is clear that deleting both snR52 and Spb1p results in severe defects in growth rates and polysome profiles, as well as paromomycin sensitivity (Bonnerot et al., 2003). This makes Spb1p an important exception to the snoRNA guided modification rule in eukaryotes. The *E. coli* homolog of Spb1p, FtsJ/RrmJ, methylates 23S rRNA residue Um_{2552} the equivalent of yeast Um_{2920} (Caldas et al., 2000). Deletion of this protein in *E. coli* results in severe growth defects, temperature sensitivity, and altered ribosome profiles (Bugl et al., 2000).

Despite their high level of conservation and distribution in functionally important areas of the ribosome, rRNA modifications belie their individual importance with a lack of defects in their absence. However, the changes in ribosome profiles and rRNA structures suggest the intriguing possibility that the translation process may indeed be altered in some way. One way to monitor the functional effects associated with these ribosomal changes is to assay for changes in translational fidelity. Here, several single and one double deletion strains of previously characterized snoRNAs known to modify the PTC of the yeast ribosome were monitored for changes in translational fidelity. The results show that defects in rRNA modification produce allele specific mutant phenotypes including increased sensitivity to translational inhibitors; defects in virus propagation; changes in translational fidelity as monitored by +1 and –1 PRF, aa-tRNA selection and non-specific nonsense suppression; changes in the rates of aa-tRNA binding to the ribosomal A-site; changes in rates of peptidyl transfer; and structural changes in the ribosome surrounding the peptidyl transferase center.

Materials and Methods

Strains, media, and genetic methods

The *S. cerevisiae* strains used in this study are presented in Table 2. *Escherichia coli* strain DH5α was used to amplify plasmids (listed in Table 3), and *E. coli* transformations were performed using the high-efficiency transformation method (Inoue et al., 1990). Yeast cells were transformed using the alkali cation method (Ito

et al., 1983). YPAD and synthetic complete medium (H-), as well as YPG, SD, and 4.7 MB plates used for testing the killer phenotype were prepared and used as described previously (Dinman and Wickner, 1994). Oligonucleotide primers were purchased from IDT (Coralville, IA) and are listed in Table 4. Yeast deletion strains *snr10*Δ, *34*Δ, *37*Δ, *42*Δ, *46*Δ and isogenic wild-type were provided by M.J. Fournier. Yeast strains s*nr52*Δ, s*pb1DA*, the double mutant and an isogenic wild-type were provided by G. Lutfalla.

Killer virus assay and viral dsRNA analyses

Cytoduction of the L-A and M_1 killer virus into snoRNA knockout strains and subsequent killer virus assays were carried out as previously described (Dinman and Wickner, 1992). Briefly, viruses were introduced into [*rho*^{0}] cells by cytoduction, cytoplamic mixing without mating. Cells were streaked for single colonies on selective media (-arg). Colonies were replica plated onto SD, YPG, and 4.7MB plates seeded with 5X47 killer indicator cells. Colonies were scored for growth on YPG, and the absence of growth on SD medium. Killer activity was observed after a few days at room temperature as a zone of growth inhibition around the Killer$^+$ (K^+) colonies. Total RNAs were extracted from cytoduced wild-type and snoRNA knockout strains as previously described (Harger and Dinman, 2003). Single stranded RNA was removed from the total RNA sample by adding 10-20μg total RNA and 0.5ng RNase A in 0.5M NaCl, 1X TE and digesting at RT for 30 min. Resulting double stranded nucleic acids were extracted once each with saturated

phenol (pH 6.6) and chloroform, precipitated, resuspended in deionized water, and separated and visualized through an ethidium bromide stained 1% agarose TAE gel.

Dual Luciferase Assays

Dual luciferase assays in yeast were performed as previously described (Harger and Dinman, 2003). These involve the use of a 0-frame control reporter and −1, +1 ribosomal frameshift, nonsense suppression, and misincorporation test reporter constructs. Miscoding efficiencies were calculated by determining the firefly/*Renilla* luminescence ratios from cell lysates expressing each the control and test reporters, then dividing the test ratio by the control ratio and normalizing by the wild-type. At least three readings derived from lysates derived from a minimum of three different yeast cultures were used. All assays were performed with enough replicates to achieve confidence levels of >95%, and standard errors were calculated as previously described (Jacobs and Dinman, 2004). Luminescence readings were obtained using a TD20/20 luminometer (Turner Designs Inc. Sunnyvale, CA). Reactions were carried out using the Dual-Luciferase® Reporter Assay system (Promega Corporation, Madison, WI).

Drug Sensitivity

For dilution spot assays, yeast cells grown to logarithmic phase were initially diluted to 1×10^6 colony forming units (CFU)/ml. Subsequent tenfold dilutions were made and 3 μl were spotted either onto rich medium on rich medium containing anisomycin

or sparsomycin (10 and 20 μg/mL) and incubated at 30°C**.** Anisomycin and sparsomycin were obtained from Sigma-Aldrich, St. Louis, MO.

Ribosome isolation

S. cerevisiae ribosomes were isolated at 4°C as previously described (Meskauskas et al., 2005). Cultures (I L) were grown in YPAD to $O.D_{595}$=1 , harvested by centrifugation and washed 1 time in 40ml cold 0.9% KCl and frozen in liquid nitrogen. Before use, frozen cells were thawed on ice and 40ml cold 0.9% KCl was added for a second wash. Cells were resuspended to a concentration of 1ml/2g pellet in Buffer A [20 mM Tris-HCl pH 7.5 at 4^o C, 5 mM $Mg(CH_3COO)_2$, 50 mM KCl, 10% Glycerol, and 1mM phenylmethylsulfonyl fluoride (PMSF), 1 mM1,4-dithioerythritol (DTE) added immediately prior to use]. Add 1 ml equivalent 0.5mm zirconia beads to a 2 ml conical tube, then fill with cell solution and vortex at 4°C to disrupt using a Mini-bead beater in 2 min bursts, with intermittent 2 min incubation on ice. Repeat two to four times until cell lysis is complete. Cells were transferred to a 5ml polycarbonate centrifuge tube. Beads were washed with Buffer A and wash solution containing cells was transferred to the 5ml polycarbonate centrifuge tube until full. Tubes were centrifuged using a Beckman micro-ultracentriguge MLS-50 rotor 25 min 20,000rpm. The supernatant was transferred, while avoiding the pellet, to a 5ml pollyallomer tube containing a 1 ml cushion of cold Buffer C [20 mM Tris-HCl pH 7.5 at $+4^o$ C, 5 mM $Mg(CH_3COO)_2$, 50 mM KCl, 25% Glycerol, and 0.1 mM PMSF, 0.1 mM DTE added immediately prior to use]. Samples were centrifuged as before except for 2 hours 20min at 50,000 rpm using the slowest acceleration and

deceleration settings. The supernatant was discarded and the fines were gently washed away from precipitate with 1ml Buffer C. Ribosomes resuspended in 100 to 300 μL cold Buffer C w/DTE and PMSF. Samples were centrifuged for 1 min 12000 rpm 4°C to clarify lysates. Supernatants were transferred to a new tube. Ribosomes were aliquoted and stored at -80°C. Concentrations were determined using optical density (1 OD_{260} = 20 pmol).

Purification of aminoacyl-tRNA synthetases

Aminoacyl-tRNA synthetases were purified as previously described with minor modifications (von der Haar F., 1979). Two pounds of frozen cake yeast (George R. Ruhl & Son, Inc., Hanover, MD) were placed in 500 ml of buffer A [0.2 M Tris-base, 0.3 M NH_4Cl, 20 mM $MgSO_4$, 1 mM EDTA, 0.15 M dextrose] and allowed to thaw and ferment overnight. Cells were disrupted by three passages through an ice-cooled Microfluidaser at ~18,000 lb/in^2, cell debris was removed by centrifugation at 4 °C in a Beckman JLA rotor at 10,000 rpm for 30 minutes, and 800 ml of supernatant was obtained. Fines and nucleic acids were precipitated by addition of polyethylenimine (1.73 g/lb of cells, equivalent to 4.32 g/liter of lysate) over a period of 5 minutes with slow stirring. Precipitates were removed by centrifugation at 4 °C using a GSA rotor at 9,000 rpm for 40 minutes. Proteins in the supernatant were precipitated by addition of 472 g of ammonium sulfate per liter of extract (70 % saturation), and precipitates were collected by centrifugation in a GSA rotor at 12,000 rpm for 45 minutes at room temperature. The pellet from this step was suspended in 43.75 ml of buffer C [30 mM potassium phosphate, pH 7.2, 1 mM EDTA, 1 mM DTE, 0.01 mM PMSF] per 100 g

of pellet and subsequently dialyzed in 2 liters of buffer C overnight with two changes of buffer. The extract then was clarified by centrifugation in a GSA rotor at 12,000 rpm for 45 minutes at 4 °C. The supernatant was diluted 2.5 times with buffer C and fractionated through a Sephadex CM50 column equilibrated with buffer C. The column was washed with buffer D [30 mM potassium phosphate, pH 7.2, 1 mM EDTA, 0.01 mM PMSF, 10 % glycerol] with 50 mM KCl. The proteins were eluted from the column using a series of step gradients composed of buffer D containing 150 mM, 300 mM, and 500 mM KCl. The material eluted by buffer D with 150 mM KCl contains phenylalanyl-tRNA synthetase activity. Proteins were precipitated by addition of 472 g/liter of ammonium sulfate, and pellets were suspended in buffer D containing 50 mM KCl. Extracts were dialyzed against 1 liter with two changes of buffer D50 for 10 h, after which they were clarified by centrifugation in a GSA rotor at 12,000 rpm for 45 minutes at 4 °C. The obtained preparations of aa-tRNA synthetases were aliquoted and flash frozen in liquid nitrogen.

Synthesis of aminoacyl-tRNA and acetylated aminoacyl-tRNA

Yeast phenylalanyl-tRNAs were aminoacylated by scaling up a previously described method (von der Haar F., 1974). The reaction mix (5 ml) contained 300 mM Tris-HCl, pH 7.6, 100 mM KCl, 20 mM $MgCl_2$, 0.4 mM ATP, 40 µM [^{14}C]Phe [496 mCi/mmole], plus 5 mg of tRNA-Phe and 475 µl of aminoacyl-tRNA synthetases (D150) purified as described above. Reaction mixtures were incubated for 30 minutes at 30 °C, and proteins were removed by extraction with acid-phenol-chloroform. [^{14}C]Phe-tRNA was separated from uncharged tRNA and free [^{14}C]Phe

by high-performance liquid chromatography (HPLC) as previously described (Triana-Alonso et al., 2000) with the following modifications. Samples were loaded onto a 4.6x250 mm JT Baker wide-pore butyl column equilibrated with buffer A [20 mM $NH_4(CH_3COO)$, 10 mM $MgCl_2$, 400 mM NaCl; pH 5.0] at 1 ml/min. The column was washed with 10 ml of buffer A, creating conditions under which free phenylalanine and aminoacyladenylate are eluted from the column. Uncharged tRNAs were eluted by isocratic elution with 19 ml at 15 % of buffer B [20 mM $NH_4(CH_3COOH)$, 10 mM $MgCl_2$, 400 mM NaCl, 60 % methanol; pH 5.0). [^{14}C]Phe-tRNA was eluted using a step gradient to 100 % of buffer B. Elution of aminoacyl-tRNA was monitored by $OD_{260/280}$ readings, and [^{14}C]Phe-tRNA peak and concentrations were determined by scintillation counting. The presence of aminoacyl-tRNA in the eluted material was confirmed by gel filtration through G-25 spin columns and by nonenzymatic hydrolysis of ester bonds at basic pH (Kaneko and Doi, 1966). Ac-[^{14}C]tRNA was obtained in a similar manner. Yeast phenylalanyl tRNA was charged with [^{14}C]Phe as above and extracted with phenol. The [^{14}C]Phe-tRNA was acetylated by addition of 64 µl of acetic anhydride at 15 minutes intervals for 1 h on ice (Triana-Alonso et al., 2000). The reaction mix was clarified by centrifugation at 15,000 rpm for 3 minutes, and Ac-[^{14}C]Phe-tRNA was purified by HPLC as described above.

Characterization of peptidyl transferase activity

Peptidyl transfer assays were performed essentially as previously described (Meskauskas et al., 2005). The protocol was carried out on ice or at 4°C at all times unless otherwise noted. Briefly, complex C [80S ribosomes, Ac-Phe-tRNA, poly(U)]

was formed by incubating 120 pmol ribosomes, 0.4 mg/ml poly(U), 0.4 mM GTP, and 100 pmol Ac- [^{14}C]Phe-tRNA in 200 µL of binding buffer P [80 mM Tris-HCl, pH 7.4, 11 mM magnesium acetate, 160 mM ammonium chloride, 6 mM β-mercaptoethanol, and 2 mM spermidine] for 20 min at 30°C. The complex was filtered through a Millipore HA filter, and washed with binding buffer. Complex C was extracted off the filter disk by gently shaking in binding buffer containing 0.05% of Zwittergent 3-12 for 30min at 4°C. Complex C extract was pre-incubated at 30°C for 5 min to activate ribosomes. 2mM puromycin was added to complex C in 100 µL of binding buffer P to begin the reaction. Time points were taken at 0, 2, 5, 10, 20, 30, 60, 120 min by removing 100 µL aliquots and terminating the reactions by addition of 100 µL of 1.0 N NaOH. Reaction products were extracted with 0.5 ml of ethyl acetate, and radioactivity was determined by scintillation counting. Control values of reaction mixture without puromycin and of extracted complex C were obtained in each experiment. The data were analyzed using Prism Graph Pad software and was fit to give the value of K_{app}, the apparent rate constant of the entire reaction at a given concentration of puromycin using the equation Y=-Ae^(-kt)+C where Y is the normalized counts per minute (CPM), C is the final value of the normalized CPM, and t is the time in minutes.

tRNA binding activity

Aminoacyl-tRNA binding to the A-site of the ribosome was carried out as previously described (Meskauskas et al., 2005). Briefly, a reaction mixture of 12-25 pmol ribosomes, 0.4 mg/ml poly (U), 0.4 mM GTP, and in 50 µl of binding buffer A

[80 mM Tris-HCl, pH 7.4, 11 mM magnesium acetate, 160 mM ammonium chloride, 6 mM β-mercaptoethanol, and 2 mM spermidine] was preincubated with uncharged tRNA (4:1 tRNA/ribosomes) at 30°C for 15 min to occupy ribosomal P- and E-sites by uncharged tRNA. The mixture is added to increasing amounts of [^{14}C]Phe-tRNA (4 to 264 pmol) and incubated at 30°C for an additional 15 min to allow formation of [14C]Phe-tRNA–80S–poly (U) complexes. Aliquots were then applied to nitrocellulose membranes, washed, and the resulting radioactivity of the membrane was measured by scintillation counting. Background levels of radioactivity were determined using a blank sample and subtracted from the test samples. The data were analyzed using Prism Graph Pad software and was fit to a nonlinear regression one site binding curve ($Y=B_{max}*X/(K_d + X)$) where Y is normalized CPM values, and X is tRNA concentration in μM.

Acetyl-aminoacyl-tRNA binding to the P-site of the ribosome was carried out as similar to the A-site binding protocol with the following modifications. Briefly, purified ribosomes in Buffer C were thawed on ice and treated with 1mM puromycin and 1mM GTP (adjust PMSF and DTE to 1mM) and incubated at 30°C for 30 min to remove aminoacyl-tRNAs. A reaction mixture of 12-25 pmol treated ribosomes, 0.4 mg/ml poly(U), and 50μl binding buffer P [80 mM Tris-HCl, pH 7.4, 11 mM magnesium acetate, 160 mM ammonium chloride, 6 mM β-mercaptoethanol, and 2 mM spermidine] is added to increasing amounts of Ac-[^{14}C]Phe-tRNA (4 to 264 pmol) and incubated at 30°C for 15 min to allow formation of [14C]Phe-tRNA–80S–

poly(U) complexes. The protocol then proceeds as described above for aminoacyl-tRNA binding reactions.

Structure Probing on Ribosomes in vitro

Purified ribosomes in Buffer C were thawed on ice and treated with 1mM puromycin and 1mM GTP (adjust PMSF and DTE to 1mM) and incubated at 30°C for 30 min to remove aminoacyl-tRNAs. Puromycin treated ribosomes were incubated with DMS (dimethyl sulfate), Kethoxal or CMCT (1-cyclohexyl-3-(2-morpholinoethyl) carbodiimide metho-p-toluene) as previously described (Kiparisov et al., 2005). Treated rRNA was extracted and slow-cool annealed in annealing buffer (250mM TrisCl pH 8.3, 200mM KCl) to ^{32}P-end-labeled primers (Table 4) which are used to investigate the ribosomal peptidyl-transferase center and A-loop. Primer extension and RNA sequencing were both performed using AMV reverse transcriptase (Roche, Mannheim, Germany) at 42°C for 30 min. Primer extensions were performed using 4μM dNTPs. Reaction products were separated through a 10% urea-polyacrylamide gel and visualized using a BioRad phosphoimager.

Results

Previous studies have implicated rRNA modification defects with changes in growth rates, translation rates and ribosome integrity. In order to more precisely determine the role of rRNA modifications in the translational fidelity of the ribosome, we have chosen several previously characterized snoRNAs and one protein that

modify residues around the peptidyl-transferase center of the ribosome and performed assays on strains deficient in these modifications to monitor changes in translational fidelity. These are single knockout strains of snoRNAs snR10, snR34, snR37, snR42, and snR46 which together pseudouridylate six rRNA residues in the PTC of the yeast ribosome, with snR34 modifying two of those residues. Additionally, single and double knockout strain snr52 and a methylase deficient mutant of the essential yeast protein Spb1, which are responsible for methylation of mG_{2921} and mU_{2920}, were analyzed (Figures 3.2 and 3.3). Since Spb1p is an essential yeast protein, a methylase deficient mutant with a D to A substitution affecting the AdoMet-binding site was used (Bonnerot et al., 2003; Lapeyre and Purushothaman, 2004). Mutant strains *snr10*Δ, *spb1DA*, and *spb1DA*/*snr52*Δ have slow growth phenotypes.

rRNA modification mutants show sensitivity to translation inhibitors

Several protein translation inhibitors are known to specifically interact with the ribosome (Tenson and Mankin, 2006) and can therefore be used as probes for changes in ribosome function. Paromomycin binds the decoding center of the A site (Vincens and Westhof, 2001) and stabilizes binding of near-cognate tRNAs (Ogle et al., 2001) can serve as a probe for A site-specific defects. Anisomycin binds the A-site crevice that normally accepts the amino acid side-chains of A-site bound aminoacyl-tRNAs (Hansen et al., 2003b) interfering with the binding of 3' end of the aa-tRNA (Grollman, 1967; Carrasco et al., 1973; Schindler, 1974) and can therefore be used as an A-site specific probe. Sparsomycin binds on top of the CCA end of a P-site bound substrate and interacts with it interfering (Hansen et al., 2003a) with the binding of

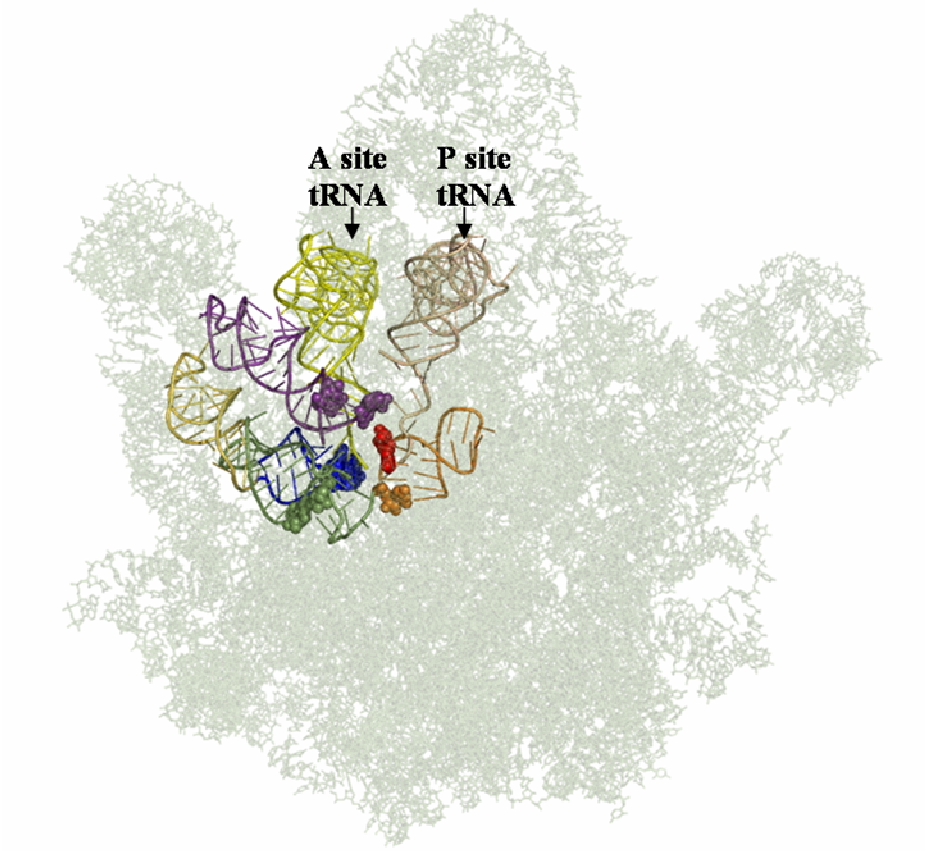

Figure 3.2

Ribosomal large subunit

The *E. coli* ribosome LSU containing A- and P-site tRNA with the helices of the peptidyl transferase center highlighted. View: looking into the PTC from the top of the ribosomal LSU. Modified residues analyzed in this study are shown highlighted in the same color as their helix location. aa-tRNA (yellow); peptidyl-tRNA (beige); Helix 89 (violet); h90 (olive); h91 (gold); h92 (blue); A2819 (red) yeast numbering.

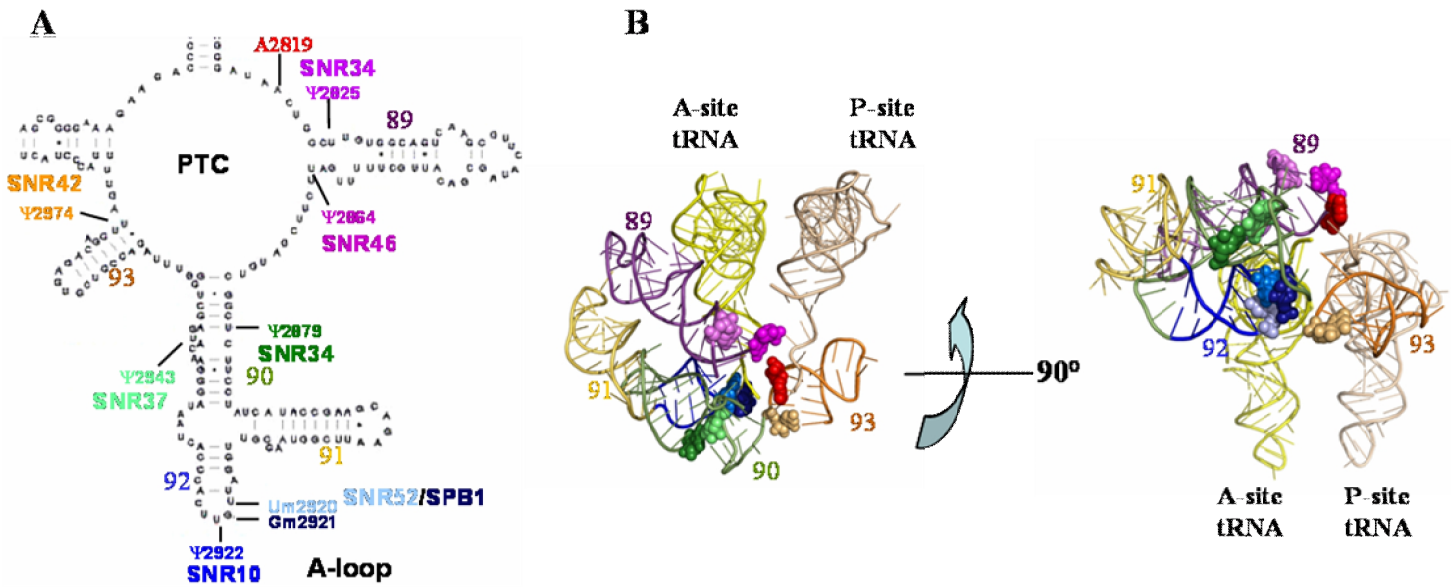

Figure 3.3

25S rRNA in the peptiptidyl transferase center of yeast.

(A) Secondary structure of yeast 25S rRNA in the PTC. SnoRNAs targeted for this study are indicated along with the residues they modify. Ψ – pseudouridylated residue; Nm – 2'-*O*-ribose methylated residue. Helices numbered in black. **(B)** Three dimensional representation of the PTC. Modified residues are labeled by the colors indicated in panel A. ***Left***: view into the PTC from the top of the LSU, ***right***: 90° rotation of ***Left***. Helices and tRNAs labeled as in Figure 3.2.

the 3' end of the peptidyl-tRNA (Jayaraman and Goldberg, 1968; Herner et al., 1969; Moazed and Noller, 1991) and can be used as a P-site specific probe. Previous studies reported that *spb1DA* mutants were sensitive to paromomycin, and that sparsomycin had no effect (Bonnerot et al., 2003). The *snr10*Δ mutant was also shown to be sensitive to paromomycin (King et al., 2003). In order to achieve a better understanding of the drug sensitivity profiles for all of the mutants, we performed standard 10-fold dilution spot assays on plates containing differing amounts for each of the translation inhibitors anisomycin and sparsomycin (Figure 3.4). The data show *spb1DA*/*snr52*Δ cells to be sensitive to anisomycin at a concentration of 20 μg/ml, with no effect on wild-type growth at this concentration. Wild-type strains show no change in growth on 20ug/ml sparsomycin, while mutants *snr34*Δ and *snr46*Δ were sensitive to the drug at this concentration.

Virus propagation in rRNA modification mutants

The yeast killer virus system is composed of the dsRNA L-A helper virus and M_1 'killer" satellite viruses. The L-A virus genome consists of two overlapping ORFs, *gag* and *pol*, which encoded the structural protein and the RNA dependent RNA polymerase respectively. The two ORFs are joined by a programmed –1 ribosomal frameshift signal where a –1 PRF event results in synthesis a gag-pol fusion protein. The M_1 satellite virus genome encodes for a secreted toxin. The pre-toxin provides the infected cell with immunity to the toxin, while secretion of the mature toxin results in death of uninfected yeast cells. A change in the efficiency of –1 PRF alters

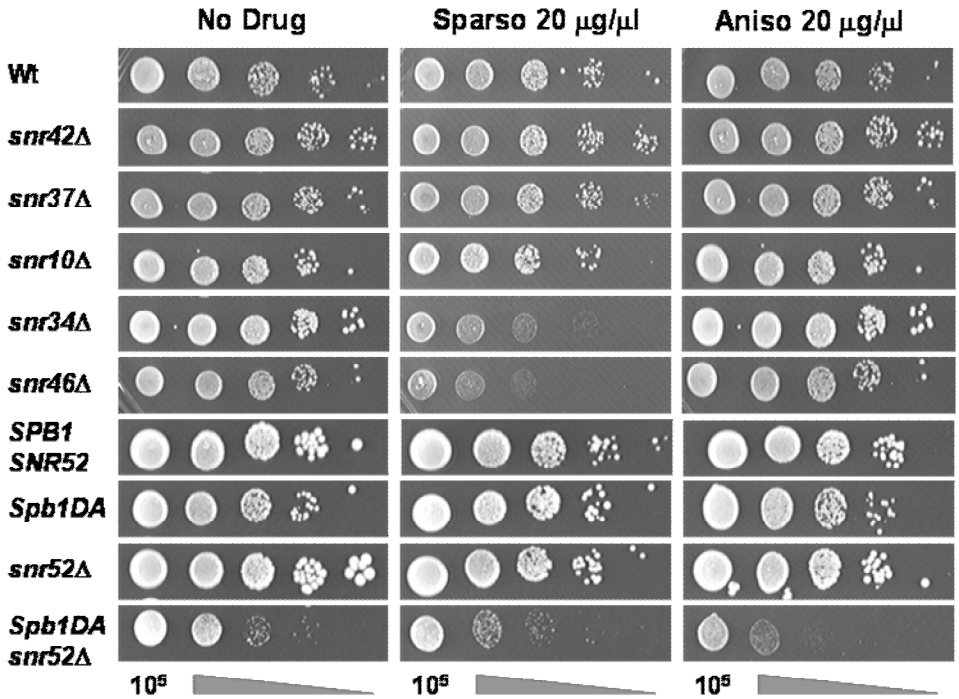

Figure 3.4

Sensitivity to Translational Inhibitors

Standard 10-fold dilution spot assays were performed to monitor growth in the presence of the translational inhibitors anisomycin and sparsomycin. Mutant and isogenic wild-type yeast strains were spotted as ten fold dilutions from 10^5 to 10^1 CFU onto YPAD media containing 20 µg/ml anisomycin or sparsomycin. Cells were incubated for 3 days at 30°C and growth was monitored as compared to growth on plates in the absence of drug. The assay was repeated at least twice. Representative pictures are shown.

the ratio of structural to enzymatic viral proteins produced for particle assembly thereby interfering with the ability of yeast to maintain the L-A helper and M_1 satellite viruses (Dinman and Wickner, 1992). M_1 propagation also depends on the level of free large subunits in yeast, such that mutants with altered amounts of free ribosomal LSU fail to maintain the M_1 virus (Wickner, 1996). The yeast killer virus model system can be utilized to identify defects in virus propagation as a possible result of altered translational fidelity, specifically programmed –1 ribosomal frameshifting. Thus, the snoRNA mutants were screened to determine their ability to maintain the M_1 killer virus as a phenotypic identifier of translational associated defects. The L-A and M_1 viruses were introduced into [rho^0] wild-type and mutant cells and assayed for the killer phenotype (Figure 3.5a). The data showed the wild-type strains and several mutants were able to maintain the killer virus (K^+). However, the mutants *snr37*Δ and *snr46*Δ showed weak killer (K^w) phenotypes, *snr10*Δ rapidly lost the killer virus (K^-), and severe viral maintenance defects were observed with the mutants *spb1DA* and *spb1DA*/*snr52*Δ. Previously published data indicates altered ribosome profiles for mutants *snr10*Δ (King et al., 2003)and *spb1DA*/*snr52*Δ (Bonnerot et al., 2003) which included ribosomal LSU defects and could be a contributing factor to their virus propagation defects.

In order to rule out the possibility that a defect in the processing or secretion of the killer toxin (Wickner, 1996) is responsible for the observed killer phenotype and not virus maintenance, double-stranded viral RNA was extracted from wild-type and

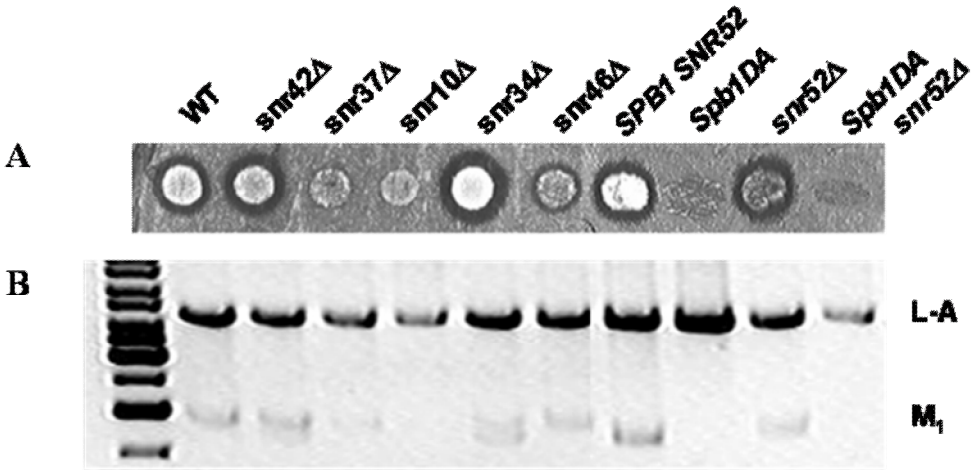

Figure 3.5

M_1 virus propagation

Yeast modification mutants were tested for their ability to maintain the yeast L-A and M_1 viruses. **(A)** Mutant and isogenic wild-type yeast strains were spotted onto YPAD plates and allowed to grow at 30°C and then replica plated to a seeded lawn of 5X47 indicator cells. Plates were incubated at room temperature for 3-5 days until a zone of inhibition was clearly visible for wild-type cells. **(B)** Total RNAs were extracted from mutant and isogenic wild-type yeast strains and digested with RNase A under high salt conditions. The resulting double-stranded RNA was separated on a 1% agarose gel and visualized with ethidium bromide. L-A and M_1 are labeled. The image was inverted for clarity.

mutant yeast cells and visualized (Figure 3.5b). The analysis revealed that M_1 dsRNA abundance correlated with the observed killer phenotypes; i.e. M_1 dsRNA was observed the in the strains which showed the K^+ phenotype and was absent or faint in strains that showed K^- or K^w phenotypes respectively.

rRNA modification mutants cause defects in translational fidelity

Defects in rRNA modification have been implicated in changes in translation rates and ribosome integrity (Gustafsson and Persson, 1998; King et al., 2003). In order to more precisely determine the role of rRNA modifications in the translational fidelity of the ribosome, we have performed assays that monitor various aspects of translational fidelity, namely changes in programmed ribosomal frameshifting, aa-tRNA selection, and nonsense suppression *in vivo*. A bicistronic dual-luciferase reporter system, described in Figure 3.6, was developed to quantitatively monitor these changes in fidelity (Harger and Dinman, 2003). The control reporter is a yeast expression vector containing *Renilla* and firefly luciferase genes, which yields active *Renilla* and firefly luciferase proteins. Programmed –1 and +1 frameshifting test reporters are constructed by inserting a frameshift signal, L-A or Ty*1* respectively, between the *Renilla* and firefly genes such that firefly luciferase is only produced in the event of a frameshift. *Renilla* luciferase serves as an internal control thereby eliminating effects due to differences in mRNA abundance, mRNA stability or translation rates between the test and control reporters. Nonsense suppression test reporters contain a stop codon (UAA, UAG, or UGA) six nucleotides into the firefly luciferase gene; therefore, firefly luciferase is only produced when nonsense suppression occurs. The misincorporation test reporters were created by mutating the

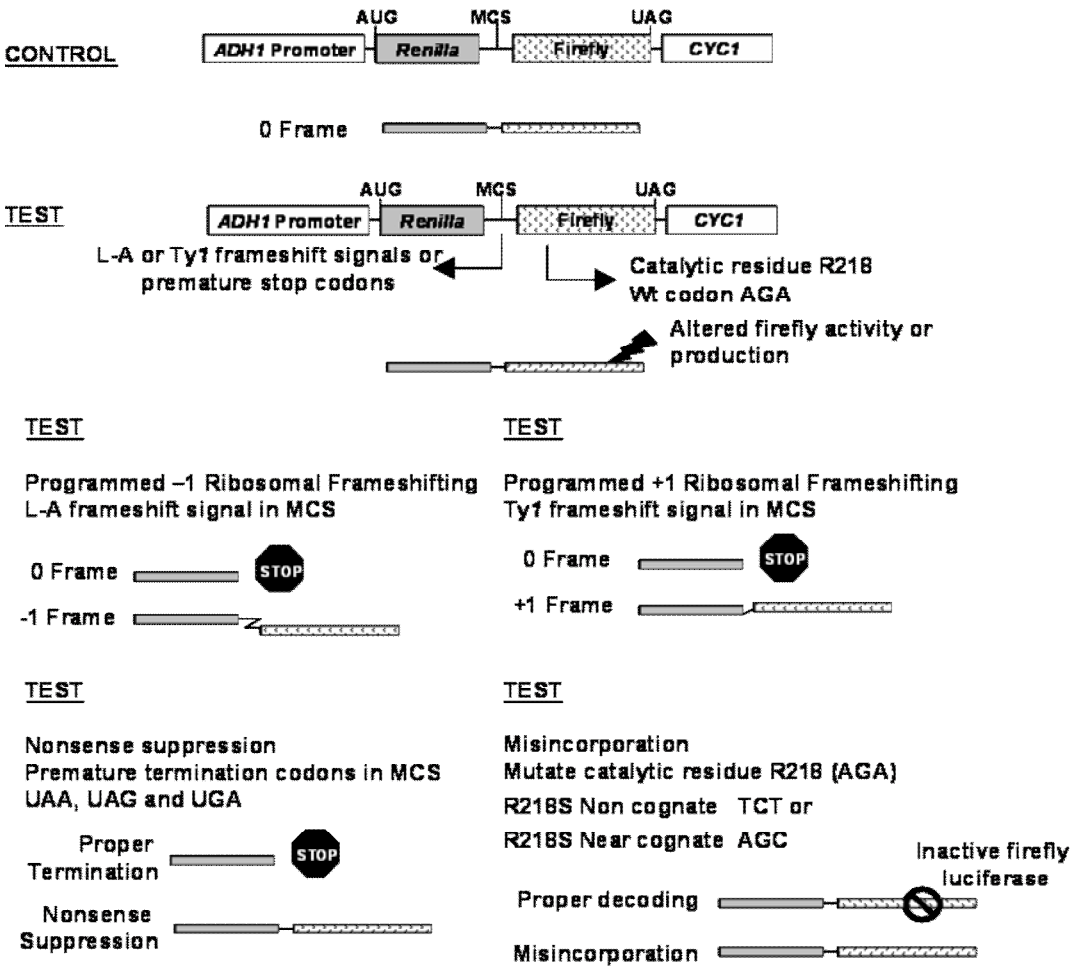

Figure 3.6
Bicistronic dual luciferase reporter system

firefly catalytic residue R218 from the wild-type AGA codon to either the near-cognate AGC codon or non-cognate TCT codon the result of which is that active firefly luciferase is only synthesized when the incorrect $tRNA^{Arg}$ is selected. Recoding efficiencies were measured for each mutant as described in the methods. The data are represented as fold wild-type values and summarized in Table 1.

The *spb1DA*/*snr52*Δ double mutant showed the largest increase in –1 PRF efficiency (1.5 fold of wild-type) (Figure 3.7). This result is in agreement with the viral propagation data as this mutant was unable to propagate the M_1 killer virus. Subtle increases in –1 PRF were observed in a few mutant strains (1.2 fold or lower). Only small (1.2 fold or lower) increases in +1 PRF were observed in any of the mutants (Figure 3.7).

Values for near and non-cognate aa-tRNA selection events are reported in Figure 3.8. The *snr10*Δ mutant strain displayed small increases in both near and non cognate aa-tRNA selection events (both 1.3 fold). The mutant *snr46*Δ shows a small increase in only non-cognate aa-tRNA selection at 1.3 fold of wild type. The double mutant *spb1DA*/*snr52*Δ shows a significant 1.9 fold increase in near cognate aa-tRNA selection events and a very slight increase in non-cognate aa-tRNA selection at 1.2 fold which is higher value than that of either of the single mutants. The *spb1DA* single mutant actually exhibits a slight (0.8 fold) decrease in non-cognate aa-tRNA selection when compared to its wild-type strain with no effect on near-cognate

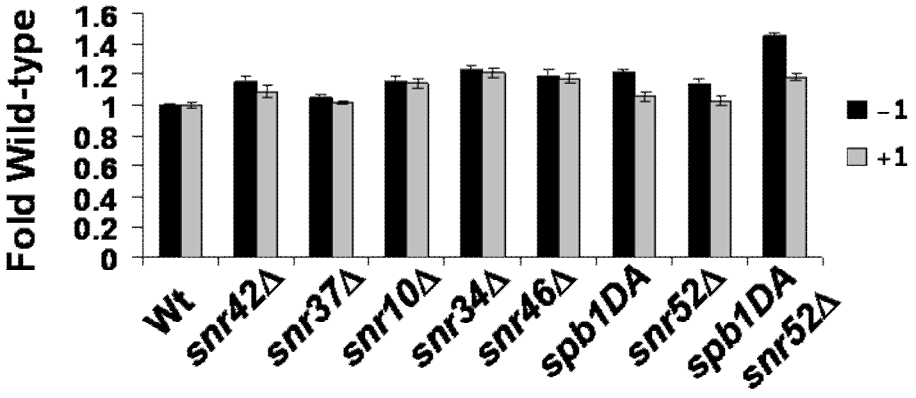

	Wt	*snr42* Δ	*snr37*Δ	*snr10*Δ	*snr34*Δ	*snr46* Δ	*spb1DA*	*snr52* Δ	*spb1DA snr52*Δ
-1PRF	**1.0** <0.1	**1.2** <0.1	**1.1** ±0.2	**1.2** <0.1	**1.2** <0.1	**1.2** ±0.1	**1.2** <0.1	**1.1** <0.1	**1.5** <0.1
+1PRF	**1.0** <0.1	**1.1** <0.1	**1.0** <0.1	**1.1** <0.1	**1.2** <0.1	**1.2** <0.1	**1.1** <0.1	**1.0** <0.1	**1.2** <0.1

Figure 3.7

Programmed Ribosomal Frameshifting

Mutant and isogenic wild-type yeast strains were each transformed with a control or test dual luciferase reporter. L-A test plasmids were used to monitor -1PRF, while Ty1 test reporter was used to monitor +1PRF. Luminescence of the *Renilla* and firefly proteins was measured and frameshifting efficiencies calculated for each strain. Frameshifting values are reported as fold change of the isogenic wild-type. Experiments were repeated at least three times or until all data were normally distributed with a confidence level >95%. Error bars represent standard error.

selection events. The *snr52*Δ single mutant shows no change in non-cognate aa-tRNA selection events, but does display a 1.4 fold increase in near-cognate values.

Nonsense suppression efficiencies were measured for each stop codon (UAA, UAG, and UGA) and reported in Figure 3.9. With the exception of *snr42*Δ, similar trends for changes in nonsense suppression are observed for all three stop codons in each mutant strain. Decreases in nonsense suppression ranging from 0.3 to 0.8 fold of wild-type were observed in mutant strains *snr37*Δ, *snr10*Δ and the double mutant *spb1DA*/*snr52*Δ. A significant increase in nonsense suppression was displayed in the *snr46*Δ mutant strain with values of 1.4, 2.0 and 1.3 fold of wild-type for stop codons UAA, UAG and UGA respectively.

Changes in aminoacyl-tRNA binding and peptidyl transfer rates

Defects in translational fidelity could possibly be due to changes in tRNA binding to the ribosome and peptidyl-transfer rates. Two phenotypically interesting mutants were chosen and biochemically characterized. The mutant strains chosen were *snr46*Δ and *spb1DA*/*snr52*Δ. The mutant *snr46*Δ showed sparsomycin sensitivity, the K^w phenotype, no significant change in +1 and –1 PRF, and exhibited increases in non-cognate aa-tRNA selection events and nonsense suppression The double mutant *spb1DA*/*snr52*Δ was anisomycin sensitive, could not propagate the M_1 virus, showed an increase in –1 PRF, an increase in near-cognate aa-tRNA selection events, and decreased nonsense suppression. Ribosomes were isolated from the isogenic wild-

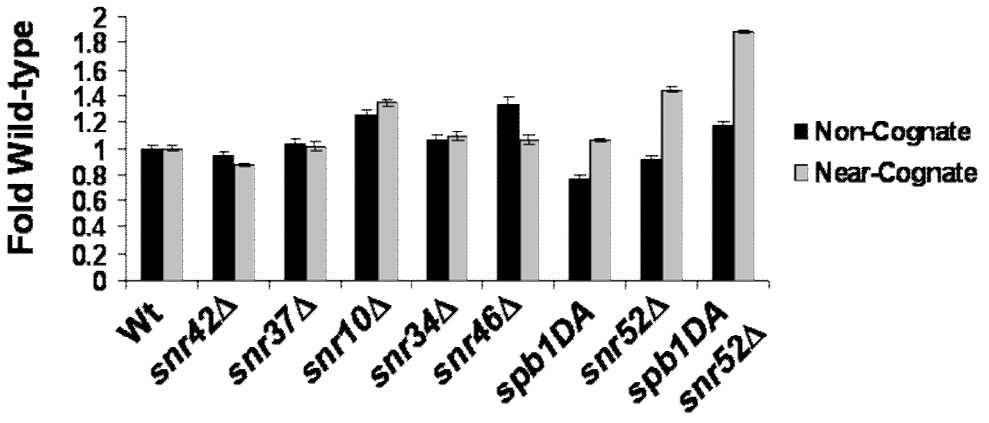

	Wt	*snr42Δ*	*snr37Δ*	*snr10Δ*	*snr34Δ*	*snr46Δ*	*spb1DA*	*snr52Δ*	*spb1DA snr52Δ*
Non cognate	**1.0** <0.1	**0.9** <0.1	**1.0** <0.1	**1.3** <0.1	**1.1** <0.1	**1.3** ±0.1	**0.8** <0.1	**0.9** <0.1	**1.2** <0.1
Near cognate	**1.0** <0.1	**0.9** <0.1	**1.0** <0.1	**1.3** <0.1	**1.1** <0.1	**1.1** <0.1	**1.1** <0.1	**1.4** <0.1	**1.9** <0.1

Figure 3.8

aminoacyl-tRNA Selection

Mutant and isogenic wild-type yeast strains were each transformed with a control or test dual luciferase reporter. Near and non-cognate test plasmids were used to monitor changes in near and non-cognate aa-tRNA selection events, respectively. Luminescence of the *Renilla* and firefly proteins was measured and efficiencies calculated for each strain. Values are reported as fold change of the isogenic wild-type. Experiments were repeated at least three times or until all data were normally distributed with a confidence level >95%. Error bars represent standard error.

types and mutant strains and the affinities for aa- and peptidyl-tRNA as well as peptidyl transfer rates were determined as described in the methods**.** The binding constants determined for aa-tRNA affinity to mutant and wild-type ribosomal A-site indicated increased binding to the A-site for both mutants (Figure 3.10). The wild-type isogenic to the mutant *snr46*Δ Kd_{app} was 1.8 μM^{-1} ±0.4 while the mutant Kd_{app} was determined to be 0.3 μM^{-1} ±0.05. Similarly, wild-type SPB1 SNR52 was shown to have a Kd_{app} of 0.6μM^{-1} ±0.2 while the mutant strain *spb1DA*/*snr52*Δ showed a Kd_{app} of 0.3 μM^{-1} ±0.1. Different wild-type binding constants are observed because the two wild-type stains are not isogenic. Affinities of tRNA for the ribosomal P-site were measured as described in methods using [^{14}C]-Ac-Phe-tRNA and the isogenic wild-type and mutant ribosomes (Figure 3.11). There was no change in Kd_{app} for P-site binding of either mutant when compared to their isogenic wild-type strain. Peptidyl-transfer rates were measured using the puromycin reaction as described in the methods. Both mutant strains displayed increases in peptidyl-transfer rates when compared to isogenic wild-type values (Figure 3.12). The K_{app} of the mutant *snr46*Δ was 0.06 min^{-1} ±0.003 while its isogenic wild-type showed a K_{app} value of 0.04 min^{-1} ±0.003. Wild-type SPB1 SNR52 was shown to have a K_{app} of 0.02 min^{-1} ±0.004 while the mutant strain *spb1DA*/*snr52*Δ showed a K_{app} of 0.04 min^{-1} ±0.007.

Structure changes observed in the PTC of a modification deficient ribosome

It has been speculated that the post-transcriptional nucleotide modification like that demonstrated in rRNA could serve to increase the stability of the local RNA structure or decrease risk of degradation (Decatur and Fournier, 2002; Helm, 2006). With this

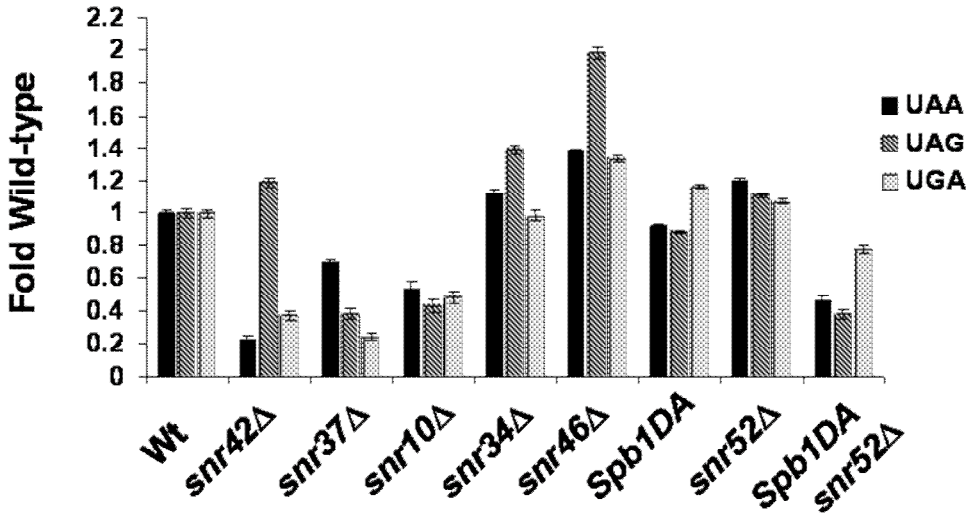

	Wt	*snr42Δ*	*snr37Δ*	*snr10Δ*	*snr34Δ*	*snr46 Δ*	*spb1DA*	*snr52 Δ*	*spb1DA snr52 Δ*
UAA	1.0 <0.1	0.2 <0.1	0.7 <0.1	0.5 ±0.1	1.1 <0.1	1.4 <0.1	0.9 <0.1	1.2 <0.1	0.5 <0.1
UAG	1.0 <0.1	1.2 <0.1	0.4 <0.1	0.4 <0.1	1.4 <0.1	2.0 <0.1	0.9 <0.1	1.1 <0.1	0.4 <0.1
UGA	1.0 <0.1	0.4 <0.1	0.3 <0.1	0.5 <0.1	1.0 <0.1	1.3 <0.1	1.2 <0.1	1.1 <0.1	0.8 <0.1

Figure 3.9

Nonsense suppression

Mutant and isogenic wild-type yeast strains were each transformed with a control or test dual luciferase reporter. Nonsense suppression test plasmids were used to monitor changes in readthough of each stop codon: UAA, UAG, and UGA. Luminescence of the *Renilla* and firefly proteins was measured and stop codon readthrough efficiencies calculated for each strain. Values are reported as fold change of the isogenic wild-type. Experiments were repeated at least three times or until all data were normally distributed with a confidence level >95%. Error bars represent standard error.

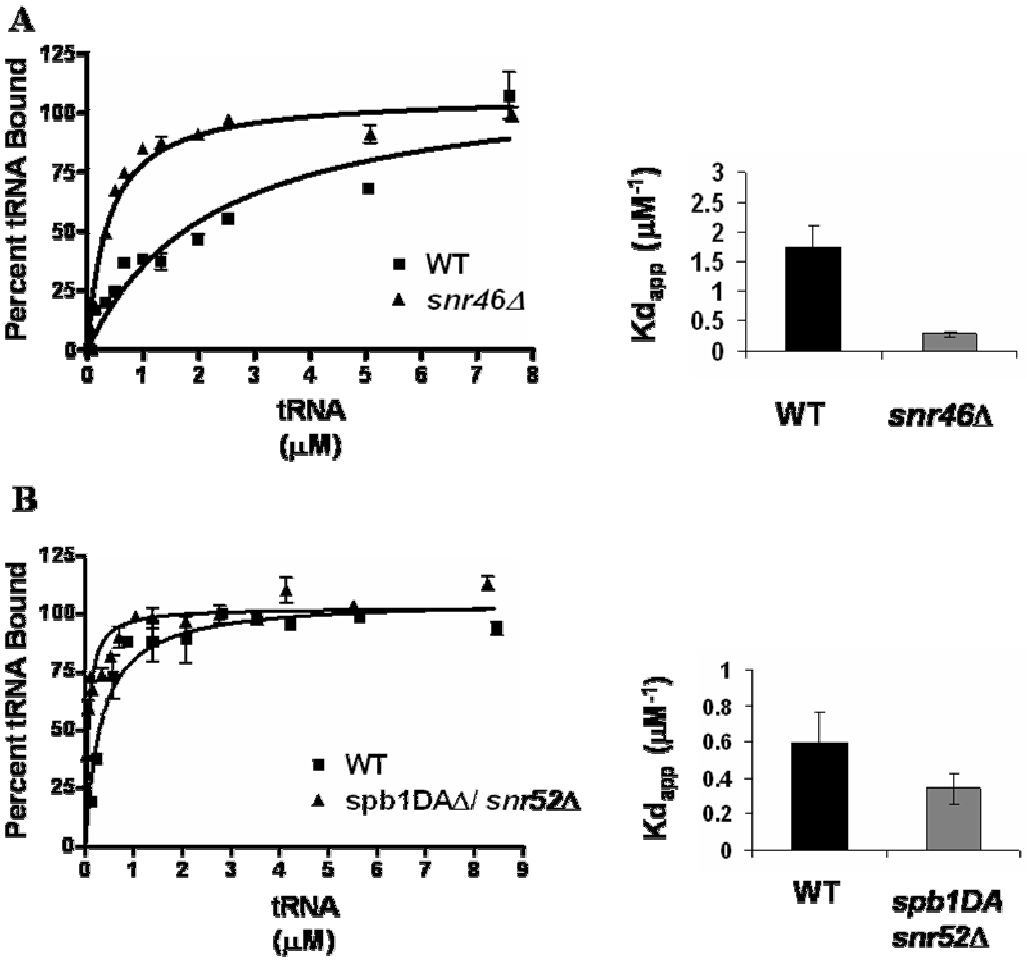

Figure 3.10

Phe-tRNA binding to the A-site of the ribosome

One site binding curves of bound tRNA as analyzed using GraphPad Prism software. Data are reported as a percentage of the total tRNA bound. Charts represent the dissociation constant values calculated from the binding curve. (A) Mutant strain *snr46Δ* and the isogenic wild-type. (B) Mutant *strain spb1DA/snr52Δ* and the isogenic wild-type. Error bars represent standard error.

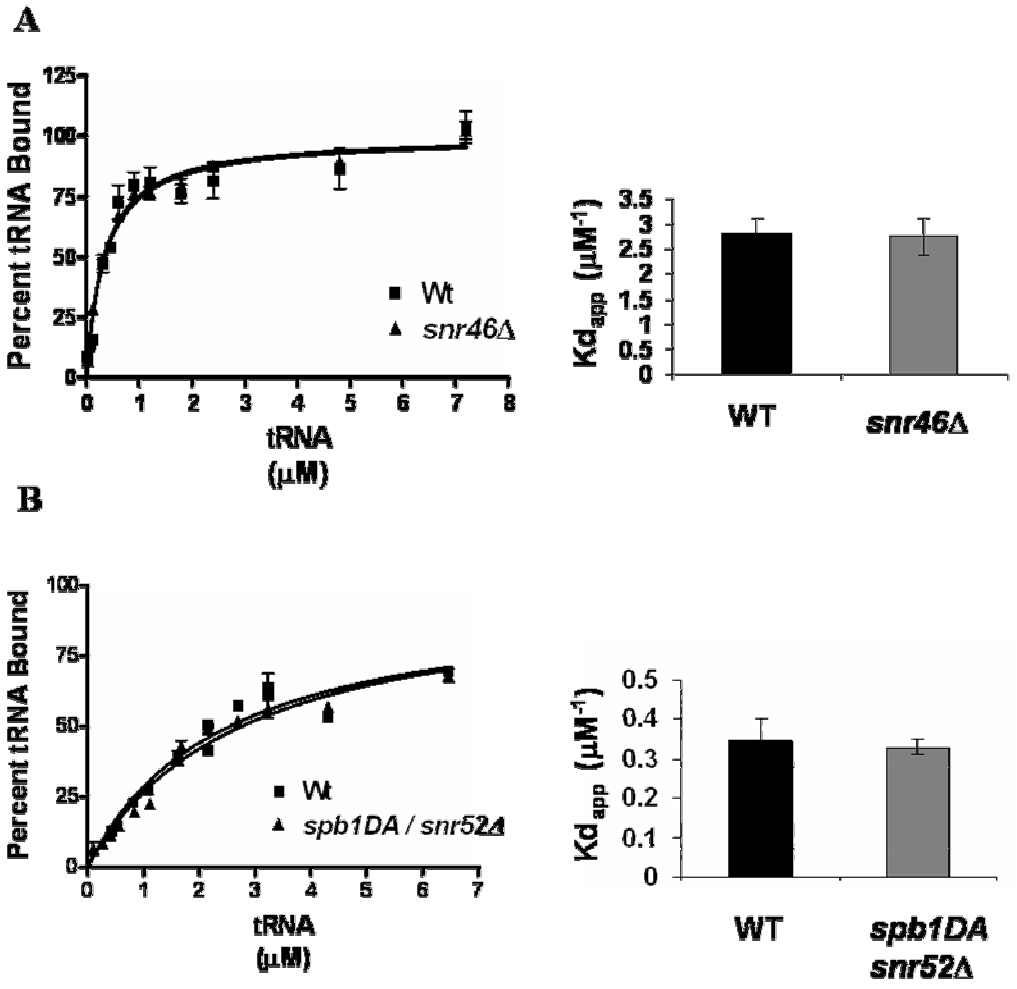

Figure 3.11

Ac-Phe-tRNA binding to the P-site of the ribosome

One site binding curves of bound tRNA as analyzed using GraphPad Prism software. Data are reported as a percentage of the total tRNA bound. Charts represent the dissociation constant values calculated from the binding curve. (A) Mutant strain *snr46Δ* and the isogenic wild-type. (B) Mutant *strain spb1DA/snr52Δ* and the isogenic wild-type. Error bars represent standard error.

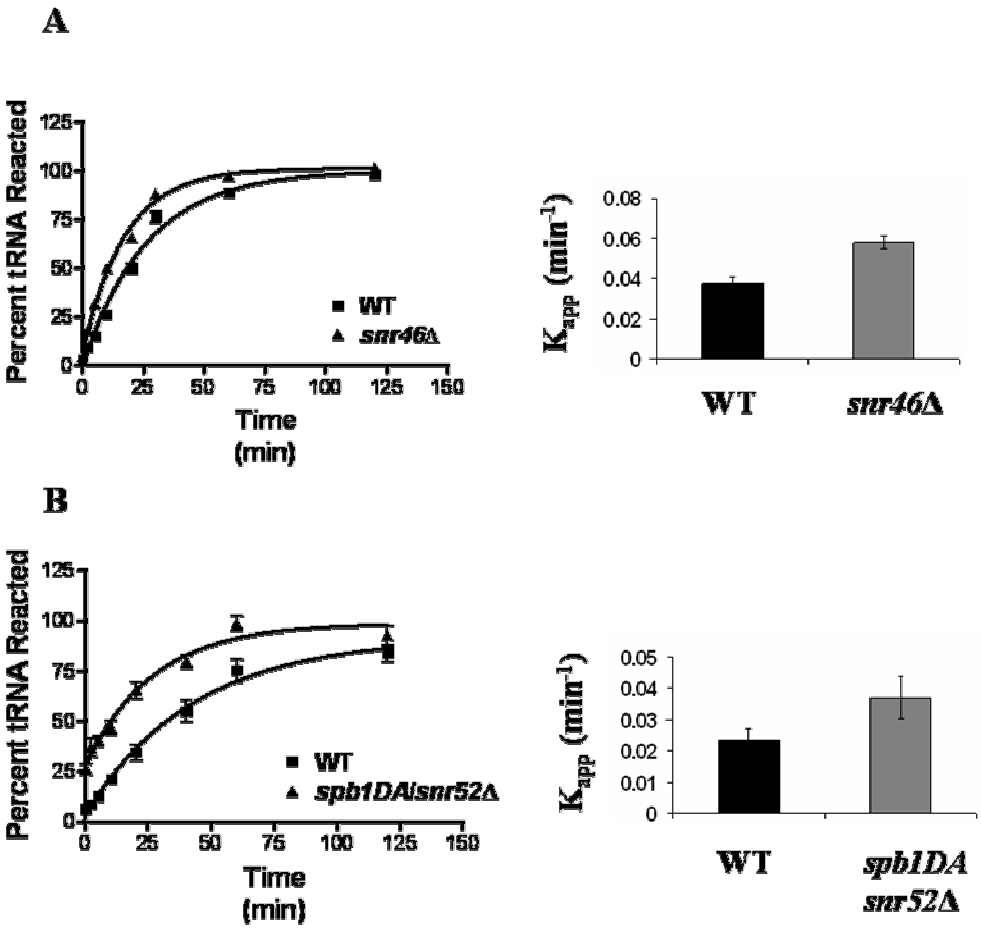

Figure 3.12

Peptidyl transfer

Curves representing peptidyl transfer as measured by the puromycin reaction. The data were analyzed using GraphPad Prism software. Data are reported as a percentage of the total tRNA reacted with puromycin. (A) Mutant strain *snr46Δ* and the isogenic wild-type. (B) Mutant *strain spb1DA/snr52Δ* the isogenic wild-type. Error bars represent standard error.

		Wt	*snr42Δ*	*snr37Δ*	*snr10Δ*	*snr34Δ*	*snr46Δ*	*spb1DA*	*snr52Δ*	*spb1DA snr52Δ*
	Killer	K^+	K^+	K^w	K^-	K^+	K^w	K^-	K^+	K^-
Drug sensitivity	Aniso	NE	NE	NE	NE	NE	NE	NE	NE	S
	Sparso	NE	NE	NE	NE	S	S	NE	NE	NE
Programmed Frameshifting	-1PRF	1.0	1.2	1.1	1.2	1.2	1.2	1.2	1.1	1.5
	+1PRF	1.0	1.1	1.0	1.1	1.2	1.2	1.1	1.0	1.2
Misincorporation	Non Cognate	1.0	0.9	1.0	1.3	1.1	1.3	0.8	0.9	1.2
	Near Cognate	1.0	0.9	1.0	1.3	1.1	1.1	1.1	1.4	1.9
Nonsense Suppression	UAA	1.0	0.2	0.7	0.5	1.1	1.4	0.9	1.2	0.5
	UAG	1.0	1.2	0.4	0.4	1.4	2.0	0.9	1.1	0.4
	UGA	1.0	0.4	0.3	0.5	1.0	1.3	1.2	1.1	0.8
Biochemical Characterization	A-site Binding	1.0	-	-	-	-	0.2	-	-	0.6
	P-site Binding	1.0	-	-	-	-	1.0	-	-	1.0
	Petidyl Transfer	1.0	-	-	-	-	1.6	-	-	1.5

Table 1:

Summary of rRNA modification mutant phenotypes

All values are reported as fold of the isogenic wild-type values except drug sensitivity and killer virus maintenance data.

in mind, *in vitro* structural probing was performed on the wild-type and mutant ribosomes biochemically characterized in the previous section. Mutants *snr46*Δ and *spb1DA*/*snr52*Δ and isogenic wild-type puromycin treated ribosomes were incubated with the chemically modifying agents CMCT, kethoxal and DMS *in vitro*. The rRNAs were extracted and primer extension analyses performed using primers sufficient to transverse the entire PTC i.e. helices 89-93. Figure 3.13 shows a representative autoradiogram for the wild-type and mutant *spb1DA*/*snr52*Δ strains with each primer 25-6 and 25-10. Observed differences between wild-type and mutant protection patterns and their nucleotide locations are indicated. Residues C2843 and C2851 in helix 93 were deprotected in the presence of DMS treatment. The A-loop residue U2923 showed increased protection from CMCT treatment. There were no significant differences between protection patterns observed for isogenic wild-type and mutant *snr46*Δ ribosomes (data not shown).

Discussion

Although decoding takes place in the small ribosomal subunit, it is not surprising that the large subunit would play a part in determining translational fidelity. The large subunit interacts with all but the anti-codon stems of both the A- and P- site tRNAs, binds elongation factors including the EF-Tu:GTP:tRNA[13] ternary complex and EF-G:GTP[14], and is the site of release factor binding. Previous studies have shown that mutations in rRNA residues of helix 89 in the peptidyl transferase center

[13] eEF-1:GTP:tRNA in eukaryotes
[14] eEF-2:GTP in eukaryotes

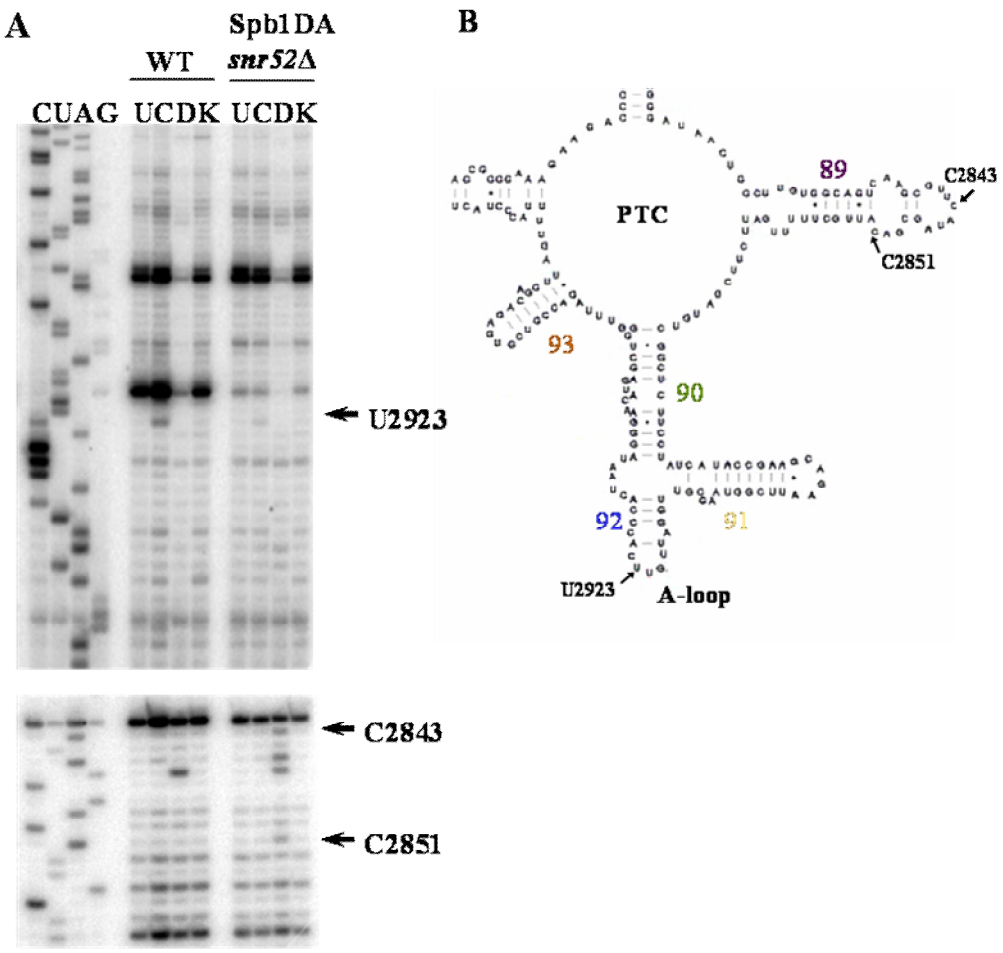

Figure 3.13

Structure Probing Analysis

Ribosomes were isolated for *spb1DA/snr52Δ* mutant and isogenic wild-type strains, puromycin treated and used for ***in vitro*** chemical probing of the structure in the peptidyl transferase center of the ribosome, specifically helices 89-93. Reactions performed in duplicate, representative autoradiographs shown in **(A)**. U - untreated; C - CMCT; D – DMS; K – Kethoxal. Residues with changes in banding pattern labeled. **(B)** Secondary structure of yeast 25S rRNA. Residues with changes in banding pattern indicated.

of *E. coli* ribosomes result in defects in stop codon recognition and reading frame maintenance (O'Connor and Dahlberg, 1995). Interestingly, residues in helix 89 along with other residues within the peptidyl transferase center are post-transcriptionally modified, although the functional contributions of this residue are unknown. The snoRNAs characterized in the current are snR10, snR34, snR37, snR42, snR46, snR52 and the essential yeast protein Spb1p which modify residues Ψ_{2922}, Ψ_{2825}/Ψ_{2879}, Ψ_{2943}, Ψ_{2864}, Um_{2920} and Gm_{2921} respectively. The modified residues are located on helices 89-93 of the PTC of the yeast ribosome (Figures 3.2 and 3.3). Modification of residue Ψ_{2825} is guided by snR34 in yeast and is conserved through evolution. However, deletion of snR34 or *RluE*, the gene responsible for the homologous modification in *E. coli*, conferred no obvious disadvantage (Samarsky et al., 1995; Del Campo et al., 2001; King et al., 2003). Residues Um_{2920} and Gm_{2921} modified by snR52 and the protein Spb1p respectively are also conserved throughout evolution. Residue Gm_{2921} has been shown to interact with the 3' end C75 of the A-site tRNA (Mueller et al., 2000). Strains lacking each of these eight PTC modifications, and one strain lacking two were investigated to determine the contributions that each of these modifications made to translational fidelity.

Biochemical characterization of the *spb1DA*/*snr52*Δ double mutant revealed an increase in peptidyl transfer rates for the mutant ribosome as determined by the puromycin reaction assay. Since peptidyl transfer is an extremely fast reaction, occurring almost instantaneously (Katunin et al., 2002), it is interesting that mutant ribosomes could perform the reaction any faster than wild-type. To understand these

data, it is necessary to analyze them in the context of the assay. Puromycin is an A-site tRNA analog that mimics its aminoacylated 3'CCA end (de Groot et al., 1970; Hansen et al., 2003a). The puromycin reaction assay involves the diffusion of puromycin into the A-site of ribosomes pre-loaded with peptidyl-tRNA, peptidyl transfer takes place and the resulting puromycin bound tRNAs are measured. Therefore, any increase in peptidyl transfer rates could result from an increase in the rate at which puromycin diffuses into the A-site. This could suggest that these mutant ribosomes have A-sites that are more accessible. Structure probing analyses of *spb1DA*/*snr52*Δ mutant ribosomes demonstrated changes in the protection patterns that are consistent with a more open A-site conformation (Figure 3.13). Two residues, C2843 and C2851, displayed decreased protection from DMS treatment, and one residue, U2923, showed increased protection from CMCT. Residue C2851 is located on helix 89 and makes direct contacts with the A-site tRNA (Figure 3.14). The fact that the residue is deprotected suggests that contacts with the A-site tRNA are abolished possibly resulting in a more open conformation around the A-site tRNA. Residue U2923 provides further insight into the A-site changes observed for this mutant. This residue is located on the A-loop and is adjacent to the gate residue C2924, one of the nucleotides which form the first gate that the 3' of the aa-tRNA has to pass through as it accommodates into the PTC (Figure 3.14). This residue is also two and three nucleotides away from residues Gm2921 and Um2920, respectively, which are lacking their modifications in this mutant. It may be that the absence of these methylations causes a shift in the local conformation causing U2923 to move into a more protected region. It would follow that the adjacent gate nucleotide would

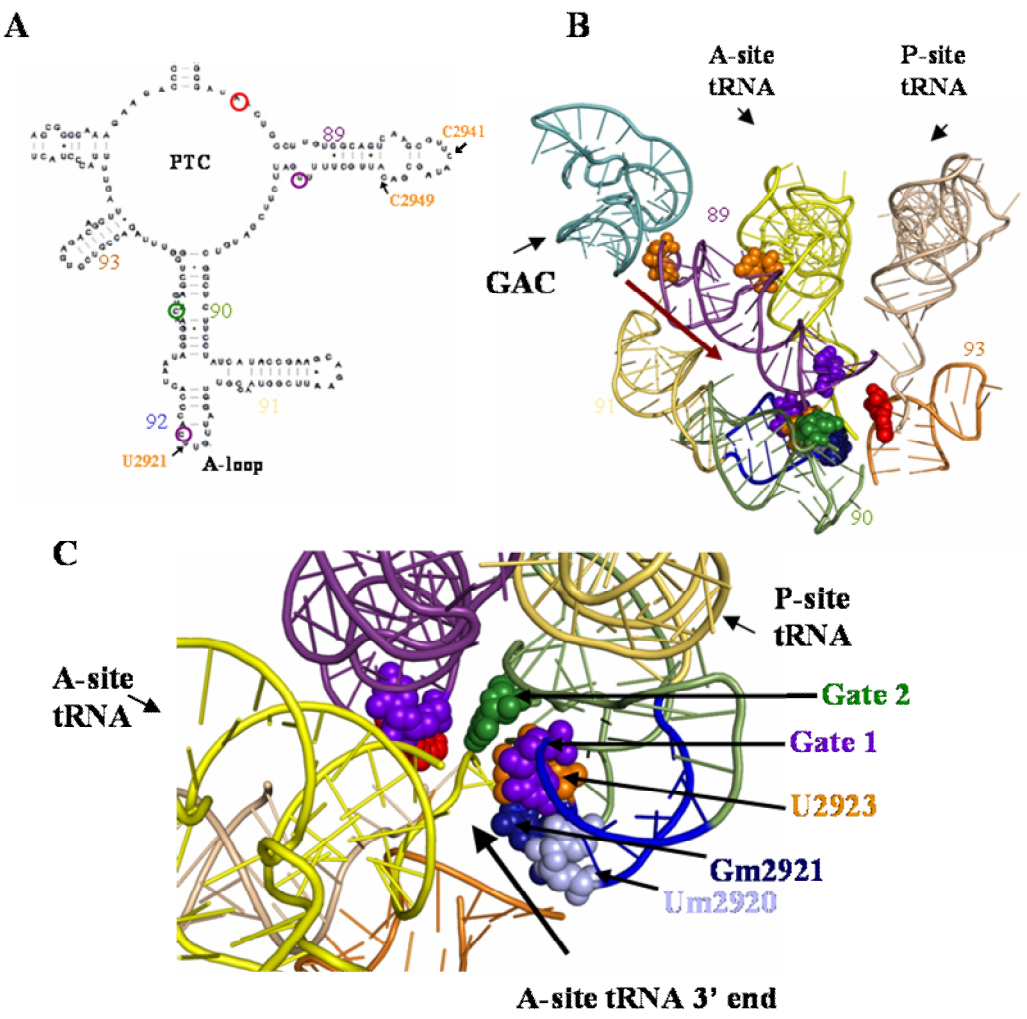

Figure 3.14

Structural changes in *spb1DA/snr52Δ* mutant ribosomes

Location of residues demonstrating changes in protection patterns from the structure probing analyses of *spb1DA/snr52Δ* mutant ribosomes when compared to wild-type. **(A)** Secondary structure of yeast 25S rRNA in the PTC. **(B)** Three dimensional representation of the PTC. Red arrow represents the path the 3' end of the aa-tRNA travels when entering the A-site. **(C)** Rotation and zoom in of Panel B. Shows the path into the A-site from the aa-tRNA perspective. Residues demonstrating changes in protection patterns are labeled in orange. A-site 'gate' residues are labeled in indigo (gate 1) and green (gate 2). Helices and other residues labeled as in Fig. 3.3.

shift as well, most likely away from its partner residue, U2860, involved in creating the first gate. This would open up the first gate producing a more accessible conformation with less steric hindrance to puromycin diffusion which would result in the observed increase in peptidyl transfer rates.

All other biochemical and genetic phenotypes observed for this mutant are in agreement with this model. Further biochemical characterization of *spb1DA*/*snr52*Δ revealed increased rates of A-site tRNA binding. The open conformation of the A-site in mutant ribosomes would allow for easier accommodation of the aa-tRNA thereby resulting in this observed increase in affinity for aa-tRNA. It would also follow that opening up the A-site and disabling the accommodation gate would produce a less discriminate A-site. This is consistent with the observed increase in near cognate aa-tRNA selection events (1.9 fold of wild-type) for the *spb1DA*/*snr52*Δ mutant strain.

The mutant also promoted increased rates of -1 PRF (1.5 fold over wild-type) and demonstrated anisomycin sensitivity. These two phenotypes are usually associated with decreased A-site binding, while increased A-site binding usually correlates with anisomycin resistance (Meskauskas et al., 2003; Meskauskas et al., 2005). Normally, defects in the ribosome that decrease its affinity for A-site tRNA also lead to increases in -1 PRF through an increased pause time during accommodation allowing more time for slippage, and since anisomycin can compete with A-site tRNA binding (Carrasco et al., 1973) , mutant strains with decreased affinity for aa-tRNA have

additional problems with accommodation resulting in reduced viability in the presence of anisomycin. Here, we see ribosomes with an increased affinity for A-site tRNA but are sensitive to anisomycin. However, these data could result from a more open, less discriminate ribosomal A-site. A less stringent A-site may promote the binding of, or increase the diffusion rates for, small molecules like anisomycin. This could interfere with peptidyl transfer causing the decreased growth in the presence of anisomycin observed for the mutant strain. It may also be that a less discriminate A-site with a more open conformation could better facilitate tRNA slippage thereby increasing -1 PRF rates. Additionally, the deprotection of residue C2851 may indicate suboptimal placement of the A-site tRNA which could also facilitate slippage thereby increasing -1 PRF rates. The inability of the *spb1DA*/*snr52*Δ mutant strain to propagate the killer virus is consistent with increased -1 PRF efficiencies. However, previous studies have also indicated that this mutant displayed altered ribosome profiles (Bonnerot et al., 2003) which could also contribute to its complete inability to maintain the killer virus independent of changes in -1 PRF (Ohtake and Wickner, 1995a). Finally, that +1 PRF, which only involves peptidyl-tRNA slippage, was not affected is consistent with the lack of effects on P-site tRNA binding and with the absence of structural changes in the area surrounding the peptidyl-tRNA.

All mutant strains were also tested for changes in nonsense suppression for all three stop codons, and phenotypic changes were observed for several mutants including *spb1DA*/*snr52*Δ. Class 1 release factors span the decoding center to the peptidyl transferase center (Rawat et al., 2003). It is not unexpected that changing the

local conformation of the large subunit in the PTC region of the yeast ribosome would have affects on translation termination. Cryo-EM structures of a class 1 release factor bound to the *E. coli* ribosome indicate that regions of the protein make contacts with portions of the large subunit including the GTPase associated center, and helices 89, 92 and 93 of the PTC (Figure 3.15) (Klaholz et al., 2003; Petry et al., 2005). Mutant strain *spb1DA*/*snr52*Δ exhibited a decrease in nonsense suppression for all three stop codons when compared to wild-type values indicating an increase in the fidelity of stop codon recognition. Since *spb1DA*/*snr52*Δ demonstrated an increase in near cognate aa-tRNA selection events, it is surprising that the fidelity of stop codon recognition was increased. It may be that the mechanisms allowing for less stringent aa-tRNA selection extends to the binding and recognition of the release factor thereby increasing stop codon recognition. It may also be that changes in the PTC of these mutants facilitate the peptidyl-tRNA hydrolysis reaction. Crystal structure analysis of the ribosome in complex with release factors 1 and 2 show the conserved RF1 GGQ motif in close proximity to the A loop of the peptidyl transferase center (Figure 13.6). Since the mutant strain *spb1DA*/*snr52*Δ lacks the methylation of two residues found on the A-loop, it is conceivable that these mutant ribosomes could alter release factor binding or activity either through direct interactions or by inducing local conformational changes. Structure probing analyses of themutant strain *spb1DA*/*snr52*Δ did demonstrate an increased protection for residue U2923 which is also located on the A-loop indicating local conformational changes for the A-loop of mutant ribosomes.

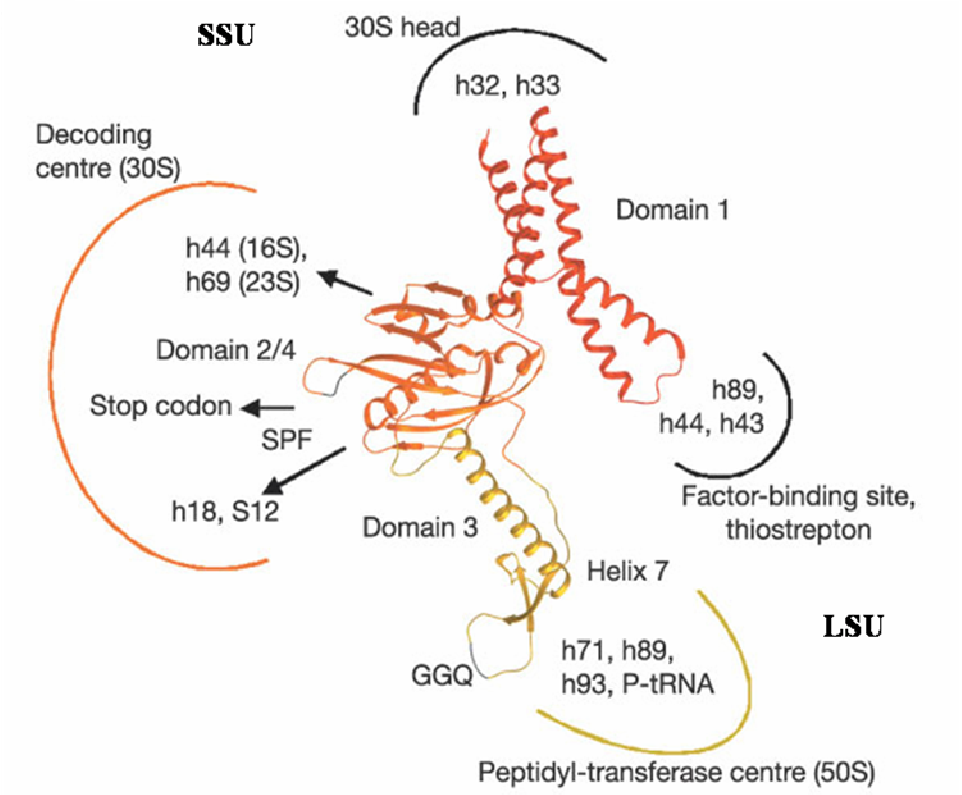

Figure 3.15

Interactions between RF2 and the *E. coli* ribosomal large and small subunit

The derived *in situ* RF2 structure and its interaction with the LSU. *In situ* RF2 areas involved in transmission of the decoding signal (left) to the PTC (bottom right). The main ribosomal proteins and RNA helices involved are indicated. Figure and legend adapted from Klaholz et al., 2003.

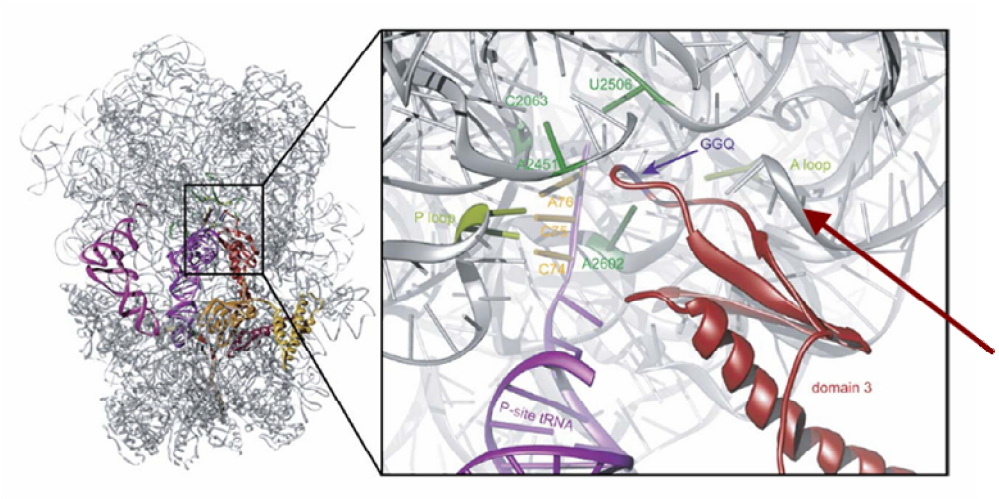

Figure 3.16

Interaction of RF1 with the PTC ribosomal large subunit

Close up of the interaction of the RF1 GGQ motif with the ribosomal large subunit. The red arrow points to the A-loop of helix 92 in the PTC of the ribosome. Figure adapted from Petry, 2005.

These data taken together suggest that the mutant ribosomes harboring methylation deficient residues U2920 and G2921 have a less discriminate A-site with a more open conformation. It would appear that residues Um2920 and Gm2921 function, at least in part, to facilitate entry of the proper aa-tRNA into the A-site by correctly positioning helix 89 and the gate residue C2924.

Structure probing of *spb1DA*/*snr52*Δ mutant ribosomes also revealed the deprotection of residue C2843 which makes direct contact with the GTPase associated center (GAC) of the ribosome. An alternative, but not mutually exclusive, explanation to the one proposed above could be that changes in the conformation of this functional center of the ribosome could also cause the changes in both nonsense suppression and the decreased discrimination in aa-tRNA selection. The GAC is a flexible region of the ribosome and its conformation changes with its functional state (Valle et al., 2003). It has been proposed that the different orientations of the GAC provide factor binding discrimination between EF-Tu:GTP and EF-G:GTP (Sergiev et al., 2005a). Interestingly, mutational studies of LSU rRNA designed to mimic the different GAC conformations demonstrates changes in chemical protection patters for helix 89 when the GAC position is altered (Sergiev et al., 2005b) It may be that the structural changes observed for the *spb1DA*/*snr52*Δ mutant ribosomes on helix 89 where it contacts the GAC indicates changes in the local conformation affecting the GAC. This could alter interactions with EF-Tu causing changes in initial tRNA binding and subsequent GTP hydrolysis which may explain the decrease in aa-tRNA discrimination and the increase in aa-tRNA binding to the A site. Similarly, changes

in the GAC that would interfere with EF-G binding and translocation could increase the pause time during -1PRF thereby increasing the chance for slippage resulting in the observed increase in -1PRF efficiencies. It has also been shown that mutations in the GAC in *E. coli* ribosomes can affect nonsense suppression by causing an increase in stop codon readthrough (Arkov et al., 1998). Therefore, it is not unreasonable to speculate that changes in the local conformation of the GAC and the PTC could cause the observed decrease in stop codon readthrough seen for the *spb1DA*/*snr52*Δ mutant strain. Further structure probing analyses of the GAC and surrounding areas would be required to investigate this model.

tRNA binding experiments performed with *snr46*Δ mutant ribosomes revealed an increase in A-site tRNA binding when compared to wild-type ribosomes, but no effect on P-site binding. This result was somewhat unexpected because the mutant strain also exhibited sparsomycin sensitivity which would suggest a P-site specific defect. This may be explained by the nature of sparsomycin. Although sparsomycin does not interfere with A-site substrate binding (Goldberg and Mitsugi, 1966; Monro et al., 1969), it does compete with A-site binding antibiotics for binding to the bacterial ribosome (Barbacid and Vazquez, 1974; Lazaro et al., 1991). Additionally, mutating residues or eliminating a modification of a residue in the PTC not in the P-site of Halobacterium results in sparsomycin resistance (Lazaro et al., 1996; Tan et al., 1996). Presumably, this is because sparsomycin stacks with the flexible A2606 (*E. coli* numbering; yeast A2970) upon binding to unoccupied ribosomes causing conformational changes throughout the PTC (Porse et al., 1999). It is possible that

the PTC of the mutant *snr46*Δ is altered in such a way as to foster increased sensitivity to sparsomycin. Increased rates of A-site tRNA binding for *snr46*Δ can be consistent with slightly increase in non-cognate aa-tRNA selection events (1.3 fold over wild-type) in that increased rates of the forward reaction involved in initial selection, GTP hydrolysis, could both increase rates of A-site tRNA binding and more easily allow for the incorporation of non-cognate tRNAs. Further biochemical analyses revealed that the mutant strain *snr46*Δ also promoted increased rates of peptidyl transfer. However, structure probing of helices 89-93 of *snr46*Δ mutant ribosomes with CMCT, DMS and kethoxal failed to reveal any major changes in structure. It may be, that since accommodation is the rate limiting step for peptidyl transfer, mutant ribosomes with increased rates of A-site tRNA binding would lead to an increased rate of peptidyl transfer when compared to wild-type ribosomes. Since these mutant ribosomes also exhibit increased accessibility to sparsomycin, this may reflect increased accessibility of the ribosome to puromycin as well. It is also possible that structural changes are present in *snr46*Δ mutant ribosomes but are too subtle to be detected by the techniques used.

Mutant strain *snr46*Δ displayed an increase in nonsense suppression indicating a decrease in the fidelity of stop codon recognition. This mutant also showed increase in non-cognate aa-tRNA selection. It would appear that defects in translational fidelity of this mutant extend into inefficient stop codon recognition as well as a less stringent aa-tRNA initial selection step. Structure probing of the helices in the PTC of the mutant ribosomes did not reveal any significant structural changes. However,

snR46 pseudouridylates a residue at the base of helix 89, and mutations made in helix 89 have previously been shown to cause increased rates of stop codon readthrough (O'Connor and Dahlberg, 1995). Helix 89 also comes in contact with the GTPase associated center of the ribosome which has also been implicated in changes in stop codon readthrough (Arkov et al., 2002). Therefore, it is conceivable that changes made in this region could produce nonsense suppression phenotypes. It may also be that structural changes are present in areas of *snr46*Δ mutant ribosomes that were not the focus of the chemical probing experiments.

These data, taken together, show that rRNA nucleotide modifications produce small but distinct changes in ribosome structure and function contributing to overall translational fidelity. The double mutant *spb1DA*/*snr52*Δ displayed the most severe phenotypic defects. This is most likely due to dramatic changes in local rRNA structure resulting from the loss of the methyl groups on two adjacent rRNA residues in the A-loop. Significant changes in translational fidelity were observed in mutant strain *snr46*Δ, although no changes in structure were perceived for this mutant. It may be that this and other mutants do result in changes in rRNA structure, but that they were too subtle to be detected by the methods employed. However, their effects were magnified by the biological process, such that they resulted in the observed phenotypes. Our conclusion is that rRNA base modification serves to fine-tune ribosome structure by facilitating structural conformations that promote optimal function.

Chapter 4: Conclusions and Future Directions

Vast amounts of cellular resources are dedicated to production of ribosomes. It is a very complex and highly coordinated process. Central to this process is the manufacture, modification and assembly of ribosomal RNA. Analyses in this study strive towards achieving a better understanding of the role modifying enzymes play in rRNA production and the resulting integrity of the final product.

The *RPD3* gene encodes a histone deacetylase that is involved in silencing of the *HM* mating loci, telomeres and rDNA in yeast. A mutant allele of *RPD3*, *mof6-1* demonstrated defects in rRNA processing resulting in changes in translational fidelity. Mutant phenotypes included sensitivity to the translational inhibitors anisomycin and paromomycin, increased rates of programmed -1 ribosomal frameshifting, decreased growth rates which was most severe in lag phase growth, and decreased protein synthesis rates. Biochemical characterization revealed decreased rates of A-site aa-tRNA binding and peptidyl transfer. Mutant phenotypes were dependent on histone deacetylase activity. These mutant phenotypes may be a result of altered timing of rRNA processing events. Alternatively, mutating *RPD3* may interfere with the transcription of rRNA processing pathway components including snoRNAs. It is also interesting to speculate that there may be a novel function for *RPD3* perhaps involving modification of ribosomal proteins or other components of the processing machinery.

An integral part of rRNA processing during ribosome biogenesis is the modification of rRNA residues. In eukaryotes, rRNA modifications are guided by box H/ACA and C/D snoRNAs. These modifications cluster in conserved regions of functional importance within the ribosomes. They are present in ribosomes of all kingdoms studied to date and their numbers increase with evolutionary complexity. However, individual modifications are usually dispensable for cell viability. Despite extensive mapping and study of these modified residues, their precise function is largely unknown. Here we have analyzed several mutants deficient in rRNA modifications of the peptidyl transferase center of the yeast ribosome for changes in translational fidelity. The data reveal a vital role for at least two rRNA modifications in ensuring the accommodation of the correct aa-tRNA into the A-site of the ribosome, and another modification that appears to be involved in the fidelity of translation termination.

The mutant strain *spb1DA/snr52*Δ was deficient in the methylation of A-loop residues Um2929 and G2921. This mutant demonstrated increased sensitivity to the translation inhibitor anisomycin and changes in translational fidelity including increased in rates of programmed -1 ribosomal frameshifting, increased near cognate aa-tRNA selection events, and a decrease in rates of nonsense suppression. Biochemical characterization of the mutant ribosomes demonstrated an increase in rates of peptidyl transfer and increased affinity of the ribosome for A-site tRNA. Structural probing revealed deprotection of two residues in helix 89 C2843 and C2851, which make contacts with the GTPase associated center and aa-tRNA

respectively. Taken together, these data suggest that the absence of these modifications produces a more available, less discriminate conformation of the ribosomal A-site. This was supported by further evidence provided by structure probing experiments. Another residue, U2923, demonstrated increased protection in mutant ribosomes. This residue is adjacent to one of three 'gate' residues in the A-loop of the PTC. These gate residues are responsible for monitoring the accommodation of the 3' end of the aa-tRNA into the A-site of the ribosome. The conformation change in a residue U2923, along with all the other data, suggests that the gate residue is no longer spatially oriented to correctly monitor the entrance of the aa-tRNA into the A-site. The resulting open conformation leads to a more promiscuous A-site. These data show that individual rRNA modifications may be dispensable for cell viability, but they provide important functional contributions to the accuracy of translation elongation and termination.

There are other functionally important areas of the ribosome that contain a high density of rRNA modifications. For example, the loop of helix 69 has at least three modified residues and it is known to make intersubunit contacts, and interacts with A- and P-site tRNAs (Yusupov et al., 2001). Functional studies in *E. coli* revealed defects in translational fidelity for mutants of helix 69 (Hirabayashi et al., 2006). Extensive genetic, biochemical and structural analysis of this helix would likely provide a wealth of information concerning translational fidelity and subunit association.

Another interesting facet of rRNA modification is its possible role in human disease. X-linked dyskeratosis congenital (X-linked DC) causes skin and bone marrow failure in humans. It is caused by point mutations in the gene encoding the nucleolar protein dyskerin. Dyskerin is present in the telomerase complex and in ribonucleoparticles that pseudouridylate rRNA residues. Mutations in dyskerin are associated with severe telomere dysfunction and defects in pre-rRNA processing and the involved machinery (Mochizuki et al., 2004). Interestingly, cells with mutant dyskerin activity also demonstrate a defect in translation of messenger RNAs containing IRES elements (Yoon et al., 2006). It would be interesting to explore the possible relationship between rRNA modification and regulation if IRES dependent translation.

Appendix A: Yeast Strains

Strain	Description
5X47	*MAT***a**/*MAT*α *his1*/+ *trp1*/+ *ura3*/+ K^-; Standard diploid killer tester
JD758	*MAT***a** *kar1-1 arg1* [L-AHN M1]
JD759	MATα *kar1-1 arg1* [L-A HN M1]
JD469-2D	*MAT_ leu2-1*::pJD85 *ura3 his4 mof6-1*
JD932D	*MAT***a** *ade2-1 trp1-1 ura3-1 leu2-3,112 his3-11,15 can1-100* [L-AHN M1]
LNY95	*MAT***a** *ura3*-SK1 *leu2-hisG trp1-hisG lys2*-SK1 *ho*::*LYS2 ade3-210S*
JD972A	*MAT***a** *ura3*-SK1 *leu2-hisG trp1-hisG lys2-SK1 ho*::*LYS2 ade3-210SPEX6*::*URA3*
YMH171	*MAT*α *ura3-52 leu2-3,112 his3 trp1*Δ
YMH265	*MAT*α *ura3-52 leu2-3,112 his3 trp1*Δ*sin3*::*LEU2*
YMH270	*MAT*α *ura3-52 leu2-3,112 his3 trp1*Δ *rpd3*::*LEU2*
YMH277	*MAT*α *ura3-52 leu2-3,112 his3 trp1*Δ *sap30*::*LEU2*
AJ82	*MAT*α *trp1 leu2 ura3 his4 UME6*
AJ82 11-2	*MAT*α *trp1 leu2 ura3 his4 ume6-11-2*
AJ82 66-2	*MAT*α *trp1 leu2 ura3 his4 ume6-66-1*
AJ82 77-2	*MAT*α *trp1 leu2 ura3 his4 ume6-72-2*
1105	*MATα ura3-52 leu2-3,112 his3 trp1Δ*
1106	*MATα ura3-52 leu2-3,112 his3 trp1Δ sin3::LEU2*
1107	*MATα ura3-52 leu2-3,112 his3 trp1Δ rpd3::LEU2*
1108	*MATα ura3-52 leu2-3,112 his3 trp1Δ sap30::LEU2*
1187	*MATα ade2-101 trp1-Δ101 ura3-52 leu2-3, 112 his3Δ200*
1188	*MATα ade2-101 trp1-Δ101 ura3-52 leu2-3, 112 his3Δ200 snr42::HIS3*
1189	*MATα ade2-101 trp1-Δ101 ura3-52 leu2-3, 112 his3Δ200 snr37::URA3*

Table 2: Yeast strains

Table 2: Yeast strains Continued

Strain	Description
1190	*MATa ade2-101 trp1-Δ101 ura3-52 leu2-3, 112 his3Δ200 snr10::LEU2*
1191	*MATα ade2-101 trp1-Δ101 ura3-52 leu2-3, 112 his3Δ200 snr34::LEU2*
1192	*MATα ade2-101 trp1-Δ101 ura3-52 leu2-3, 112 his3Δ200 snr46::HIS3*
1316	*MATa ade2-1 his3-11 leu2-3 112 trpΔ ura3-1 can1-100 spb1Δ::TRP1 pSEY18-SPB1-OR19(CEN, URA3,Spb1)*
1317	*MATa ade2-1 his3-11 leu2-3 112 trpΔ ura3-1 can1-100 spb1Δ::TRP1 p(CEN, LEU2,HASpb1DA)*
1318	*MATα ade2-1 his3-11 leu2-3 112 trpΔ ura3-1 can1-100 snR52Δ::TRP1*
1319	*MATa ade2-1 his3-11 leu2-3 112 trpΔ ura3-1 can1-100 spb1Δ::TRP1 snR52Δ::TRP1 p(CEN, LEU2,HASpb1DA)*

Appendix B: Plasmid List

Strain	Description
pJD375	0-frame control dual luciferase reporter test (DLR). Described previously (Harger and Dinman, 2003) and Figure 3.6. Harbors a *URA3* selectable marker.
pJD376	-1 PRF test DLR. Described previously (Harger and Dinman, 2003) and Figure 3.6. Harbors a *URA3* selectable marker.
pJD 377	+1 PRF test DLR. Described previously (Harger and Dinman, 2003) and Figure 3.6. Harbors a *URA3* selectable marker.
pJD 419	0-frame control dual luciferase reporter test (DLR). DLR cassette identical to that in pJD375. Harbors a *LEU2* selectable marker.
pJD 420	-1 PRF test DLR. DLR cassette identical to that in pJD376. Harbors a *LEU2* selectable marker.
pJD 421	+1 PRF test DLR. DLR cassette identical to that in pJD377. Harbors a *LEU2* selectable marker.
pJD431	Nonsense suppression test DLR. Contain the UAA premature termination codon. Described in Figure 3.6. Harbors a *URA3* selectable marker.
pJD 432	Nonsense suppression test DLR. Contain the UAG premature termination codon. Described in Figure 3.6. Harbors a *URA3* selectable marker.
pJD433	Nonsense suppression test DLR. Contain the UGA premature termination codon. Described in Figure 3.6. Harbors a *URA3* selectable marker.
pJD633	0-frame control dual luciferase reporter test (DLR). DLR cassette identical to that in pJD375. Harbors a *TRP1* selectable marker.
pJD634	-1 PRF test DLR. DLR cassette identical to that in pJD376. Harbors a *TRP1* selectable marker.
pJD635	+1 PRF test DLR. DLR cassette identical to that in pJD377. Harbors a *TRP1* selectable marker.
pJD642	Non-cognate tRNA misincorporation test DLR. Described in Figure 3.6. Harbors a *URA3* selectable marker.

Table 3: Plasmid List

Table 3: Plasmid List Continued

Strain	Description
pJD643	Near-cognate tRNA misincorporation test DLR. Described in Figure 3.6. Harbors a *URA3* selectable marker.
pJD676	Non-cognate tRNA misincorporation test DLR. DLR cassette identical to that of pJD643. Harbors a *TRP1* selectable marker.
pJD677	Near-cognate tRNA misincorporation test DLR. DLR cassette identical to that of pJD644. Harbors a *TRP1* selectable marker.
pJD699	Non-cognate tRNA misincorporation test DLR. Described in Figure 3.6. Harbors a *URA3* selectable marker.
pJD700	Near-cognate tRNA misincorporation test DLR. DLR cassette identical to that of pJD644. Harbors a *TRP1* selectable marker.
pJD702	Non-cognate tRNA misincorporation test DLR. Described in Figure 3.6. Harbors a *URA3* selectable marker.
pJD703	Nonsense suppression test DLR. Contain the UAG premature termination codon. DLR cassette identical to that of pJD43. Harbors a *LEU2* selectable marker.
pJD704	Nonsense suppression test DLR. Contain the UGA premature termination codon. DLR cassette identical to that of pJD433. Harbors a *LEU2* selectable marker.
p0	*lacZ* containing 0 frame control reporter for measuring -1PRF using β-galactosidase activity
p-1	*lacZ* containing -1 frame control reporter for measuring -1PRF using β-galactosidase activity

Appendix C: Oligonucleotide List

Name and Description	Sequence 5' – 3'
Reverse sequencing primer	TTCACACAGGAAACAG
Universal sequencing primer	GTAAAACGACGGCCAGT
RPD3 sequencing oligo 1	GCCGCATAGAATAAGAATGG
RPD3 sequencing oligo 2	GGTTCAAACACAGATCTATACG
RPD3 sequencing oligo 2	GCTGTCGTGTTACAGTGTGG
PCR primer 1 (forward *Xho*I)	CCCCCTCGAGTGTCCCATATTTTGCCTTG
PCR primer 2 (forward *Pst*I)	CCCCCTGCAGTTGTCATGCTCAACATGTAGG
PCR primer 3 (forward *Kpn*I)	CCCCGGTACCTCATGTAGCCAATTGCTACAC
PCR primer 4 (forward SalI)	CCCCGTCGACTCAAAATTAGCTCTCACCGC
PCR primer 5 (forward *Xho*I)	CCCCCTCGAGTCAAATAAGTTGCATTGTTCG
PCR primer 6 (forward *Pst*I)	CCCCCTGCAGTCAAAAGCTATCCTGGCAGA
Oligo H151A	GCTTCCGATTTTTTTGCAGCATGCAAACCACCCGC
25-6 Ribosome structure probing helices 93-89	AACCTGTCTCACGACGG
25-10 Ribosome structure probing h89	GGTATGATAGGAAGAGC

Table 3: Oligonucleotide List

Reference List

Abraham,A.K. and Pihl,A. (1983). Effect of protein synthesis inhibitors on the fidelity of translation in eukaryotic systems. Biochim. Biophys. Acta *741*, 197-203.

Agrawal,R.K., Heagle,A.B., Penczek,P., Grassucci,R.A., and Frank,J. (1999). EF-G-dependent GTP hydrolysis induces translocation accompanied by large conformational changes in the 70S ribosome. Nature Structural Biology *6*, 643-647.

Agris,P.F. (1996). The importance of being modified: roles of modified nucleosides and Mg2+ in RNA structure and function. Prog. Nucleic Acid Res. Mol. Biol. *53*, 79-129.

Aigner,S., Lingner,J., Goodrich,K.J., Grosshans,C.A., Shevchenko,A., Mann,M., and Cech,T.R. (2000). Euplotes telomerase contains an La motif protein produced by apparent translational frameshifting. EMBO J. *19*, 6230-6239.

Arkov,A.L., Freistroffer,D.V., Ehrenberg,M., and Murgola,E.J. (1998). Mutations in RNAs of both ribosomal subunits cause defects in translation termination. EMBO J. *17*, 1507-1514.

Arkov,A.L., Freistroffer,D.V., Pavlov,M.Y., Ehrenberg,M., and Murgola,E.J. (2000). Mutations in conserved regions of ribosomal RNAs decrease the productive association of peptide-chain release factors with the ribosome during translation termination. Biochimie *82*, 671-682.

Arkov,A.L., Hedenstierna,K.O., and Murgola,E.J. (2002). Mutational eidence for a functional connection between two domains of 23S rRNA in translation termination. J. Bacteriol. *184*, 5052-5057.

Baim,S.B., Pietras,D.F., Eustice,D.C., and Sherman,F. (1985). A mutation allowing an mRNA secondary structure diminishes translation of Saccharomyces cerevisiae iso-1-cytochrome c. Molecular & Cellular Biology *5*, 1839-1846.

Balakin,A.G., Smith,L., and Fournier,M.J. (1996a). The RNA world of the nucleolus: two major families of small RNAs defined by different box elements with related functions. Cell *86*, 823-834.

Balakin,A.G., Smith,L., and Fournier,M.J. (1996b). The RNA world of the nucleolus: two major families of small RNAs defined by different box elements with related functions. Cell *86*, 823-834.

Balasundaram,D., Dinman,J.D., Tabor,C.W., and Tabor,H. (1994). Two essential genes in the biosynthesis of polyamines that modulate +1 ribosomal frameshifting in *Saccharomyces cerevisiae*. J. Bacteriol. *176*, 7126-7128.

Ban,N., Nissen,P., Hansen,J., Moore,P.B., and Steitz,T.A. (2000). The complete atomic structure of the large ribosomal subunit at 2.4 A resolution. Science *289*, 905-920.

Baranov,P.V., Gesteland,R.F., and Atkins,J.F. (2002). Recoding: translational bifurcations in gene expression. Gene *286*, 187-201.

Barbacid,M. and Vazquez,D. (1974). (3H)anisomycin binding to eukaryotic ribosomes. J. Mol. Biol *84*, 603-623.

Beier,H. and Grimm,M. (2001). Misreading of termination codons in eukaryotes by natural nonsense suppressor tRNAs. Nucleic Acids Res. *29*, 4767-4782.

Belcourt,M.F. and Farabaugh,P.J. (1990). Ribosomal frameshifting in the yeast retrotransposon Ty: tRNAs induce slippage on a 7 nucleotide minimal site. Cell *62*, 339-352.

Blanchard,S.C., Kim,H.D., Gonzalez,R.L., Jr., Puglisi,J.D., and Chu,S. (2004). tRNA dynamics on the ribosome during translation. Proc. Natl. Acad. Sci. U. S. A *101*, 12893-12898.

Blinkowa,A.L. and Walker,J.R. (1990). Programmed ribosomal frameshifting generates the Escherichia coli DNA polymerase III gamma subunit from within the tau subunit reading frame. Nucleic Acids Research *18*, 1725-1729.

Bonnerot,C., Pintard,L., and Lutfalla,G. (2003). Functional redundancy of Spb1p and a snR52-dependent mechanism for the 2 '-O-ribose methylation of a conserved rRNA position in yeast. Molecular Cell *12*, 1309-1315.

Brierley,I. (1995). Ribosomal frameshifting on viral RNAs. J. Gen. Virol. *76*, 1885-1892.

Bugl,H., Fauman,E.B., Staker,B.L., Zheng,F., Kushner,S.R., Saper,M.A., Bardwell,J.C., and Jakob,U. (2000). RNA methylation under heat shock control. Mol. Cell *6*, 349-360.

Caldas,T., Binet,E., Bouloc,P., Costa,A., Desgres,J., and Richarme,G. (2000). The FtsJ/RrmJ heat shock protein of Escherichia coli is a 23 S ribosomal RNA methyltransferase. J. Biol. Chem. *275*, 16414-16419.

Carr-Schmid,A., Durko,N., Cavallius,J., Merrick,W.C., and Kinzy,T.G. (1999). Mutations in a GTP-binding motif of eukaryotic elongation factor 1A reduce both translational fidelity and the requirement for nucleotide exchange. J. Biol. Chem. *274*, 30297-30302.

Carrasco,L., Barbacid,M., and Vazquez,D. (1973). The tricodermin group of antibiotics, inhibitors of peptide bond formation by eukaryotic ribosomes. Biochim. et Biophys. Acta. *312*, 368-376.

Carter,A.P., Clemons,W.M., Brodersen,D.E., Morgan-Warren,R.J., Wimberly,B.T., and Ramakrishnan,V. (2000). Functional insights from the structure of the 30S ribosomal subunit and its interactions with antibiotics. Nature *407*, 340-348.

Cavaille,J. and Bachellerie,J.P. (1998). SnoRNA-guided ribose methylation of rRNA: structural features of the guide RNA duplex influencing the extent of the reaction. Nucleic Acids Res. *26*, 1576-1587.

Chandler,M. and Fayet,O. (1993). Translational Frameshifting in the Control of Transposition in Bacteria. Molecular Microbiology *7*, 497-503.

Charette,M. and Gray,M.W. (2000). Pseudouridine in RNA: what, where, how, and why. IUBMB. Life *49*, 341-351.

Chavatte,L., Seit-Nebi,A., Dubovaya,V., and Favre,A. (2002). The invariant uridine of stop codons contacts the conserved NIKSR loop of human eRF1 in the ribosome. EMBO J. *21*, 5302-5311.

Chernoff,Y.O., Newnam,G.P., and Liebman,S.W. (1996). The translational function of nucleotide C1054 in the small subunit rRNA is conserved throughout evolution: genetic evidence in yeast. Proc. Natl. Acad. Sci. U. S. A *93*, 2517-2522.

Christianson,T.W., Sikorski,R.S., Dante,M., Shero,J.H., and Hieter,P. (1992). Multifunctional yeast high-copy-number shuttle vectors. Yeast *110*, 119-122.

Chu,C.K., Wempen,I., Watanabe,K.A., and Fox,J.J. (1976). Nucleosides. 100. General synthesis of pyrimidine C-5 cucleosides related to pseudouridine. Synthesis of 5-(beta-D-ribofuranosyl) isocytosine (pseudoisocytidine),5-(beta-D-ribofuranosyl)-2-thiouracil(2-thiopseudourid ine) and 5-(beta-D-ribofuranosyl)uracil(pseudouridine). J. Org. Chem. *41*, 2793-2797.

Condron,B.G., Atkins,J.F., and Gesteland,R.F. (1991). Frameshifting in gene 10 of bacteriophage T7. J. Bacteriol. *173*, 6998-7003.

Courey,A.J. and Jia,S. (2001). Transcriptional repression: the long and the short of it. Genes Dev. *15*, 2786-2796.

Craigen,W.J. and Caskey,C.T. (1986). Expression of peptide chain release factor 2 requires high- efficiency frameshift. Nature *322*, 273-275.

Cui,Y., Dinman,J.D., Kinzy,T.G., and Peltz,S.W. (1998). The Mof2/Sui1 protein is a general monitor of translational accuracy. Mol. Cell. Biol. *18*, 1506-1516.

Cui,Y., Dinman,J.D., and Peltz,S.W. (1996). *mof4-1* is an allele of the *UPF1/IFS2* gene which affects both mRNA turnover and -1 ribosomal frameshifting efficiency. EMBO J. *15*, 5726-5736.

de Groot,N., Panet,A., and Lapidot,Y. (1970). Reaction of puromycin with chemically prepared peptidyl transfer RNA. Eur. J. Biochem. *15*, 215-221.

Decatur,W.A. and Fournier,M.J. (2002). rRNA modifications and ribosome function. Trends Biochem. Sci. *27*, 344-351.

Decatur,W.A. and Fournier,M.J. (2003). RNA-guided nucleotide modification of ribosomal and other RNAs. J. Biol. Chem. *278*, 695-698.

Del Campo,M., Kaya,Y., and Ofengand,J. (2001). Identification and site of action of the remaining four putative pseudouridine synthases in Escherichia coli. RNA. *7*, 1603-1615.

Diedrich,G., Spahn,C.M., Stelzl,U., Schafer,M.A., Wooten,T., Bochkariov,D.E., Cooperman,B.S., Traut,R.R., and Nierhaus,K.H. (2000). Ribosomal protein L2 is involved in the association of the ribosomal subunits, tRNA binding to A and P sites and peptidyl transfer. EMBO J. *19*, 5241-5250.

Dinman,J.D. (1995). Ribosomal frameshifting in yeast viruses. Yeast *11*, 1115-1127.

Dinman,J.D., Icho,T., and Wickner,R.B. (1991). A -1 ribosomal frameshift in a double-stranded RNA virus forms a Gag-pol fusion protein. Proc. Natl. Acad. Sci. USA *88*, 174-178.

Dinman,J.D. and Kinzy,T.G. (1997). Translational misreading: Mutations in translation elongation factor 1α differentially affect programmed ribosomal frameshifting and drug sensitivity. RNA *3*, 870-881.

Dinman,J.D., Ruiz-Echevarria,M.J., Czaplinski,K., and Peltz,S.W. (1997). Peptidyl transferase inhibitors have antiviral properties by altering programmed -1 ribosomal frameshifting efficiencies: development of model systems. Proc. Natl. Acad. Sci. USA *94*, 6606-6611.

Dinman,J.D. and Wickner,R.B. (1992). Ribosomal frameshifting efficiency and Gag/Gag-pol ratio are critical for yeast M_1 double-stranded RNA virus propagation. J. Virology *66*, 3669-3676.

Dinman,J.D. and Wickner,R.B. (1994). Translational maintenance of frame: mutants of *Saccharomyces cerevisiae* with altered -1 ribosomal frameshifting efficiencies. Genetics *136*, 75-86.

Dinman,J.D. and Wickner,R.B. (1995). 5S rRNA is involved in fidelity of translational reading frame. Genetics *141*, 95-105.

Donly,B.C., Edgar,C.D., Adamski,F.M., and Tate,W.P. (1990). Frameshift autoregulation in the gene for Escherichia coli release factor 2: partly functional mutants result in frameshift enhancement. Nucleic Acids Research *18*, 6517-6522.

Dunbar,D.A., Wormsley,S., Agentis,T.M., and Baserga,S.J. (1997). Mpp10p, a U3 small nucleolar ribonucleoprotein component required for pre-18S rRNA processing in yeast. Mol. Cell Biol. *17*, 5803-5812.

Durant,P.C., Bajji,A.C., Sundaram,M., Kumar,R.K., and Davis,D.R. (2005). Structural effects of hypermodified nucleosides in the Escherichia coli and human tRNALys anticodon loop: the effect of nucleosides s2U, mcm5U, mcm5s2U, mnm5s2U, t6A, and ms2t6A. Biochemistry *44*, 8078-8089.

Farabaugh,P.J. (1996). Programmed translational frameshifting. Microbiol. Rev. *60*, 103-134.

Farabaugh,P.J. (2000). Translational frameshifting: implications for the mechanism of translational frame maintenance. Prog. Nucleic Acid Res. Mol. Biol. *64*, 131-170.

Fath,S., Milkereit,P., Podtelejnikov,A.V., Bischler,N., Schultz,P., Bier,M., Mann,M., and Tschochner,H. (2000). Association of yeast RNA polymerase I with a nucleolar substructure active in rRNA synthesis and processing. Journal of Cell Biology *149*, 575-589.

Frank,J. and Agrawal,R.K. (2000). A ratchet-like inter-subunit reorganization of the ribosome during translocation. Nature *406*, 318-322.

Fried,H.M. and Fink,G.R. (1978). Electron microscopic heteroduplex analysis of "killer" double-stranded RNA species from yeast. Proc. Natl. Acad. Sci. USA *75*, 4224-4228.

Frolova,L.Y., Tsivkovskii,R.Y., Sivolobova,G.F., Oparina,N.Y., Serpinsky,O.I., Blinov,V.M., Tatkov,S.I., and Kisselev,L.L. (1999). Mutations in the highly conserved GGQ motif of class 1 polypeptide release factors abolish ability of human eRF1 to trigger peptidyl-tRNA hydrolysis. RNA. *5*, 1014-1020.

Gabashvili,I.S., Agrawal,R.K., Grassucci,R., Squires,C.L., Dahlberg,A.E., and Frank,J. (1999). Major rearrangements in the 70S ribosomal 3D structure caused by a conformational switch in 16S ribosomal RNA. EMBO J. *18*, 6501-6507.

Ganot,P., Bortolin,M.L., and Kiss,T. (1997a). Site-specific pseudouridine formation in preribosomal RNA is guided by small nucleolar RNAs. Cell *89*, 799-809.

Ganot,P., Caizergues-Ferrer,M., and Kiss,T. (1997b). The family of box ACA small nucleolar RNAs is defined by an evolutionarily conserved secondary structure and ubiquitous sequence elements essential for RNA accumulation. Genes Dev. *11*, 941-956.

Gautier,T., Berges,T., Tollervey,D., and Hurt,E. (1997). Nucleolar KKE/D repeat proteins Nop56p and Nop58p interact with Nop1p and are required for ribosome biogenesis. Mol. Cell Biol. *17*, 7088-7098.

Gesteland,R.F. and Atkins,J.F. (1996). Recoding: Dynamic reprogramming of translation. Annu. Rev. Biochem. *65*, 741-768.

Goldberg,I.H. and Mitsugi,K. (1966). Sparsomycin, an inhibitor of aminoacyl transfer to polypeptide. Biochem. Biophys. Res. Commun. *23*, 453-459.

Green,R. and Noller,H.F. (1996). In vitro complementation analysis localizes 23S rRNA posttranscriptional modifications that are required for Escherichia coli 50S ribosomal subunit assembly and function. RNA. *2*, 1011-1021.

Grollman,A.P. (1967). Inhibitors of protein biosynthesis. II. Mode of action of anisomycin. J. Biol. Chem. *242*, 3226-3233.

Gromadski,K.B. and Rodnina,M.V. (2004). Kinetic determinants of high-fidelity tRNA discrimination on the ribosome. Mol. Cell *13*, 191-200.

Gustafsson,C. and Persson,B.C. (1998). Identification of the rrmA gene encoding the 23S rRNA m1G745 methyltransferase in Escherichia coli and characterization of an m1G745-deficient mutant. J. Bacteriol. *180*, 359-365.

Haenni,A.L. and Chapeville,F. (1966). The behaviour of acetylphenylalanyl soluble ribonucleic acid in polyphenylalanine synthesis. Biochim. Biophys. Acta *114*, 135-148.

Hansen,J.L., Moore,P.B., and Steitz,T.A. (2003a). Structures of five antibiotics bound at the peptidyl transferase center of the large ribosomal subunit. J. Mol. Biol. *330*, 1061-1075.

Hansen,T.M., Baranov,P.V., Ivanov,I.P., Gesteland,R.F., and Atkins,J.F. (2003b). Maintenance of the correct open reading frame by the ribosome. Embo Reports *4*, 499-504.

Harger,J.W. and Dinman,J.D. (2003). An in vivo dual-luciferase assay system for studying translational recoding in the yeast *Saccharomyces cerevisiae*. RNA *9*, 1019-1024.

Harger,J.W., Meskauskas,A., and Dinman,J.D. (2002). An 'integrated model' of programmed ribosomal frameshifting and post-transcriptional surveillance. TIBS *27*, 448-454.

Harris,R. and Pestka,S. (1973). Studies on the formation of transfer ribonucleic acid-ribosome complexes. XXIV. Effects of antibiotics on binding of aminoacyl-oligonucleotides to ribosomes. J. Biol. Chem. *248*, 1168-1174.

Hassig,C.A., Fleischer,T.C., Billin,A.N., Schreiber,S.L., and Ayer,D.E. (1997). Histone deacetylase activity is required for full transcriptional repression by mSin3A. Cell *89*, 341-347.

Hatfield,D.L. and Gladyshev,V.N. (2002). How selenium has altered our understanding of the genetic code. Mol. Cell Biol. *22*, 3565-3576.

Hayashi,S.-I. and Murakami,Y. (1995). Rapid and regulated degradation of ornithine decarboxylase. Biochem. J. *306*, 1-10.

Hayes,S. and Bull,H.J. (1999). Translational frameshift sites within bacteriophage lambda genes rexA and cI. Acta Biochim. Pol. *46*, 879-884.

Hellen,C.U. and Sarnow,P. (2001). Internal ribosome entry sites in eukaryotic mRNA molecules. Genes Dev. *15*, 1593-1612.

Helm,M. (2006). Post-transcriptional nucleotide modification and alternative folding of RNA. Nucleic Acids Res. *34*, 721-733.

Henras,A., Henry,Y., Bousquet-Antonelli,C., Noaillac-Depeyre,J., Gelugne,J.P., and Caizergues-Ferrer,M. (1998). Nhp2p and Nop10p are essential for the function of H/ACA snoRNPs. EMBO J. *17*, 7078-7090.

Herner,A.E., Goldberg,I.H., and Cohen,L.B. (1969). Stabilization of N-acetylphenylalanyl transfer ribonucleic acid binding to ribosomes by sparsomycin. Biochemistry *8*, 1335-1344.

Hirabayashi,N., Sato,N.S., and Suzuki,T. (2006). Conserved loop sequence of helix 69 in Escherichia coli 23 S rRNA is involved in A-site tRNA binding and translational fidelity. J. Biol Chem. *281*, 17203-17211.

Inoue,H., Nojima,H., and Okayama,H. (1990). High efficiency transformation of Escherichia coli with plasmids. Gene *96*, 23-28.

Ito,H., Fukuda,Y., Murata,K., and Kimura,A. (1983). Transformation of intact yeast cells treated with alkali cations. J. Bacteriol. *153*, 163-168.

Ito,K., Ebihara,K., Uno,M., and Nakamura,Y. (1996). Conserved motifs in prokaryotic and eukaryotic polypeptide release factors: tRNA-protein mimicry hypothesis. Proc. Natl. Acad. Sci. U. S. A *93*, 5443-5448.

Ivanov,I.P., Gesteland,R.F., and Atkins,J.F. (2000). SURVEY AND SUMMARY: antizyme expression: a subversion of triplet decoding, which is remarkably conserved by evolution, is a sensor for an autoregulatory circuit. Nucleic Acids Res. *28*, 3185-3196.

Jacks,T., Madhani,H.D., Masiraz,F.R., and Varmus,H.E. (1988). Signals for ribosomal frameshifting in the Rous Sarcoma Virus gag-pol region. Cell *55*, 447-458.

Jacks,T. and Varmus,H.E. (1985). Expression of the Rous Sarcoma Virus pol gene by ribosomal frameshifting. Science *230*, 1237-1242.

Jacobs,J.L. and Dinman,J.D. (2004). Systematic analysis of bicistronic reporter assay data. Nucleic Acids Res. *32*, e160-e170.

Jayaraman,J. and Goldberg,I.H. (1968). Localization of sparsomycin action to the peptide-bond-forming step. Biochemistry *7*, 418-421.

Jones,M.H., Frank,D.N., and Guthrie,C. (1995). Characterization and functional ordering of Slu7p and Prp17p during the second step of pre-mRNA splicing in yeast. Proceedings of the National Academy of Sciences of the United States of America *92*, 9687-9691.

Kadosh,D. and Struhl,K. (1998). Histone deacetylase activity of Rpd3 is important for transcriptional repression in vivo. Genes Dev. *12*, 797-805.

Kaneko,I. and Doi,R.H. (1966). Alteration of valyl-sRNA during sporulation of bacillus subtilis. Proc. Natl. Acad. Sci. U. S. A. *55*, 564-571.

Kasten,M.M., Dorland,S., and Stillman,D.J. (1997). A large protein complex containing the yeast Sin3p and Rpd3p transcriptional regulators. Mol. Cell Biol. *17*, 4852-4858.

Katunin,V.I., Muth,G.W., Strobel,S.A., Wintermeyer,W., and Rodnina,M.V. (2002). Important contribution to catalysis of peptide bond formation by a single ionizing group within the ribosome. Mol. Cell *10*, 339-346.

Kawakami,K., Paned,S., Faioa,B., Moore,D.P., Boeke,J.D., Farabaugh,P.J., Strathern,J.N., Nakamura,Y., and Garfinkel,D.J. (1993). A rare tRNA-Arg(CCU) that regulates Ty*1* element ribosomal frameshifting is essential for Ty*1* retrotransposition in *Saccharomyces cerevisiae*. Genetics *135*, 309-320.

King,T.H., Liu,B., McCully,R.R., and Fournier,M.J. (2003). Ribosome structure and activity are altered in cells lacking snoRNPs that form pseudouridines in the peptidyl transferase center. Molecular Cell *11*, 425-435.

Kiparisov,S., Petrov,A., Meskauskas,A., Sergiev,P.V., Dontsova,O.A., and Dinman,J.D. (2005). Structural and functional analysis of 5S rRNA. Molecular Genetics and Genomics *27*, 235-247.

Kiss,T. (2001). Small nucleolar RNA-guided post-transcriptional modification of cellular RNAs. EMBO J. *20*, 3617-3622.

Kiss-Laszlo,Z., Henry,Y., and Kiss,T. (1998). Sequence and structural elements of methylation guide snoRNAs essential for site-specific ribose methylation of pre-rRNA. EMBO J. *17*, 797-807.

Klaholz,B.P., Pape,T., Zavialov,A.V., Myasnikov,A.G., Orlova,E.V., Vestergaard,B., Ehrenberg,M., and van Heel,M. (2003). Structure of the Escherichia coli ribosomal termination complex with release factor 2. Nature *421*, 90-94.

Klobutcher,L.A. and Farabaugh,P.J. (2002). Shifty ciliates: frequent programmed translational frameshifting in euplotids. Cell *111*, 763-766.

Kowalak,J.A., Dalluge,J.J., McCloskey,J.A., and Stetter,K.O. (1994). The role of posttranscriptional modification in stabilization of transfer RNA from hyperthermophiles. Biochemistry *33*, 7869-7876.

Kozak,M. (1999). Initiation of translation in prokaryotes and eukaryotes. Gene *234*, 187-208.

Kressler,D., Linder,P., and de La,C.J. (1999). Protein trans-acting factors involved in ribosome biogenesis in Saccharomyces cerevisiae. Mol. Cell Biol. *19*, 7897-7912.

Kuchino,Y. and Muramatsu,T. (1996). Nonsense suppression in mammalian cells. Biochimie *78*, 1007-1015.

Kunkel,T. (1985). Rapid and efficient site-specific mutagenesis without phenotype selection. Proc. Natl. Acad. Sci. USA *82*, 488-492.

Kutay,U., Lipowsky,G., Izaurralde,E., Bischoff,F.R., Schwarzmaier,P., Hartmann,E., and Gorlich,D. (1998). Identification of a tRNA-specific nuclear export receptor. Mol. Cell *1*, 359-369.

Lafontaine,D.L., Bousquet-Antonelli,C., Henry,Y., Caizergues-Ferrer,M., and Tollervey,D. (1998). The box H + ACA snoRNAs carry Cbf5p, the putative rRNA pseudouridine synthase. Genes Dev. *12*, 527-537.

Lafontaine,D.L. and Tollervey,D. (1999). Nop58p is a common component of the box C+D snoRNPs that is required for snoRNA stability. RNA. *5*, 455-467.

Lafontaine,D.L. and Tollervey,D. (2000). Synthesis and assembly of the box C+D small nucleolar RNPs. Mol. Cell Biol. *20*, 2650-2659.

Lapeyre,B. and Purushothaman,S.K. (2004). Spb1p-directed formation of Gm2922 in the ribosome catalytic center occurs at a late processing stage. Mol. Cell *16*, 663-669.

Lazaro,E., Rodriguez-Fonseca,C., Porse,B., Urena,D., Garrett,R.A., and Ballesta,J.P. (1996). A sparsomycin-resistant mutant of Halobacterium salinarium lacks a modification at nucleotide U2603 in the peptidyl transferase centre of 23 S rRNA. J. Mol. Biol. *261*, 231-238.

Lazaro,E., van den Broek,L.A., San Felix,A., Ottenheijm,H.C., and Ballesta,J.P. (1991). Biochemical and kinetic characteristics of the interaction of the antitumor antibiotic sparsomycin with prokaryotic and eukaryotic ribosomes. Biochemistry *30*, 9642-9648.

Leary,D.J. and Huang,S. (2001). Regulation of ribosome biogenesis within the nucleolus. FEBS Lett. *509*, 145-150.

Lee,S.J. and Baserga,S.J. (1999). Imp3p and Imp4p, two specific components of the U3 small nucleolar ribonucleoprotein that are essential for pre-18S rRNA processing. Mol. Cell Biol. *19*, 5441-5452.

Levin,M.E., Hendrix,R.W., and Casjens,S.R. (1993). A programmed translational frameshift is required for the synthesis of a bacteriophage lambda tail assembly protein. J. Mol. Biol. *234*, 124-139.

Liermann,R.T., Dinman,J.D., Sylvers,L.A., and Jackson,J.C. (2000). Improved purification of the double-stranded RNA from killer strains of yeast. Biotechniques *28*, 64-65.

Lowe,T.M. and Eddy,S.R. (1999). A computational screen for methylation guide snoRNAs in yeast. Science *283*, 1168-1171.

Manktelow,E., Shigemoto,K., and Brierley,I. (2005). Characterization of the frameshift signal of Edr, a mammalian example of programmed -1 ribosomal frameshifting. Nucleic Acids Res. *33*, 1553-1563.

Matsufuji,S., Matsufuji,T., Miyazaki,Y., Murakami,Y., Atkins,J.F., Gesteland,R.F., and Hayashi,S. (1995). Autoregulatory frameshifting in decoding mammalian ornithine decarboxylase antizyme. Cell *80*, 51-60.

Meroueh,M., Grohar,P.J., Qiu,J., SantaLucia,J., Jr., Scaringe,S.A., and Chow,C.S. (2000). Unique structural and stabilizing roles for the individual pseudouridine residues in the 1920 region of Escherichia coli 23S rRNA. Nucleic Acids Res. *28*, 2075-2083.

Merrick,W.C. (1979). Assays for eukaryotic protein synthesis. Met. Enzymol. *60*, 108-123.

Meskauskas,A., Baxter,J.L., Carr,E.A., Yasenchak,J., Gallagher,J.E.G., Baserga,S.J., and Dinman,J.D. (2003). Delayed rRNA processing results in significant ribosome biogenesis and functional defects. Mol. Cell Biol. *23*, 1602-1613.

Meskauskas,A. and Dinman,J.D. (2001). Ribosomal protein L5 helps anchor peptidyl-tRNA to the P-site in Saccharomyces cerevisiae. RNA. *7*, 1084-1096.

Meskauskas,A., Petrov,A.N., and Dinman,J.D. (2005). Identification of functionally important amino acids of ribosomal protein L3 by saturation mutagenesis. Molecular & Cellular Biology *25*, 10863-10874.

Moazed,D. and Noller,H.F. (1989). Intermediate states in the movement of transfer RNA in the ribosome. Nature *342*, 142-148.

Moazed,D. and Noller,H.F. (1991). Sites of interaction of the CCA end of peptidyl-tRNA with 23S rRNA. Proc. Natl. Acad. Sci. U. S. A *88*, 3725-3728.

Mochizuki,Y., He,J., Kulkarni,S., Bessler,M., and Mason,P.J. (2004). Mouse dyskerin mutations affect accumulation of telomerase RNA and small nucleolar RNA, telomerase activity, and ribosomal RNA processing. Proc. Natl. Acad. Sci. U. S. A *101*, 10756-10761.

Monro,R.E., Celma,M.L., and Vazquez,D. (1969). Action of sparsomycin on ribosome-catalysed peptidyl transfer. Nature *222*, 356-358.

Mueller,F., Sommer,I., Baranov,P., Matadeen,R., Stoldt,M., Wohnert,J., Gorlach,M., van Heel,M., and Brimacombe,R. (2000). The 3D arrangement of the 23 S and 5 S rRNA in the Escherichia coli 50 S ribosomal subunit based on a cryo-electron microscopic reconstruction at 7.5 A resolution. J. Mol. Biol. *298*, 35-59.

Muth,G.W., Ortoleva-Donnelly,L., and Strobel,S.A. (2000). A single adenosine with a neutral pK(a) in the ribosomal peptidyl transferase center. Science *289*, 947-950.

Namy,O., Hatin,I., and Rousset,J.P. (2001). Impact of the six nucleotides downstream of the stop codon on translation termination. EMBO Rep. *2*, 787-793.

Namy,O., Rousset,J.P., Napthine,S., and Brierley,I. (2004). Reprogrammed genetic decoding in cellular gene expression. Mol. Cell *13*, 157-168.

Ni,J., Tien,A.L., and Fournier,M.J. (1997). Small nucleolar RNAs direct site-specific synthesis of pseudouridine in ribosomal RNA. Cell *89*, 565-573.

Nissen,P., Hansen,J., Ban,N., Moore,P.B., and Steitz,T.A. (2000). The structural basis of ribosome activity in peptide bond synthesis. Science *289*, 920-930.

Nissen,P., Ippolito,J.A., Ban,N., Moore,P.B., and Steitz,T.A. (2001). RNA tertiary interactions in the large ribosomal subunit: the A-minor motif. Proc. Natl. Acad. Sci. U. S. A *98*, 4899-4903.

Nissen,P., Kjeldgaard,M., Thirup,S., Polekhina,G., Reshetnikova,L., Clark,B.F., and Nyborg,J. (1995). Crystal structure of the ternary complex of Phe-tRNAPhe, EF-Tu, and a GTP analog [see comments]. Science *270*, 1464-1472.

Noller,H.F., Yusupov,M.M., Yusupova,G.Z., Baucom,A., and Cate,J.H. (2002). Translocation of tRNA during protein synthesis. FEBS Lett. *514*, 11-16.

O'Connor,M. and Dahlberg,A.E. (1995). The involvement of two distinct regions of 23 S ribosomal RNA in tRNA selection. J. Mol. Biol. *254*, 838-847.

Ofengand,J. (2002). Ribosomal RNA pseudouridines and pseudouridine synthases. FEBS Lett. *514*, 17-25.

Ofengand,J., Bakin,A., Wrzesinski,J., Nurse,K., and Lane,B.G. (1995). The pseudouridine residues of ribosomal RNA. Biochem. Cell Biol. *73*, 915-924.

Ogle,J.M., Brodersen,D.E., Clemons,W.M., Jr., Tarry,M.J., Carter,A.P., and Ramakrishnan,V. (2001). Recognition of cognate transfer RNA by the 30S ribosomal subunit. Science *292*, 897-902.

Ogle,J.M. and Ramakrishnan,V. (2005). Structural Insights into Translational Fidelity. Annu. Rev. Biochem. *74*, 129-177.

Ohtake,Y. and Wickner,R.B. (1995a). KRB1, a suppressor of mak7-1 (a mutant RPL4A), is RPL4B, a second ribosomal protein L4 gene, on a fragment of Saccharomyces chromosome XII. Genetics *140*, 129-137.

Ohtake,Y. and Wickner,R.B. (1995b). Yeast virus propagation depends critically on free 60S ribosomal subunit concentration. Mol. Cell. Biol. *15*, 2772-2781.

Pagel,F.T., Zhao,S.Q., Hijazi,K.A., and Murgola,E.J. (1997). Phenotypic heterogeneity of mutational changes at a conserved nucleotide in 16 S ribosomal RNA. J. Mol. Biol. *267*, 1113-1123.

Pape,T., Wintermeyer,W., and Rodnina,M. (1999). Induced fit in initial selection and proofreading of aminoacyl-tRNA on the ribosome. EMBO J. *18*, 3800-3807.

Pape,T., Wintermeyer,W., and Rodnina,M.V. (1998). Complete kinetic mechanism of elongation factor Tu-dependent binding of aminoacyl-tRNA to the A site of the E. coli ribosome. EMBO J. *17*, 7490-7497.

Pegg,A.E. (1986). Recent advances in the biochemistry of polyamines in eukaryotes. Biochem. J. *234*, 249-262.

Peltz,S.W., Hammell,A.B., Cui,Y., Yasenchak,J., Puljanowski,L., and Dinman,J.D. (1999). Ribosomal Protein L3 Mutants Alter Translational Fidelity and Promote Rapid Loss of the Yeast Killer Virus. Mol. Cell Biol. *19*, 384-391.

Pestka,S., Hishizawa,T., and Lessard,J.L. (1970). Studies on the formation of transfer ribonucleic acid-ribosome complexes. 8. Aminoacyl oligonucleotide binding to ribosomes: characteristics and requirements. J. Biol. Chem. *245*, 6208-6219.

Pestova,T.V., Shatsky,I.N., Fletcher,S.P., Jackson,R.J., and Hellen,C.U. (1998). A prokaryotic-like mode of cytoplasmic eukaryotic ribosome binding to the initiation codon during internal translation initiation of hepatitis C and classical swine fever virus RNAs. Genes Dev. *12*, 67-83.

Petry,S., Brodersen,D.E., Murphy,F.V., Dunham,C.M., Selmer,M., Tarry,M.J., Kelley,A.C., and Ramakrishnan,V. (2005). Crystal structures of the ribosome in complex with release factors RF1 and RF2 bound to a cognate stop codon. Cell *123*, 1255-1266.

Pisarev,A.V., Shirokikh,N.E., and Hellen,C.U. (2005). Translation initiation by factor-independent binding of eukaryotic ribosomes to internal ribosomal entry sites. C. R. Biol. *328*, 589-605.

Plant,E.P., Jacobs,K.L.M., Harger,J.W., Meskauskas,A., Jacobs,J.L., Baxter,J.L., Petrov,A.N., and Dinman,J.D. (2003). The 9-angstrom solution: How mRNA pseudoknots promote efficient programmed -1 ribosomal frameshifting. RNA *9*, 168-174.

Porse,B.T., Kirillov,S.V., Awayez,M.J., Ottenheijm,H.C., and Garrett,R.A. (1999). Direct crosslinking of the antitumor antibiotic sparsomycin, and its derivatives, to A2602 in the peptidyl transferase center of 23S-like rRNA within ribosome-tRNA complexes. Proc. Natl. Acad. Sci. U. S. A *96*, 9003-9008.

Pyronnet,S., Pradayrol,L., and Sonenberg,N. (2000). A cell cycle-dependent internal ribosome entry site. Mol Cell *5*, 607-616.

Rawat,U.B.S., Zavialov,A.V., Sengupta,J., Valle,M., Grassucci,R.A., Linde,J., Vestergaard,B., Ehrenberg,M., and Frank,J. (2003). A cryo-electron microscopic study of ribosome-bound termination factor RF2. Nature *421*, 87-90.

Raychaudhuri,S., Conrad,J., Hall,B.G., and Ofengand,J. (1998). A pseudouridine synthase required for the formation of two universally conserved pseudouridines in ribosomal RNA is essential for normal growth of Escherichia coli. RNA. *4*, 1407-1417.

Raychaudhuri,S., Niu,L., Conrad,J., Lane,B.G., and Ofengand,J. (1999). Functional effect of deletion and mutation of the Escherichia coli ribosomal RNA and tRNA pseudouridine synthase RluA. J. Biol. Chem. *274*, 18880-18886.

Robinson,D.N. and Cooley,L. (1997). Examination of the function of two kelch proteins generated by stop codon suppression. Development *124*, 1405-1417.

Rodnina,M.V., Fricke,R., Kuhn,L., and Wintermeyer,W. (1995). Codon-dependent conformational change of elongation factor Tu preceding GTP hydrolysis on the ribosome. EMBO Journal *14*, 2613-2619.

Rodnina,M.V., Gromadski,K.B., Kothe,U., and Wieden,H.J. (2005). Recognition and selection of tRNA in translation. FEBS Lett. *579*, 938-942.

Rom,E. and Kahana,C. (1994). Polyamines regulate the expression of ornithine decarboxylase antizyme *in vitro* by inducing ribosomal frameshifting. Proc. Natl. Acad. Sci. USA *91*, 3959-3963.

Rose,M.D., Novick,P., Thomas,J.H., Botstein,D., and Fink,G.R. (1987). A *Saccharomyces cerevisiae* genomic plasmid bank based on a centromere-containing shuttle vector. Gene *60*, 237-243.

Rozenski,J., Crain,P.F., and McCloskey,J.A. (1999). The RNA Modification Database: 1999 update. Nucleic Acids Res. *27*, 196-197.

Ruiz-Echevarria,M.J., Yasenchak,J.M., Han,X., Dinman,J.D., and Peltz,S.W. (1998). The Upf3p is a component of the surveillance complex that monitors both translation and mRNA turnover and affects viral maintenance. Proc. Natl. Acad. Sci. USA *95*, 8721-8726.

Samarsky,D.A., Balakin,A.G., and Fournier,M.J. (1995). Characterization of three new snRNAs from Saccharomyces cerevisiae: snR34, snR35 and snR36. Nucleic Acids Res. *23*, 2548-2554.

Samarsky,D.A. and Fournier,M.J. (1999). A comprehensive database for the small nucleolar RNAs from Saccharomyces cerevisiae. Nucleic Acids Res. *27*, 161-164.

Sambrook,J., Fritsch,E.F., and Maniatis,T. (1989). Molecular cloning, a laboratory manual., C.Nolan, N.Ford, and M.Ferguson, eds. (Cold Spring Harbor, NY: Cold Spring Harbor Press).

Sanbonmatsu,K.Y., Joseph,S., and Tung,C.S. (2005). Simulating movement of tRNA into the ribosome during decoding. Proc. Natl. Acad. Sci. U. S. A *102*, 15854-15859.

Schena,M. and Yamamoto,K. (1988). Mammalian glucocorticoid receptor derivitives enhance transcription transcription in yeast. Science *241*, 965-967.

Schimmang,T., Tollervey,D., Kern,H., Frank,R., and Hurt,E.C. (1989). A yeast nucleolar protein related to mammalian fibrillarin is associated with small nucleolar RNA and is essential for viability. EMBO J. *8*, 4015-4024.

Schindler,D. (1974). Two classes of inhibitors of peptidyl transferase activity in eukaryotes. Nature *249*, 38-41.

Schmeing,T.M., Huang,K.S., Kitchen,D.E., Strobel,S.A., and Steitz,T.A. (2005a). Structural insights into the roles of water and the 2' hydroxyl of the P site tRNA in the peptidyl transferase reaction. Mol. Cell *20*, 437-448.

Schmeing,T.M., Huang,K.S., Strobel,S.A., and Steitz,T.A. (2005b). An induced-fit mechanism to promote peptide bond formation and exclude hydrolysis of peptidyl-tRNA. Nature *438*, 520-524.

Sergiev,P.V., Bogdanov,A.A., and Dontsova,O.A. (2005a). How can elongation factors EF-G and EF-Tu discriminate the functional state of the ribosome using the same binding site? FEBS Lett. *579*, 5439-5442.

Sergiev,P.V., Lesnyak,D.V., Burakovsky,D.E., Kiparisov,S.V., Leonov,A.A., Bogdanov,A.A., Brimacombe,R., and Dontsova,O.A. (2005b). Alteration in location of a conserved GTPase-associated center of the ribosome induced by mutagenesis

influences the structure of peptidyltransferase center and activity of elongation factor G. J. Biol. Chem. *280*, 31882-31889.

Sharma,D., Southworth,D.R., and Green,R. (2004). EF-G-independent reactivity of a pre-translocation-state ribosome complex with the aminoacyl tRNA substrate puromycin supports an intermediate (hybrid) state of tRNA binding. RNA *10*, 102-113.

Shigemoto,K., Brennan,J., Walls,E., Watson,C.J., Stott,D., Rigby,P.W.J., and Reith,A.D. (2001). Identification and characterisation of a developmentally regulated mammalian gene that utilises –1 programmed ribosomal frameshifting. Nucleic Acids Res. *29*, 4079-4088.

Sikorski,R.S. and Hieter,P. (1989). A system of shuttle vectors and yeast host strains designed for efficient manipulation of DNA in *Saccharomyces cerevisiae*. Genetics *122*, 19-27.

Skuzeski,J.M., Nichols,L.M., Gesteland,R.F., and Atkins,J.F. (1991). The signal for a leaky UAG stop codon in several plant viruses includes the two downstream codons. J. Mol. Biol. *218*, 365-373.

Somogyi,P., Jenner,A.J., Brierley,I.A., and Inglis,S.C. (1993). Ribosomal pausing during translation of an RNA pseudoknot. Mol. Cell. Biol. *13*, 6931-6940.

Song,H., Mugnier,P., Das,A.K., Webb,H.M., Evans,D.R., Tuite,M.F., Hemmings,B.A., and Barford,D. (2000). The crystal structure of human eukaryotic release factor eRF1--mechanism of stop codon recognition and peptidyl-tRNA hydrolysis. Cell *100*, 311-321.

Spahn,C.M., Gomez-Lorenzo,M.G., Grassucci,R.A., Jorgensen,R., Andersen,G.R., Beckmann,R., Penczek,P.A., Ballesta,J.P., and Frank,J. (2004). Domain movements of elongation factor eEF2 and the eukaryotic 80S ribosome facilitate tRNA translocation. EMBO J. *23*, 1008-1019.

Stark,H., Rodnina,M.V., Wieden,H.J., Zemlin,F., Wintermeyer,W., and van Heel,M. (2002). Ribosome interactions of aminoacyl-tRNA and elongation factor Tu in the codon-recognition complex. Nat. Struct. Biol. *9*, 849-854.

Steitz,T.A. and Moore,P.B. (2003). RNA, the first macromolecular catalyst: the ribosome is a ribozyme. Trends Biochem. Sci. *28*, 411-418.

Steneberg,P. and Samakovlis,C. (2001). A novel stop codon readthrough mechanism produces functional Headcase protein in Drosophila trachea. EMBO Rep. *2*, 593-597.

Stoneley,M., Chappell,S.A., Jopling,C.L., Dickens,M., MacFarlane,M., and Willis,A.E. (2000). c-Myc protein synthesis is initiated from the internal ribosome entry segment during apoptosis. Mol. Cell Biol *20*, 1162-1169.

Struhl,K. (1998). Histone acetylation and transcriptional regulatory mechanisms. Genes Dev. *12*, 599-606.

Suka,N., Carmen,A.A., Rundlett,S.E., and Grunstein,M. (1998). The regulation of gene activity by histones and the histone deacetylase RPD3. Cold Spring Harb. Symp. Quant. Biol. *63*, 391-399.

Sumita,M., Desaulniers,J.P., Chang,Y.C., Chui,H.M., Clos,L., and Chow,C.S. (2005). Effects of nucleotide substitution and modification on the stability and structure of helix 69 from 28S rRNA. RNA. *11*, 1420-1429.

Sun,Z.W. and Hampsey,M. (1999). A general requirement for the Sin3-Rpd3 histone deacetylase complex in regulating silencing in Saccharomyces cerevisiae. Genetics *152*, 921-932.

Sundaram,M., Durant,P.C., and Davis,D.R. (2000). Hypermodified nucleosides in the anticodon of tRNALys stabilize a canonical U-turn structure. Biochemistry *39*, 12575-12584.

Tan,G.T., DeBlasio,A., and Mankin,A.S. (1996). Mutations in the peptidyl transferase center of 23 S rRNA reveal the site of action of sparsomycin, a universal inhibitor of translation. J. Mol. Biol. *261*, 222-230.

Taunton,J., Hassig,C.A., and Schreiber,S.L. (1996). A mammalian histone deacetylase related to the yeast transcriptional regulator Rpd3p [see comments]. Science *272*, 408-411.

Tenson,T. and Mankin,A. (2006). Antibiotics and the ribosome. Mol. Microbiol. *59*, 1664-1677.

Thompson,J.D., Higgins,D.G., and Gibson,T.J. (1994). CLUSTAL W: improving the sensitivity of progressive multiple sequence alignment through sequence weighting, position-specific gap penalties and weight matrix choice. Nucleic Acids Res. *22*, 4673-4680.

Tollervey,D., Lehtonen,H., Jansen,R., Kern,H., and Hurt,E.C. (1993). Temperature-sensitive mutations demonstrate roles for yeast fibrillarin in pre-rRNA processing, pre-rRNA methylation, and ribosome assembly. Cell *72*, 443-457.

Triana-Alonso,F.J., Spahn,C.M., Burkhardt,N., Rohrdanz,B., and Nierhaus,K.H. (2000). Experimental prerequisites for determination of tRNA binding to ribosomes from Escherichia coli. Methods Enzymol. *317*, 261-276.

Tu,C., Tzeng,T.-H., and Bruenn,J.A. (1992). Ribosomal movement impeded at a pseudoknot required for ribosomal frameshifting. Proc. Natl. Acad. Sci. USA *89*, 8636-8640.

Tumer,N.E., Parikh,B., Li,P., and Dinman,J.D. (1998). Pokeweed antiviral protein specifically inhibits Ty*1* directed +1 ribosomal frameshifting and Ty*1* retrotransposition in *Saccharomyces cerevisiae*. J. Virol. *72*, 1036-1042.

Valadkhan,S. and Manley,J.L. (2003). Characterization of the catalytic activity of U2 and U6 snRNAs. RNA. *9*, 892-904.

Valle,M., Zavialov,A., Li,W., Stagg,S.M., Sengupta,J., Nielsen,R.C., Nissen,P., Harvey,S.C., Ehrenberg,M., and Frank,J. (2003). Incorporation of aminoacyl-tRNA into the ribosome as seen by cryo-electron microscopy. Nat. Struct. Biol *10*, 899-906.

Vanrobays,E., Gleizes,P.E., Bousquet-Antonelli,C., Noaillac-Depeyre,J., Caizergues-Ferrer,M., and Gelugne,J.P. (2001). Processing of 20S pre-rRNA to 18S ribosomal RNA in yeast requires Rrp10p, an essential non-ribosomal cytoplasmic protein. EMBO J. *20*, 4204-4213.

Venema,J. and Tollervey,D. (1999). Ribosome synthesis in Saccharomyces cerevisiae. Annu. Rev. Genet. *33*, 261-311.

Vershon,A.K., Hollingsworth,N.M., and Johnson,A.D. (1992). Meiotic induction of the yeast HOP1 gene is controlled by positive and negative regulatory sites. Mol. Cell Biol. *12*, 3706-3714.

Vicens,Q. and Westhof,E. (2001). Crystal structure of paromomycin docked into the eubacterial ribosomal decoding A site. Structure. (Camb.) *9*, 647-658.

Vidal,M. and Gaber,R.F. (1991). RPD3 encodes a second factor required to achieve maximum positive and negative transcriptional states in Saccharomyces cerevisiae. Mol. Cell Biol. *11*, 6317-6327.

von der Haar F. (1974). Affinity elution: principles and applications to purification of aminoacyl-tRNA synthetases. Methods Enzymol. *34*, 163-171.

von der Haar F. (1979). Purification of aminoacyl-tRNA synthetases. Methods Enzymol. *59*, 257-267.

Wang,A.H., Bertos,N.R., Vezmar,M., Pelletier,N., Crosato,M., Heng,H.H., Th'ng,J., Han,J., and Yang,X.J. (1999). HDAC4, a human histone deacetylase related to yeast HDA1, is a transcriptional corepressor. Mol. Cell Biol. *19*, 7816-7827.

Warner,J.R. (1999). The economics of ribosome biosynthesis in yeast. Trends Biochem. Sci. *24*, 437-440.

Watkins,N.J., Gottschalk,A., Neubauer,G., Kastner,B., Fabrizio,P., Mann,M., and Luhrmann,R. (1998). Cbf5p, a potential pseudouridine synthase, and Nhp2p, a putative RNA-binding protein, are present together with Gar1p in all H BOX/ACA-motif snoRNPs and constitute a common bipartite structure. RNA. *4*, 1549-1568.

Weinger,J.S., Parnell,K.M., Dorner,S., Green,R., and Strobel,S.A. (2004). Substrate-assisted catalysis of peptide bond formation by the ribosome. Nat. Struct. Mol. Biol. *11*, 1101-1106.

Wickner,R.B. (1996). Double-stranded RNA viruses of *Saccharomyces cerevisiae*. Microbiol. Rev. *60*, 250-265.

Wickner,R.B. and Leibowitz,M.J. (1976). Two chromosomal genes required for killing expression in killer strains of Saccharomyces cerevisiae. Genetics *82*, 429-442.

Williams,D.J., Boots,J.L., and Hall,K.B. (2001). Thermodynamics of 2'-ribose substitutions in UUCG tetraloops. RNA. *7*, 44-53.

Wills,N., Moore B., Hammer A., Gesteland,R.F., and Atkins,J.F. (2006). A Functional -1 Ribosomal Frameshift Signal in the Human Paraneoplastic Ma3 Gene. J. Biol Chem. *281*, 7082-7088.

Wilson,J.E., Pestova,T.V., Hellen,C.U., and Sarnow,P. (2000). Initiation of protein synthesis from the A site of the ribosome. Cell *102*, 511-520.

Wilson,K.S. and Noller,H.F. (1998). Molecular movement inside the translational engine. Cell *92*, 337-349.

Yarus,M., Valle,M., and Frank,J. (2003). A twisted tRNA intermediate sets the threshold for decoding. RNA *9*, 384-385.

Yoon,A., Peng,G., Brandenburger,Y., Zollo,O., Xu,W., Rego,E., and Ruggero,D. (2006). Impaired control of IRES-mediated translation in X-linked dyskeratosis congenita. Science *312*, 902-906.

Yusupov,M.M., Yusupova,G.Z., Baucom,A., Lieberman,K., Earnest,T.N., Cate,J.H., and Noller,H.F. (2001). Crystal Structure of the Ribosome at 5.5 A Resolution. Science *292*, 883-896.

Zebarjadian,Y., King,T., Fournier,M.J., Clarke,L., and Carbon,J. (1999). Point mutations in yeast CBF5 can abolish in vivo pseudouridylation of rRNA. Mol. Cell Biol. *19*, 7461-7472.

Zhao,X. and Yu,Y.T. (2004). Pseudouridines in and near the branch site recognition region of U2 snRNA are required for snRNP biogenesis and pre-mRNA splicing in Xenopus oocytes. RNA. *10*, 681-690.